To the Graduate Council:

I am submitting herewith a dissertation written by George Brock Williams entitled "Discrete Conformal Welding." I have examined the final copy of this dissertation for form and content and recommend that it be accepted in partial fulfillment of the requirements for the degree of Doctor of Philosophy, with a major in Mathematics.

Ken Stephenson

Ken Stephenson, Major Professor

We have read this dissertation
and recommend its acceptance:

Stefan Richter

Accepted for the Council:

Associate Vice Chancellor and
Dean of The Graduate School

DISCRETE CONFORMAL WELDING

A Dissertation

Presented for the

Doctor of Philosophy

Degree

The University of Tennessee, Knoxville

George Brock Williams, Jr.

May 1999

Acknowledgments

I would first like to thank my Doctoral Committee, Geoffrey Canright, Conrad Plaut, Ken Stephenson, and Stefan Richter. Their many thoughtful suggestions have greatly improved the quality of this work. Dr. Stephenson's tireless assistance and encouragement have proven priceless. I will be forever grateful not only for his help in conducting this research, but also for his contagious enthusiasm for circle packing.

Many thanks are also due to my high school mathematics teacher, Sherman Livingston. His encouragement sparked my love for mathematics, and his example has shown me what teaching can be.

I must also express my deepest gratitude to my parents, George and Dorothy Williams, for the tremenous sacrifices they have made to further my education. I can never forget "who I am and where I came from."

Through her constant support and tireless assistance, my wife Carol has been my greatest blessing. I could never thank her enough for all she has done. Most of all, I must thank my Lord for the strength and insights He has given me.

Abstract

We develop a discrete version of conformal welding for discs and half-planes. Using circle packings, we induce discrete welding maps which approximate the classical conformal welding maps. A type of converse is also developed, allowing the approximation of quasisymmetries given the conformal welding curves they induce. We also discuss the practical issues involved in computing the discrete maps.

Contents

1 Introduction **1**

2 Conformal Welding **5**

2.1 Conformal Structures 5

2.2 Quasiconformal Maps 6

2.3 Quasisymmetries 12

2.4 Quasicircles 15

2.5 Conformal Welding Theorem 20

3 Circle Packing **25**

3.1 Triangulations and Complexes 25

3.2 Circle Packings 27

3.3 Existence of Packings 29

3.4 Geometric Lemmas 31

3.5 Discrete Analytic Functions 38

3.6 Discrete Analytic Function Theory 38

4 Combinatorial Welding **41**

4.1 The Discrete Approach 41

4.2 Augmentation of the Complexes 43

4.3 Discrete Quasisymmetries 48

4.4 Conditions on the Degree 51

4.5 Conditions on Angles 52

5 Welding of Discs **57**

5.1 Prototype Triangulations 58

5.2 Geometric Realization of Prototypes 59

5.3 Construction of Discrete Welding Maps 64

5.4 Quasiconformality of the Discrete Maps 67

5.5 Extension of the Discrete Maps 73

5.6 Convergence of the Discrete Maps 75

5.7 Conformality of the Limit Maps 77

5.8 Welding Property of the Limit Maps 78

5.9 Quasisymmetric Identification Maps 79

6 Welding of Half-Planes **81**

6.1 Prototype Triangulations 82

6.2 Construction of Discrete Welding Maps 82

6.3 Extension of the Discrete Maps 84

6.4 Convergence of the Discrete Maps 86

6.5 Conformality of the Limit Maps 87

6.6 Welding Property of the Limit Maps 87

6.7 Quasisymmetric Identification Maps 88
6.8 Locally Quasisymmetric Maps 89
6.9 Discrete Local Approximation 90

7 Approximation of Quasisymmetries **95**

7.1 Construction of Range Packings 96
7.2 Geometric Lemmas 99
7.3 Construction of Domain Packings 110
7.4 Construction of the Approximating Maps 115
7.5 Extension of the Approximating Maps 116
7.6 Convergence of the Approximating Maps 117

8 Computational Aspects **119**

8.1 Experimentation 119
8.2 Successful Failures 122
8.3 Monomial Quasisymmetries 125
8.4 Quasisymmetries Induced by Blaschke Products 127
8.5 Practical Limitations 129

Bibliography **132**

Index **140**

Vita **146**

List of Figures

4.1 Addition of Vertices 44

4.2 Augmentation of Complexes 46

4.3 An Augmented Face 54

4.4 Adding a Perpendicular Segment 55

5.1 A Prototype Triangulation 58

5.2 The packing $P_{14,8}$ on S^2. 61

5.3 The packing $P_{14,8}$ projected to the plane. 63

7.1 A Cow-Shaped Quasicircle. 97

7.2 The Jordan curve J. 102

7.3 The image of J lying in $\mathbb{D}$. 104

7.4 Curves for which $\Gamma_{l_n(w),l_n(z)} \neq l_n(A_{w,z})$ 107

7.5 A Doubled Complex. 111

7.6 A Euclidean Complex 112

8.1 Welding a Contraction 121

8.2 An Early Discrete Welding 123

8.3 A Spiraling Welding 124

8.4 A Discrete Welding for $\varphi(x) = x^3$. 126

8.5 A Discrete Welding for $\varphi(x) = x^5$. 126

8.6 Discrete Blaschke Welding for Small y. 128

8.7 Discrete Blaschke Welding for Large y. 128

8.8 A Double Spiral. 130

Chapter 1

Introduction

Imagine two discs positioned one above the other. If the boundaries of the discs are sewn together, a sphere with a "seam" about its equator emerges. Suppose, however, that the sewing is done unevenly, stretching the top disc in some places while compressing it in others. For example, if we had a homeomorphism φ from the boundary of the top disc onto the boundary of the bottom disc, we could sew the discs by attaching points to their images under φ. Now if we require the discs to maintain their conformal structures even after being joined together, they will push and pull against each other, warping their seam in the process. It will be possible for the discs to settle in locations so that their conformal structures mesh, precisely when they can be mapped conformally onto complementary Jordan domains of S^2 by maps whose boundary values respect the identification. If such maps exist, then we say the discs have been *conformally welded* and refer to their seam as a *conformal welding curve.*

Of great importance to the study of conformal structures on Riemann surfaces, is the case in which the above sewing is performed using a quasisymmetric identification map. A conformal welding will always exist for such a map, and the conformal welding curve will be a quasicircle. Moreover, every quasicircle arises as the conformal welding curve for some quasisymmetric map. Indeed, both the space of quasicircles and the space of quasisymmetric identification maps provide a model for the Universal Teichmüller Space, the set of all conformal structures of all Riemann surfaces. Conformal welding thus provides the mechanism for switching between these two models. The Universal Teichmüller Space has gained attention by physicists recently [36, 40, 41] as a setting for bosonic string theory.

After describing some background results in Chapters 2 and 3, we construct a discrete version of conformal welding in Chapter 4. Instead of welding discs, we will weld triangulations of discs. This *combinatorial welding* then yields a triangulation T of a sphere which can be realized as a geometric complex by a circle packing on S^2, that is, a configuration of circles in S^2 in which each circle corresponds to a vertex of T and two circles are externally tangent if their corresponding vertices are connected by an edge in T. Just as there is a unique conformal structure on S^2, so there is an essentially unique circle packing on S^2 for each T. The circles must push and pull against each other to settle in locations compatible with the global pattern provided by T in the same way that two welded discs settle in locations compatible with the global conformal structure on S^2. By connecting centers of tangent circles with spherical geodesics, this circle packing provides a geometric realization of the once purely combinatorial welding. In particular, the "seam" between the original triangulations is realized as a polygonal Jordan curve, a discretized version of the conformal welding curve.

In Chapter 5, we will show that the discrete version is more than just analogous to the classical case – it approximates it as well. Indeed, welding finer and finer triangulations using the same quasisymmetric map produces discrete welding curves that converge in the Hausdorff metric to the classical conformal welding curve. Moreover, the construction produces discrete maps of the discs onto S^2 which converge locally uniformly to the classical conformal welding maps.

In Chapter 6, we develop similar methods for the discrete welding of half-planes. Moreover, in this case we need not restrict ourselves to only quasisymmetric identification maps; any locally bilipschitz identification map will possess a conformal welding [38, 54, 56], which we can then approximate with our discrete techniques.

Next, in Chapter 7 we develop a method for approximating the quasisymmetry φ from the quasicircle Γ it induces. We first construct a circle packing lying inside Γ and one lying outside Γ. The inside packing will be repacked to cover the unit disc $\mathbb{D}$, and the outside packing will be repacked to lie in $\mathbb{D}^* = \mathbb{C} \setminus \mathbb{D}$. These packings then induce a discrete analytic maps which will approximate the classical conformal welding maps. The boundary values of the discrete maps can then be used to approximate φ itself.

We conclude with a discussion in Chapter 8 of the computational aspects of these results, including examples of progress and problems of computer implementation.

Chapter 2

Conformal Welding

2.1 Conformal Structures

The development of the theory of Riemann surfaces is one of the great achievements of mathematics in the last 150 years. Lying at the intersection of complex analysis and geometry, it has been a major theme of pure mathematics. Some of the many excellent references on the general aspects of this theory include [3, 8, 10].

Definition 2.1. A **Riemann Surface** R is a 1-complex-dimensional manifold with a **conformal structure**, that is, a maximal collection $\{\phi_\alpha : R \to \mathbb{C}\}$ of charts such that all transition maps $\phi_\alpha \circ \phi_\beta^{-1}$ are analytic where defined. Two surfaces R_1 and R_2 with conformal structures $\{\phi_\alpha\}$ and $\{\phi_\beta\}$, respectively, are **conformally equivalent** if there exists a homeomorphism f between them so that the complex maps $\phi_\beta \circ f \circ \phi_\alpha^{-1}$ are analytic for all charts ϕ_α and ϕ_β for which they are defined.

One natural question to ask is whether surfaces which are topologically equivalent can be conformally inequivalent; that is, can two homeomorphic surfaces have different conformal structures. It is not hard to show that the answer must be "yes," and this observation forms the starting point for Teichmüller theory [19, 33, 35].

In one important case, however, the answer is "no."

Proposition 2.1. *The sphere S^2 admits only one conformal structure.*

2.2 Quasiconformal Maps

Following the work of Herbert Grötzsch [21] in the 1920's and Lars Ahlfors [2, 5], Lipman Bers [12], and Arne Beurling [13] in the 1950's, the study of quasiconformal maps has grown into a well-developed field. Quasiconformal maps behave like "distorted" analytic homeomorphisms and provide the link between different conformal structures for the same topological surfaces. We first make some preliminary definitions [34].

Definition 2.2. Given a family of curves G in a domain $\Omega \subset S^2$, the **extremal length** of G is

$$EL(G) = \sup_{\rho \in P} \frac{\left(\inf_{\gamma \in G} \int_\gamma \rho(z)\, |dz|\right)^2}{\iint_\Omega \rho^2(z)\, dx\, dy},$$

where $P = \{\rho : \Omega \to \mathbb{C} \mid \rho \geq 0,\ \rho \text{ Borel-measurable}\}$. The **modulus** $M(G)$ of G is $\frac{1}{EL(G)}$.

We will usually be more concerned with two special types of curve families.

Definition 2.3. A **quadrilateral** is a Jordan domain in S^2 with four distinguished boundary points (and four distinguished boundary arcs - the top, bottom, left, and right sides). The **modulus of a quadrilateral** is the modulus of the family of curves joining its top and bottom sides. A **ring domain** is a doubly connected open subset of S^2. The **modulus of a ring domain** is 2π times the modulus of the family of curves separating its two complementary components.

It is not hard to prove that the modulus of a euclidean rectangle whose left and right sides have length a and whose top and bottom sides have length b is $\frac{b}{a}$. Moreover, an annulus whose outer circle is the unit circle and whose inner circle is the circle $\{|x| = r\}$ has modulus $\log \frac{1}{r}$. A punctured disc will then be said to have infinite modulus. The following result [34] will prove useful for estimating the moduli of ring domains.

Proposition 2.2. *If $R \subset S^2$ is a ring domain and l is a lower bound on the spherical length of Jordan curves separating the components of R, then*

$$M(R) \leq \frac{2\pi^2}{l^2}.$$

Also, if R separates the pair p_1, p_2 from the pair q_1, q_2 such that the spherical distance between p_1 and p_2 and the spherical distance between q_1 and q_2 are less than d, then

$$M(R) \leq \frac{\pi^2}{2d^2}.$$

Thus, if a ring is to have very large modulus, it must contain very short curves separating its complementary components.

It is not difficult to prove that conformal maps preserve the modulus of curve families [34]. Quasiconformal maps then are those homeomorphisms which distort moduli by only a bounded amount.

Definition 2.4. A homeomorphism f on a domain Ω in S^2 is K-**quasiconformal** if

$$\frac{1}{K}M(f(G)) \leq M(G) \leq KM(f(G))$$

for all curve families in Ω. Note that f is conformal if and only if it is 1-quasiconformal.

Fortunately, it is sufficient to check the modulus of only rings or quadrilaterals [34].

Proposition 2.3. *A homeomorphism f on a domain Ω in S^2 is K-quasiconformal if either*

$$\frac{1}{K}M(f(Q)) \leq M(Q) \leq KM(f(Q))$$

for all quadrilaterals $Q \subset \Omega$ or

$$\frac{1}{K}M(f(R)) \leq M(R) \leq KM(f(R))$$

for all rings $R \subset \Omega$.

Using this idea that quasiconformality measures the distortion of moduli, it is not difficult to show the following very useful result.

Proposition 2.4. *If f is K_1-quasiconformal and g is K_2-quasiconformal, then $f \circ g$ is K_1K_2-quasiconformal (where defined). In particular, if g and h are conformal, then $h \circ f \circ g$ is K_1-quasiconformal.*

The preceeding *geometric* definition of quasiconformality was developed by Lars Ahlfors [2] and Albert Pfluger [42]. However, there is also an *analytic* characterization developed by Herbert Grötzsch [21].

Lemma 2.5. *A homeomorphism f on a domain Ω in S^2 is K-quasiconformal if and only if for all $z \in \Omega$*

$$D_f(z) = \limsup_{r \to 0^+} \frac{\max_{w \in \partial B(z;r)} |f(w) - f(z)|}{\min_{w \in \partial B(z;r)} |f(w) - f(z)|} \leq K.$$

$D_f(z)$ is called the **dilatation** *of f at z. Note that a map f is conformal if and only if its dilatation is* 1 *everywhere.*

This characterization can be restated in terms of the complex derivatives of f.

Lemma 2.6. *A homeomorphism f on a domain Ω in S^2 is K-quasiconformal if*

$$\bar{\partial} f = \mu \, \partial f$$

for some **Beltrami differential** *μ in the unit ball of $L^2(\Omega)$ with $K \leq \frac{1+\|\mu\|_\infty}{1-\|\mu\|_\infty}$.*

The function μ is then called the **complex dilatation** *of f. Note that f is conformal if and only if f satisfies the Cauchy-Riemann equation $\bar{\partial} f = 0$; hence f is conformal if and only if its complex dilatation is 0 almost everywhere (with respect to Lebesque measure).*

Given this definition, we have the following existence theorem [34].

Theorem 2.7. *Given a Beltrami differential $\|\mu\|_\infty < 1$ on a region Ω then there exists a quasiconformal map f satisfying $\bar{\partial} f = \mu\, \partial f$. If g is any other such map, then there exists a conformal homeomorphism $h : \Omega \to \Omega$ such that $g = f \circ h$.*

Remark 2.1. Since Beltrami differentials are only defined almost everywhere with respect to Lebesque measure, if a homeomorphism $f : \Omega \to S^2$ is K-quasiconformal off a set $E \subset \Omega$ of Lebesgue measure zero, then f is K-quasiconformal on E as well.

It is a well-known fact [34], that a quasiconformal homeomorphism between Jordan domains extends continuously to the boundary. We follow the common practice of referring to a quasiconformal map and its extension by the same name. Note that we have defined quasiconformality only on open subsets of S^2; in referring to quasiconformality on the closure of Jordan domains, we shall mean quasiconformality on the interior.

Since quasiconformal maps act as "distorted" conformal maps, they possess many of the same function theoretic properties.

Theorem 2.8 (Liouville's Theorem). *A non-constant K-quasiconformal map cannot map the entire plane into a proper subset of itself.*

One of the great advantages in working with quasiconformal maps is the relative ease with which one can construct a family of quasiconformal maps which are normal.

Theorem 2.9. *If a sequence $\{f_n\}$ of K-quasiconformal homeomorphisms satisfies any one of the following conditions for some triple of points a, b, and c,*

1. *Each f_n fixes a, b, and c.*
2. *Each f_n fixes a and b and omits c.*
3. *Each f_n fixes a and omits b and c.*

then some subsequence $\{f_{n_k}\}$ converges locally uniformly to either a constant function or a K-quasiconformal homeomorphism whose range is

$$\begin{aligned} \operatorname{range}(f) &= \operatorname{kernel}(\{\operatorname{range}(f_{n_k})\}) \\ &= \bigcup_j \operatorname{int}\left(\bigcap_{k>j} \operatorname{range}(f_{n_k})\right). \end{aligned}$$

Moreover, in cases 1 and 2, the limit map cannot be constant.

Theorem 2.9 makes it very easy to construct a convergent sequence of quasiconformal maps. Thus even if one is interested in only conformal maps, it is often fruitful instead to construct a sequence of quasiconformal maps with dilatation decreasing to 1 and then use Theorem 2.9 to extract a convergent subsequence.

2.3 Quasisymmetries

We now turn our focus to the 1-dimensional analog of quasiconformal maps.

Notation 2.1. Given a rectifiable Jordan curve J,

$$|x - y|_J$$

will denote the length of the shorter subarc of J connecting x and y. That is, $|x - y|$ is the distance from x to y inside J. If I is a subarc of J, then

$$|I|_J$$

will denote the length of I.

Definition 2.5. An orientation preserving homeomorphism $\varphi : \partial\mathbb{D} \to \partial\mathbb{D}$ is called a k-**quasisymmetry** if

$$\frac{1}{k} \leq \frac{|\varphi(I)|_{\mathbb{D}}}{|\varphi(J)|_{\mathbb{D}}} \leq k$$

for any two adjacent intervals (subarcs) I and J of $\partial\mathbb{D}$ having equal length. Similarly, an increasing homeomorphism $\varphi : \mathbb{R} \to \mathbb{R}$ is a k-quasisymmetry if

$$\frac{1}{k} \leq \frac{\varphi(x+t) - \varphi(x)}{\varphi(x) - \varphi(x-t)} \leq k$$

for any $x \in \mathbb{R}$, $t > 0$. A map φ is called **locally quasisymmetric on** E if every point of E has a neighborhood on which φ is quasisymmetric.

Note that the definition of a quasisymmetry is unaffected by composition with a rotation of $\partial\mathbb{D}$ or an affine map of $\mathbb{R}$. Thus unless otherwise stated, we will assume that any real quasisymmetry has been normalized to fix 0 and 1 and any quasisymmetry on $\partial\mathbb{D}$ fixes 1. (Note that as described in [31], we could actually require a quasisymmetry on $\partial\mathbb{D}$ to fix both 1 and -1.)

Example 2.1. Suppose φ is k-bilipschitz on $\mathbb{D}$; that is, for all x and y in its domain,

$$\frac{1}{k} \leq \frac{|\varphi(x) - \varphi(y)|_{\mathbb{D}}}{x - y} \leq k.$$

Then for all adjacent intervals I and J having equal length t,

$$\frac{1}{k^2} \leq \frac{\frac{t}{k}}{kt} \leq \frac{|\varphi(I)|_{\mathbb{D}}}{|\varphi(J)|_{\mathbb{D}}} \leq \frac{kt}{\frac{t}{k}} \leq k^2.$$

Thus any such φ is a k^2-quasisymmetry. The corresponding result also holds of course for bilipschitz homeomorphisms of $\mathbb{R}$.

Remark 2.2. One should note that there is no analog of Lemma 2.5 for quasisymmetries; that is, one cannot tell if a function is quasisymmetric by observing its behavior only in a neighborhood of each point. Thus, unlike quasiconformality, quasisymmetry is a global property. However, John Kelingos [29] proved the following.

Lemma 2.10. *Any real k-quasisymmetric function φ defined on an interval $[a, b]$ can be extended to a k'-quasisymmetry on all of $\mathbb{R}$, where k' depends only on k.*

In fact, it was Kelingos who coined the term "quasisymmetry" because such functions map symmetric intervals to intervals of comparable length, just as quasiconformal homeomorphisms map path families to path families of comparable extremal length. Another justification for considering quasisymmetries as 1-dimensional quasiconformal maps lies in the following theorem [13].

Theorem 2.11. *Any K-quasiconformal homeomorphism of the disc $\mathbb{D}$ or the upper-half plane $\mathbb{U}$ onto itself can be extended continuously to the boundary. This extension will be k-quasisymmetric, where k depends only on K.*

Beurling and Ahlfors [13], proved that the converse also holds.

Theorem 2.12 (Beurling-Ahlfors Extension Theorem). *Any $\varphi : \mathbb{R} \to \mathbb{R}$ which is k-quasisymmetric can be extended to a K-quasiconformal homeomorphism Φ of the upper half-plane, where K depends only on k.*

The following proposition follows easily from the construction of the Beurling-Ahlfors extension.

Proposition 2.13. *If a sequence of real quasisymmetries $\{\varphi_n\}$ converges locally uniformly to a quasisymmetry φ, then the Beurling-Ahlfors extensions $\{\Phi_n\}$ of $\{\varphi_n\}$ converge locally uniformly on the upper half-plane to the Beurling-Ahlfors extension Φ of φ.*

Adrien Douady and Earle [16] have constructed quasiconformal extensions of quasisymmetries of $\partial\mathbb{D}$. Alternative proofs are contained in [32, 44], while [1] describes numerical issues involved in computing the extension.

Theorem 2.14 (Douady-Earle Extension Theorem). *Any $\varphi : \partial\mathbb{D} \to \partial\mathbb{D}$ which is k-quasisymmetric can be extended to a K-quasiconformal homeomorphism f of $\mathbb{D}$, where K depends only on k. Moreover, this extension is conformally natural in that the extension of $M^{-1} \circ \varphi \circ M$ is $M^{-1} \circ f \circ M$ for any Möbius transformation M.*

We note that the corresponding result to Proposition 2.13 also holds in this case.

2.4 Quasicircles

We now turn our attention from the boundary values of quasiconformal maps to the images of discs under quasiconformal maps.

Definition 2.6. A Jordan curve Γ is a K-**quasicircle** if it is the image of the unit circle under a K-quasiconformal map F of S^2. A Jordan domain whose boundary is a K-quasicircle is then called a K-**quasidisc**.

Recall that a K-quasiconformal map remains K-quasiconformal after composition with a conformal map. Thus we can always normalize Γ by post-composing F with a Möbius transformation to ensure Γ passes through 1 and separates 0 from ∞ or that Γ passes through each of $0, 1$, and ∞.

Example 2.2. Consider a regular n-gon Γ_n having the unit circle as its inscribed circle. The most obvious homeomorphism of Γ_n onto $\partial\mathbb{D}$ is the one which merely radially projects each point $re^{i\theta} \in \Gamma_n$ onto $e^{i\theta} \in \partial\mathbb{D}$. This shrinking of rays through the origin can obviously be extended to a homeomorphism p_n of $\mathbb{C}$ onto itself. In particular, if we assume Γ_n is rotated such that one of the points at which Γ_n is tangent to $\partial\mathbb{D}$ lies at 1, then this map becomes

$$p_n(re^{i\theta}) = \begin{cases} \cos(\theta)re^{i\theta} & \text{if } 0 \leq \theta < \frac{\pi}{n}; \\ \cos(\theta - \frac{2\pi}{n})re^{i\theta} & \text{if } \frac{\pi}{n} \leq \theta < \frac{3\pi}{n}; \\ \cos(\theta - \frac{4\pi}{n})re^{i\theta} & \text{if } \frac{3\pi}{n} \leq \theta < \frac{5\pi}{n}; \\ \vdots & \vdots \\ \cos(\theta - \frac{2(n-1)\pi}{n})re^{i\theta} & \text{if } \frac{(2n-3)\pi}{n} \leq \theta < \frac{(2n-1)\pi}{n}. \\ \cos(\theta)re^{i\theta} & \text{if } \frac{(2n-1)\pi}{n} \leq \theta < 2\pi \end{cases} \tag{2.1}$$

Note that the scaling factor in p_n is periodic so that to show the quasiconformality of p_n it suffices to work only on the sector $0 \leq \theta < \frac{\pi}{n}$.

Since p_n is expressed using polar coordinates, we will need the polar form of the complex derivatives; that is, if $f(re^{i\theta}) = u(r,\theta) + iv(r,\theta)$, then

$$\begin{aligned} \partial f(re^{i\theta}) &= \cos\theta\left(u_r + \frac{1}{r}v_\theta\right) + \sin\theta\left(v_r - \frac{1}{r}u_\theta\right) \\ &\quad + i\left(\cos\theta\left(v_r - \frac{1}{r}u_\theta\right) + \sin\theta\left(-u_r - \frac{1}{r}v_\theta\right)\right) \end{aligned} \tag{2.2}$$

and

$$\begin{aligned}\bar{\partial} f(re^{i\theta}) &= \cos\theta\left(u_r - \frac{1}{r}v_\theta\right) + \sin\theta\left(-v_r - \frac{1}{r}u_\theta\right) \\ &\quad + i\left(\cos\theta\left(v_r + \frac{1}{r}u_\theta\right) + \sin\theta\left(u_r - \frac{1}{r}v_\theta\right)\right).\end{aligned} \tag{2.3}$$

After a somewhat lengthy computation, we then find

$$\begin{aligned}\partial p_n(re^{i\theta}) &= 2\cos\theta + i\sin\theta \\ \bar{\partial} p_n(re^{i\theta}) &= (2\cos\theta\sin^2\theta) - i\sin\theta\cos(2\theta),\end{aligned} \tag{2.4}$$

and

$$\begin{aligned}|\partial p_n(re^{i\theta})| &= \sqrt{3\cos^2\theta + 1} \\ |\bar{\partial} p_n(re^{i\theta})| &= \sin\theta.\end{aligned} \tag{2.5}$$

Another calculation shows that the minimum of

$$|\partial p_n| - |\bar{\partial} p_n| = \sqrt{3\cos^2\theta + 1} - \sin\theta$$

on $[0, \frac{\pi}{n}]$ occurs at $\frac{\pi}{n}$. Thus we have

$$\frac{|\partial p_n| + |\bar{\partial} p_n|}{|\partial p_n| - |\bar{\partial} p_n|} \le \frac{2 + \sin(\frac{\pi}{n})}{\sqrt{3\cos^2(\frac{\pi}{n}) + 1} - \sin(\frac{\pi}{n})}. \tag{2.6}$$

Hence Γ_n is a b_n-quasicircle, where

$$b_n = \frac{2 + \sin(\frac{\pi}{n})}{\sqrt{3\cos^2(\frac{\pi}{n}) + 1} - \sin(\frac{\pi}{n})}. \tag{2.7}$$

Note that in later work, we will assume one of the *vertices* of our polygon lies at 1, rather than one of the tangency points. In this case the radial projection map will be the above map p_n conjugated by a (conformal) rotation and dilation. Our estimates of the dilatation of this projection will of course remain unchanged; any regular n-gon, $n \geq 4$, is a b-quasicircle, where $b = b_4 = \max_{n \geq 4} b_n$.

We also note that p_n can stretch the distance between two points by no more that a factor of $\cos(\frac{\pi}{n})$; that is, p_n is bilipschitz with constant $\cos(\frac{\pi}{n}) < b$.

There are a great many other characterizations of quasicircles [20]; one particularly nice geometric result is due to Ahlfors [4, 5].

Proposition 2.15. *A curve Γ in S^2 is a quasicircle if and only if it is of* **bounded turning***; that is, there exists $\widetilde{K}$ such that for all points $x, y \in \Gamma$*

$$\operatorname{diam}(\Gamma_{x,y}) \leq \widetilde{K}|x - y|, \tag{2.8}$$

where $\Gamma_{x,y}$ is the sub-arc of Γ connecting x and y which has the smaller diameter. If Γ is a K-quasicircle, then $\widetilde{K}$ depends only on K. Similarly, if (2.8) *holds, then Γ is a K-quasicircle where K depends only on $\widetilde{K}$.*

For our work, the most useful property of quasicircles is the following [4].

Lemma 2.16. *If Γ is a K_1-quasicircle, then there exists an orientation-reversing K_1^2-quasiconformal involution $\imath_\Gamma$ fixing each point of Γ and interchanging the components of the complement of Γ. Such a map will be called a* **quasiconformal reflection** *in Γ. Moreover, if f is a K_2-quasiconformal map of a K_3-quasidisc onto a Jordan domain with boundary Γ, then f has a $K_1^2 K_2 K_3^2$-quasiconformal extension to all of S^2.*

Proof. If Γ is the image of $\partial\mathbb{D}$ under a K_1-quasiconformal map F, then we set

$$\imath_\Gamma = F \circ \imath \circ F^{-1},$$

where $\imath$ is the reflection in $\partial\mathbb{D}$. By Proposition 2.4, $\imath_\Gamma$ is K_1^2-quasiconformal.

If $f : \mathbb{D} \to \mathbb{C}$ is a K_2-quasiconformal map of a K_3-quasidisc bounded by Σ onto the region bounded by Γ, then we can extend f to all of S^* by putting

$$f = \imath_\Gamma \circ f \circ \imath_\Sigma$$

on the complement of the region bounded by Σ. Again by Proposition 2.4, this extension is $K_1^2 K_2 K_3^2$-quasiconformal.

□

2.5 Conformal Welding Theorem

This finally brings us to the process of conformal welding.

Given two Jordan domains D_1 and D_2 on the Riemann sphere and a homeomorphism $\varphi : \partial D_1 \to \partial D_2$, we may form a topological sphere S by identifying points x of ∂D_1 with points $\varphi(x)$ of ∂D_2. We may equip D_1 and D_2 with the conformal structures they inherit as subsets of the Riemann sphere; however, since S is a sphere, it admits exactly one conformal structure no matter how φ glues D_1 and D_2 together.

We say a *conformal welding* exists for φ if this conformal structure on S extends the conformal structures of D_1 and D_2; that is, if there exist *conformal welding maps* g and f of D_1 and D_2, respectively, onto complementary regions of S^2 with boundary values satisfying

$$g = f \circ \varphi.$$

The interplay between the two domains as they find their new positions as complementary regions of S will pull their "seam" Γ into a *conformal welding curve.*

In the case in which D_1 and D_2 are both discs or both half-planes, it is well-known that if φ is quasisymmetric, then a welding will exist and Γ will be a quasicircle [34].

Theorem 2.17 (Conformal Welding Theorem). *Let $\varphi : \partial\mathbb{D} \to \partial\mathbb{D}$ be a quasisymmetry. Then there exist conformal maps $f : \mathbb{D} \to \Omega$ and $g : \mathbb{D}^* \to \Omega^*$ onto disjoint Jordan domains of S^2 such that their boundary values satisfy*

$$g(e^{i\theta}) = f \circ \varphi(e^{i\theta})$$

Moreover the Jordan curve $\Gamma = f(\partial\mathbb{D}) = g(\partial\mathbb{D})$ is an essentially unique quasicircle; that is, Γ is unique up to Möbius transformations. A similar result holds for real quasisymmetries.

The Conformal Welding Theorem for half-planes was first proved by Albert Pfluger [43] using Lipman Bers's "μ-trick" and Theorem 2.7; a constructive proof was later given by Ollie Lehto [34]. The disc case was then proved by Dariusz Partyka [39] using the same techniques as Lehto and the characterization of quasisymmetries of $\mathbb{D}$ by Jan Krzyż [31]. Since that time, various other forms of the welding have been developed. For example, Kinjiro Nishikawa and Fumio Maitani [37] have studied the welding of two sides of a quadrilateral to form a ring, and Kôtaro Oikawa [38] has discussed the welding of half-infinite strips to form a half-infinite cylinder. The type of the surface formed by welding has also been studied by several people, including Oikawa [38], Jussi Väisälä [57], and Juhani Vainio [54–56].

In the special case in which φ is bilipschitz, the conformal welding curve is a **Bishop-Jones** curve [9, 14]. The approximation techniques we will develop allow us to approximate Bishop-Jones curves directly and general quasicircles via a diagonalization argument.

Example 2.3. Consider the real quasisymmetry $\varphi(x) = x^3$ and the maps $f : \mathbb{L} \to \mathbb{C}$ and $g : \mathbb{U} \to \mathbb{C}$ defined on the lower and upper half-planes, respectively, by

$$f(z) = z^{\frac{1}{2}}$$
$$g(z) = z^{\frac{3}{2}}.$$

If we take different branch cuts for f and g, we see that the images of f and g are complementary regions of the Jordan curve Γ consisting of two rays meeting at the origin (and at ∞) at angle $\frac{\pi}{2}$. Moreover,

$$g(x) = x^{\frac{3}{2}} = (x^3)^{\frac{1}{2}} = f \circ \varphi(x).$$

Since φ, f, and g are all normalized to fix 0, 1 and ∞, then f and g must be the conformal welding maps for φ, and Γ must be its conformal welding curve.

In fact, one can similarly show [13, 28] that a real quasisymmetry of the form $\varphi(x) = x|x|^{\alpha-1}$ will have as its conformal welding curve two rays meeting at the origin at angle $\frac{2\pi}{\alpha+1}$. Moreover, the conformal welding maps must be given by $f(z) = z^{\frac{2}{\alpha+1}}$ and $g(z) = z^{2-\frac{2}{\alpha+1}} = z^{\frac{2\alpha}{\alpha+1}}$.

Next we observe that not only does every quasisymmetry induce a quasicircle, but every quasicircle has a naturally associated normalized quasisymmetry.

Theorem 2.18. *Suppose Γ is a K-quasicircle separating S^2 into two domains Ω and Ω^* with $0 \in \Omega$ and $\infty \in \Omega^*$. If*

$$f : \Omega \to \mathbb{D}$$

$$g : \Omega^* \to \mathbb{D}^*$$

are conformal homeomorphisms, then the homeomorphism

$$\varphi = f^{-1} \circ g : \partial\mathbb{D} \to \partial\mathbb{D}$$

formed from the boundary values of f and g is a k-quasisymmetry, where k depends only on K. If we normalize so that

$$f(0) = 0$$

$$g(\infty) = \infty$$

$$\varphi(1) = 1,$$

then this quasisymmetry is unique.

The corresponding result also holds for conformal maps f and g of Ω and Ω^* onto the lower and upper half-planes, respectively. In this case we will usually require Γ to pass through 0, 1, and ∞ and normalize so that

$$f(0) = g(0) = \varphi(0) = 0$$
$$f(1) = g(1) = \varphi(1) = 1$$
$$f(\infty) = g(\infty) = \varphi(\infty) = \infty.$$

It is well-known [33] that both the space of normalized quasisymmetries and the space of normalized quasicircles provide models for the Universal Teichmüller Space, which contains all conformal structures of all Riemann surfaces. The correspondence produced by conformal welding thus provides the mechanism for switching between these two models.

Although this correspondence is of great importance in the study of conformal structures on Riemann surfaces, aside from a few special cases [26–28], such as Example 2.3, there is as yet no known general formula for finding a quasicircle given a quasisymmetry or vice versa.

In Chapters 4, 5, 6, and 7 we will develop discrete techniques to compute this correspondence, and in Chapter 8, we discuss the computational aspects of these techniques.

Chapter 3

Circle Packing

3.1 Triangulations and Complexes

Before assembling the machinery needed to construct a discrete version of conformal welding, we first collect the pieces [48].

Definition 3.1. A **topological triangle** is a closed topological disc with three distingished boundary points called **vertices** (and consequently three distingished boundary arcs, or **edges**). A **triangulation** T of a topological surface S is a decomposition of S into a countable collection of closed topological triangles which are either disjoint or intersect in exactly one vertex or one edge. The triangles in a triangulation are usually referred to as **faces**. Vertices and edges which lie on the boundary (interior) of S are called boundary (interior) vertices and edges.

We will often be concerned only with the combinatorial information encoded by a triangulation. Thus we consider the following abstraction.

Definition 3.2. A n-**simplex** is a set consisting of $n+1$ elements. We will write a 0-simplex $\{v\}$ as simply v, a 1-simplex $\{v, w\}$ as $[v, w]$, and a 2-simplex $\{u, v, w\}$ as $\langle u, v, w\rangle$. A (2-dimensional) **simplicial complex** $\mathcal{K}$ is a countable collection of 0, 1, and 2-simplices such that

1. Every subsimplex of a simplex of $\mathcal{K}$ is in $\mathcal{K}$.

2. Any two simplices of $\mathcal{K}$ intersect in a simplex of $\mathcal{K}$ or not at all.

Note that a triangulation of a surface is a geometric representation of some underlying simplicial complex. The vertices, edges, and topological triangles correspond to the 0, 1, and 2-simplices, respectively, of this complex. Moreover, we can form a topological representation of a simplicial complex by gluing points, euclidean line segments, and euclidean triangles. Given this topology, we will often consider a geometric realization as an "embedding" of the complex in a geometric space. It is the existence of embeddings of "welded" complexes with very nice geometric properties which will allow us to approximate conformal weldings.

Definition 3.3. If a simplicial complex $\mathcal{K}$ can be realized as a (locally finite) triangulation of an orientable topological surface S, then we will call $\mathcal{K}$ an **abstract triangulation** for S. Such a complex is called a **CP-complex** triangulating S if additionally

1. Every boundary vertex has an interior neighbor.

2. The collection of interior vertices is nonempty and edge-connected.

3. If $\mathcal{K}$ is infinite, then the degree of $\mathcal{K}$, that is, the maximum degree of any vertex, is bounded.

When no possiblity of confusion exists, we will often drop the term "abstract." Indeed, we will not be overly rigorous about the distinction between an abstract triangulation and its geometric realization. For example, if T is realized in $D \subset \mathbb{C}$, we will feel free to refer to triangles in D corresponding to faces of T as "faces in D."

Often we will want to consider the subcomplex of a triangulation T formed by removing all the open faces containing a given vertex w. For simplicity of notation, we will denote this complex simply as $T \setminus w$.

3.2 Circle Packings

Since William Thurston's conjecture [52] at the International Symposium on the Occasion of the Proof of the Bieberbach Conjecture, the maps induced by circle packings have been intensely studied as a discrete analog of classical conformal mappings. Several sources of background information are available, including [18] and [48], from which we take the following definition.

Definition 3.4. Given an abstract triangulation $\mathcal{K}$ of a topological surface and $S = S^2$, $\mathbb{C}$, or, $\mathbb{H}^2$, a **circle packing** P for $\mathcal{K}$ in S is a configuration of circles in S such that

1. P contains a circle C_v for each vertex v in $\mathcal{K}$,

2. C_v is externally tangent to C_u if $[v, u]$ is an edge of $\mathcal{K}$,

3. $\langle C_v, C_u, C_w \rangle$ forms a positively oriented mutually tangent triple of circles in S if $\langle v, u, w \rangle$ is a positively oriented face of $\mathcal{K}$.

A circle packing is called **univalent** if no pair of its circles overlap, that is, if no pair intersects in more than one point. A univalent packing P for $\mathcal{K}$ in S provides a geometric realization of $\mathcal{K}$ in S by taking geodesics between the centers of circles as edges. The subset of S formed by the union of the closed faces in this realization will be called the **carrier** of P, denoted carr P.

We note that a triangulation $\mathcal{K}$ can also be thought of as a graph [49]. Thus we will often use terms, such as neighbor and edge path, relating to these viewpoints. We will also use a few terms suggested by the use of circles themselves. For example, if v_0 is an interior vertex, then the circle C_{v_0} together with its neighboring circles C_{v_1},C_{v_2}, ... ,C_{v_n} is called the **flower** of v and denoted $(v_0; v_1, v_2, \ldots, v_n)$. A few terms will be unique to this paper. For example, we will refer to the set of interior vertices sharing an edge with a boundary vertex as the **fringe** of the complex.

Given an vertex v of $\mathcal{K}$ we will denote the collection of neighbors of v in $\mathcal{K}$ by $\mathfrak{G}_{\mathcal{K}}(v,1)$, the first generation about v. In general, $\mathfrak{G}_{\mathcal{K}}(v,n)$ will denote the n^{th} generation about v in $\mathcal{K}$, that is the collection of neighbors of $\mathfrak{G}_{\mathcal{K}}(v,n-1)$ which are not contained in $\mathfrak{G}_{\mathcal{K}}(v,n-1)$ or $\mathfrak{G}_{\mathcal{K}}(v,n-2)$.

3.3 Existence of Packings

One might wonder whether circle packings always exist for a given triangulation [6,7,30,51]. Can the circles somehow push themselves around so that they fit together coherently?

Theorem 3.1 (Koebe-Andreev-Thurston Theorem). *Given a fixed CP-complex $\mathcal{K}$ triangulating a sphere, there exists a univalent circle packing P for $\mathcal{K}$ in S^2. This packing is essentially unique, that is, unique up to Möbius transformations.*

As an immediate corollary, we get an existence result for (necessarily finite) abstract triangulations of a closed disc.

Corollary 3.2. *Given a CP-complex $\mathcal{K}$ triangulating a closed disc, there exists a univalent circle packing for P for $\mathcal{K}$ in $\mathbb{D}$ with all boundary circles internally tangent to $\partial\mathbb{D}$.*

Proof. First add a simplicial cone over the boundary of $\mathcal{K}$ to form an abstract triangulation $\widetilde{\mathcal{K}} = \mathcal{K} \cup \{w_\infty\}$ of a sphere. By Theorem 3.1, there exists a circle packing for $\widetilde{\mathcal{K}}$ on S^2 which we may normalize so that C_{w_∞} corresponds to $\partial\mathbb{D}$ and the remainder of the packing lies in the lower hemisphere of S^2. Stereographic projection then yields the desired euclidean packing. $\square$

A more subtle case is that of (necessarily infinite) CP-complexes triangulating an open disc. The twin possiblities for existence of locally finite packings provides a discrete analog [11,24,46] of the classical Uniformization Theorem.

Theorem 3.3. *Given a CP-complex $\mathcal{K}$ triangulating an open disc, there exists a locally finite univalent packing for $\mathcal{K}$ in exactly one of $\mathbb{C}$ or $\mathbb{D}$. In the first case, the complex is called* **parabolic**; *in the second case, the complex is called* **hyperbolic**.

Example 3.1. The simplest infinite circle packing is the regular hexagonal packing. It is an easy geometric exercise to show that 7 euclidean circles with the same radii always fit together to form a univalent flower. Repeating this pattern yields a parabolic packing H consisting of infinitely many generations of circles of the same radius. The underlying complex consists of infinitely many degree 6 vertices and is realized by carr H as a tiling of $\mathbb{C}$ by equilateral triangles.

The packing H for this triangulation is unique up to maps of the form $z \mapsto az + b, \quad a, b \in \mathbb{R}$, that is, up to scaling and translation. Thus we can form a sequence $\{H_n\}$ of regular hexagonal packings normalized such that every circle of H_n has radius $\frac{1}{2n}$, some distinguished vertex is located at the origin while one of its neighbors is located on the positive x-axis.

Minor modifications to this complex still result in a parabolic complex; for example, if all but finitely many vertices of a triangulation of an open disc have degree 6, then the complex is parabolic [24, 46].

3.4 Geometric Lemmas

One of the central themes of the theory of circle packing is controlling the geometry of a packing by controlling the combinatorics of its underlying triangulation. Our first stop is the Length-Area Lemma of Burt Rodin and Sullivan [47]. This result has its origins in the Length-Area Method of Ahlfors and Beuring [13] and definition of extremal length of curve families in Section 2.2. Here the role of a curve will be played by a **chain**, a collection $\{C_{v_1}, C_{v_2}, \ldots, C_{v_n}\}$ of circles in our packing such that $v_1, v_2, \ldots, v_n$ describes an edge path in the underlying triangulation that does not cross itself. Such a chain will be called closed if $v_1 = v_n$.

Lemma 3.4 (Length-Area Lemma). *Let P be a packing in $\mathbb{D}$ and C_v a circle in P with radius r. Assume there exist m disjoint chains of circles in P having lengths $n_1, \ldots, n_m$, and each separating v from either 0 or a point on $\partial\mathbb{D}$. Then*

$$r < \frac{4}{\sqrt{\sum_{i=1}^{m} \frac{1}{n_i}}}. \tag{3.1}$$

Proposition 3.5. *If C is a circle on S^2 with spherical radius $r \in (0, .72\pi)$, then its diameter is less than its circumference.*

Proof. Recall the circumference of C is $2\pi \sin r$. It is easy to verify $f(x) = 2x - 2\pi \sin x$ is positive for x between 0 and $\approx .73\pi$. $\square$

This allows a spherical version of the Length-Area Lemma. Its proof is similar to the original.

Lemma 3.6 (Spherical Length-Area Lemma). *Let P be a univalent circle packing on S^2 and C_v a circle in P with spherical radius r. Assume there exist m disjoint chains of circles in P having combinatorial lengths $n_1, \ldots, n_m$, and each separating v from two of the three points 0, 1, and ∞. Then*

$$r < \frac{2\pi}{\sqrt{\sum_{i=1}^{m} \frac{1}{n_i}}}. \tag{3.2}$$

Recall that ring domains with large modulii are characterized as containing short curves which separate the complementary components of the domain. If C_v is surrounded by many short chains separating it from two of the three points 0, 1, and ∞, then then radius of C_v must be small. Hence the modulus of the ring domain having boundary components C_v and the line segment joining two of the three points 0, 1, and ∞ as above, must be large. In this way, the Spherical Length-Area Lemma can be considered a combinatorial companion to Proposition 2.2. This ability to control the geometry of a packing by purely combinatorial means will prove invaluable.

Proof of Lemma 3.6. Label vertex corresponding to the j^{th} circle in the i^{th} chain as w_{ij} and label the radius of $C_{w_{i,j}}$ as r_{ij}. Let α_i be the closed curve in S^2 realizing the edge path described by $w_{i,1}, w_{i,2}, \ldots, w_{i,n_i}$. Let l_i be the spherical length of α_i and note

$$l_i = \sum_j 2r_{ij}.$$

First note that by requiring our chains surround two of the three points 0, 1, and ∞, we ensure each circle in each chain must have radius less than $\frac{\pi}{2}$. Thus by Proposition 3.5,

$$\begin{aligned} l_i &= \sum_j 2r_{ij} \\ &< \sum_j \text{circumference}(C_{w_{ij}}). \end{aligned} \tag{3.3}$$

Now note [45] that a circle on S^2 with spherical radius r has circumference $2\pi \sin r$. Thus (3.3) becomes

$$l_i < \sum_j \text{circumference}(C_{w_{ij}}) = \sum_j 2\pi \sin r_{ij}. \tag{3.4}$$

Now we use the Cauchy-Schwartz inequality to compute

$$
\begin{aligned}
l_i^2 &< 4\pi^2(\sum_j \sin r_{ij})^2 \\
&\leq 4\pi^2 n_i \sum_j \sin^2 r_{ij} \\
&= 4\pi^2 n_i \sum_j 1 - \cos^2 r_{ij} \\
&= 4\pi^2 n_i \sum_j (1 - \cos r_{ij})(1 + \cos r_{ij}) \\
&\leq 4\pi^2 n_i \sum_j 2(1 - \cos r_{ij}) \\
&= 4\pi n_i \sum_j 2\pi(1 - \cos r_{ij}).
\end{aligned} \tag{3.5}
$$

But [45] a circle on S^2 with spherical radius r has area $2\pi(1-\cos r)$. Thus

$$
\begin{aligned}
\frac{1}{n_i} l_i^2 &< 4\pi \sum_j 2\pi(1 - \cos r_{ij}) \\
&= 4\pi \sum_j \text{area}(C_{w_{ij}}).
\end{aligned} \tag{3.6}
$$

If we take the sum over i, we see

$$
\begin{aligned}
\sum_{i=1}^{m} \frac{1}{n_i} l_i^2 &< 4\pi \sum_{ij} \text{ area } (C_{w_{ij}}) \\
&< \text{ area } S^2 = (4\pi)^2.
\end{aligned} \tag{3.7}
$$

Now we let $l = \min\{l_i | i = 1, \ldots, m\}$, and observe

$$l^2 \sum_{i=1}^{m} \frac{1}{n_i} \le \sum_{i=1}^{m} \frac{1}{n_i} l_i^2 < (4\pi)^2.$$

Hence

$$l^2 < (4\pi)^2 \left(\sum_i \frac{1}{n_i} \right)^{-1}.$$

Now note our separation assumptions imply $r < \frac{\pi}{2}$, since C_v must lie entirely in a hemisphere. Thus by another application of Proposition 3.5,

$$2r < \text{ circumference } (C_v).$$

Moreover, each α_i separates C_v from two points whose spherical distance is $\frac{\pi}{2}$ and thus must be longer than $\min\{$ circumference $(C_v), \frac{\pi}{2}\} =$ circumference (C_v). Consequently,

$$\begin{aligned}
(2r)^2 &< (\text{ circumference}(C_v))^2 \\
&< l^2 \\
&< (4\pi)^2 \left(\sum_i \frac{1}{n_i} \right)^{-1}.
\end{aligned}$$

Thus

$$r < \frac{2\pi}{\sqrt{\sum_{i=1}^{m} \frac{1}{n_i}}}.$$

□

Next we consider the Ring Lemma and Hex Packing Lemma of Rodin and Sullivan [47]. These results form the heart of their proof of the Rodin-Sullivan Theorem and led to development of discrete analytic function theory.

Lemma 3.7 (Ring Lemma). *Given a univalent flower* $(v_0; v_1, v_2, \ldots, v_n)$ *in* $\mathbb{C}$, *there is a lower bound* C_n, *depending only on* n, *on the ratio of the radius* r_i *of* C_{v_i} *and the radius* r_0 *of* C_{v_0}; *that is,*

$$C_n < \frac{r_i}{r_0},$$

for $i = 1, 2, \ldots, n$.

A spherical version also exists for the Ring Lemma.

Lemma 3.8 (Spherical Ring Lemma). *If* $(v_0; v_1, v_2, \ldots, v_n)$ *is a univalent flower in* S^2 *with each circle having spherical radius less that* $\frac{\pi}{2}$, *then there is a lower bound* C_n, *depending only on* n, *on the ratio of the spherical radius* s_i *of* C_{v_i} *and the spherical radius* s_0 *of* C_{v_0}; *that is,*

$$C_n < \frac{s_i}{s_0},$$

for $i = 1, 2, \ldots, n$.

Proof. Without loss of generality we may rotate the flower so that C_{v_1} lies in the lower hemisphere and C_{v_0} lies in the upper hemisphere. Let r_0 denote the euclidean radius (that is, the radius of the stereographic projection) of C_{v_0}, and let r_1 denote the euclidean radius of C_{v_1}.

Recall that the spherical metric is given by $|ds| = \frac{1}{1+|z|^2}|dz|$. Thus in the lower hemisphere the spherical metric density is higher than the euclidean, while in the upper hemisphere, the euclidean metric density is higher. Hence we see

$$s_1 > r_1 > C_n r_0 > C_n s_0,$$

where C_n is the bound promised by the Rodin-Sullivan Ring Lemma. Clearly the same holds for any other petal C_{v_i} of the flower. □

The Ring Lemma gives us some control over the relationship between circles and their immediate neighbors; by considering more generations , we can gain much better control.

Lemma 3.9 (Hex Packing Lemma). *If a circle C_v is surrounded by n univalent generations of degree 6 circles in a euclidean circle packing, then the ratio between the radius of C_v and the radius of any neighboring circle C_u is bounded above and below by constants depending only on n and decreasing to 1 as $n \to \infty$.*

3.5 Discrete Analytic Functions

Two euclidean packings for the same complex $\mathcal{K}$ give two embeddings for $\mathcal{K}$. There is a natural map from one embedding to the other using barycentric coordinates [58].

Definition 3.5. Every point x in a euclidean triangle Δ having vertices v_1, v_2, and, v_3 can be represented by a triple (t_1, t_2, t_3) where $x = t_1 v_1 + t_2 v_2 + t_3 v_3$ and $\sum_i t_i = 1$. The triple (t_1, t_2, t_3) is called the **barycentric coordinates** for x.

Proposition 3.10. *If P and $\widetilde{P}$ are both univalent euclidean packings for the same triangulation T, then define a map $f : \operatorname{carr} P \to \operatorname{carr} \widetilde{P}$ as follows: If Δ and $\widetilde{\Delta}$ are embeddings in $\operatorname{carr} P$ and $\operatorname{carr} \widetilde{P}$, respectively, of the same face in T, then we map each point $x \in \Delta$ to the point having the same barycentric coordinates as x in the triangle $\widetilde{\Delta}$. The map f is then continuous and piecewise affine.*

Maps induced by circle packings in this way will be referred to as **discrete analytic functions** [49].

3.6 Discrete Analytic Function Theory

We first note the following fact about piecewise affine maps of the plane.

Proposition 3.11. *If f is a piecewise affine map from some euclidean triangle T_1 to a euclidean triangle T_2, then f is K-quasiconformal on T_1, where*

K depends only on the maximum difference between angles in T_1 and corresponding angles in T_2.

Now the Ring Lemma implies that triangles in the carriers of univalent circle packings have angles which are bounded away from 0 and π, and this bound depends only on the degree of the underlying triangulation. Thus discrete analytic functions are quasiconformal, if the degree of $\mathcal{K}$ is bounded.

Corollary 3.12. *If P and Q are two univalent packings in $\mathbb{C}$ for the same complex $\mathcal{K}$, with $\deg \mathcal{K} < \infty$, then the induced discrete analytic function $f : \operatorname{carr}(P) \to \operatorname{carr}(Q)$ is K-quasiconformal on faces which do not contain a boundary vertex. Moreover, K depends only on the degree of $\mathcal{K}$.*

Moreover, as a consequence of the Hex Packing Lemma, discrete analytic functions are almost analytic "deep inside" a hexagonal packing.

Corollary 3.13. *If a vertex v in $\mathcal{K}$ is surrounded by n generations of degree 6 vertices, and $f : \operatorname{carr} P \to \operatorname{carr} \widetilde{P}$ is a discrete analytic function between univalent packings for $\mathcal{K}$, then the dilatation of f on faces containing v decreases to 1 as $n \to \infty$.*

These corollaries were used by Rodin and Sullivan [47] to prove

Theorem 3.14 (Rodin-Sullivan Theorem). *Fix a simply connected domain $\Omega \subsetneq \mathbb{C}$ and points $p, q \in \Omega$. Let P_n be the portion of the infinite regular hexagonal packing H_n which intersects Ω and $\mathcal{K}_n$ its underlying complex. Let $\widetilde{P}_n$ be the packing for $\mathcal{K}_n$ in $\mathbb{D}$ promised by Corollary 3.2 and $f_n : \operatorname{carr} P_n \to \operatorname{carr} \widetilde{P}_n$ the induced discrete analytic function. If each $\widetilde{P}_n$ has* *been normalized so that* $f_n(p) = 0$ *and* $f_n(q) > 0$*, then* $\{f_n\}$ *converges locally uniformly to the Riemann map* $f : \Omega \to \mathbb{D}$ *which satisfies* $f(p) = 0$ *and* $f(q) > 0$*.*

This result has been extended by Ken Stephenson [50], who replaced the strictly hexagonal combinatorics by a requirement that radii be uniformly comparable and the degree of $\mathcal{K}_n$ be uniformly bounded. Zheng-Xu He and Oded Schramm [25] have since removed even these conditions.

The moral of our story is that given a triangulation $\mathcal{K}$, circle packings exist for $\mathcal{K}$ and in any two packings for the same triangulation, the circles somehow re-arrange their carriers in nearly the same way an analytic map would.

Chapter 4

Combinatorial Welding

4.1 The Discrete Approach

We are now ready to develop a discrete analog of the classical conformal welding described in Chapter 2. Rather than gluing together two discs in the plane, we will glue together two *triangulations* of discs. Instead of requiring that the welded discs maintain their *conformal* structures, we will require that they maintain their *combinatorial* structures.

Throughout this chapter T and T^* will denote abstract triangulations of closed discs. We will assume the faces of T and T^* which contain boundary vertices have been embedded in the plane in such a way that each face is realized as a euclidean triangle. We will denote by ∂T and ∂T^* the embedded image of the collection of boundary edges of T and T^*, respectively.

Suppose $\varphi : \partial T^* \to \partial T$ is a k-bilipschitz homeomorphism; that is, for all $x, y \in \partial T^*$

$$\frac{1}{k}|x-y|_{\partial T^*} \leq |\varphi(x) - \varphi(y)|_{\partial T} \leq k|x-y|_{\partial T^*}. \tag{4.1}$$

To simplify our discussion will also assume that φ maps the embedded image of some boundary vertex w_1 of T^* to the embedded image of a boundary vertex v_1 of T, but φ need not otherwise respect the combinatorial structures of ∂T and ∂T^*.

Just as classical conformal weldings are constructed by gluing boundary points to their images under a homeomorphism, our combinatorial welding will be constructed by gluing boundary edges of T^* to their images under φ . Since φ need not respect the combinatorial structure of T^*, some care must be taken to ensure that the image of a boundary edge of T^* is actually an edge of T. Once such technicalities are dealt with, our procedure will yield a triangulation $\mathcal{K}$ of a sphere. The combinatorial structures of both T and T^* will be preserved in complementary portions of $\mathcal{K}$.

It should be emphasized that although we require portions of T and T^* to be embedded in $\mathbb{C}$, the spherical triangulation $\mathcal{K}$ is purely abstract. No metric or geometric information will be assumed on this spherical complex until the triangulation is realized via circle packing. It is the circle packing which will provide a discrete conformal structure approximating the classical one. The packing will impose exactly the correct geometry to allow our discrete welding to approximate the classical welding.

It should also be noted that while we will describe the combinatorial welding procedure by welding the entire boundary of one triangulation to the entire boundary of another, the same construction can be used to weld only portions of each boundary. This will be explored in Chapter 6.

4.2 Augmentation of the Complexes

Recall a boundary vertex of T and a boundary vertex of T^* have previously been distinguished in our assumption that $\varphi(w_1) = v_1$. We begin our combinatorial welding by labeling the boundary vertices of T as $v_1, v_2, \ldots, v_n$, beginning with v_1 and continuing in the positive direction around ∂T. Similarly, we label the boundary vertices of T^* as $w_1, w_2, \ldots, w_m$, beginning with w_1 and continuing in the negative direction around ∂T^*. With all circular lists of this form, we adopt the convention $v_{n+1} = v_1$ and $w_{m+1} = w_1$.

Now since φ may not as yet respect the combinatorial structure of ∂T^*, we add new boundary vertices to T corresponding to the images under φ of boundary vertices of T^*. See Figure 4.1. That is, for each boundary vertex w_i of T^*, we define

$$\tilde{v_i} = \begin{cases} v_j, & \text{if } |\varphi(w_i) - v_j|_{\partial T} < \frac{r}{3k} \\ \varphi(w_i), & \text{otherwise,} \end{cases}$$

where $r = \min\{|w_i - w_{i+1}|_{\partial T^*}, |v_j - v_{j+1}|_{\partial T} : i = 1, 2, \ldots, m, j = 1, 2, \ldots, n\}$. Note that each v_j is at least r units from v_{j+1}; thus $\varphi(w_i)$ can be within $\frac{r}{3k}$

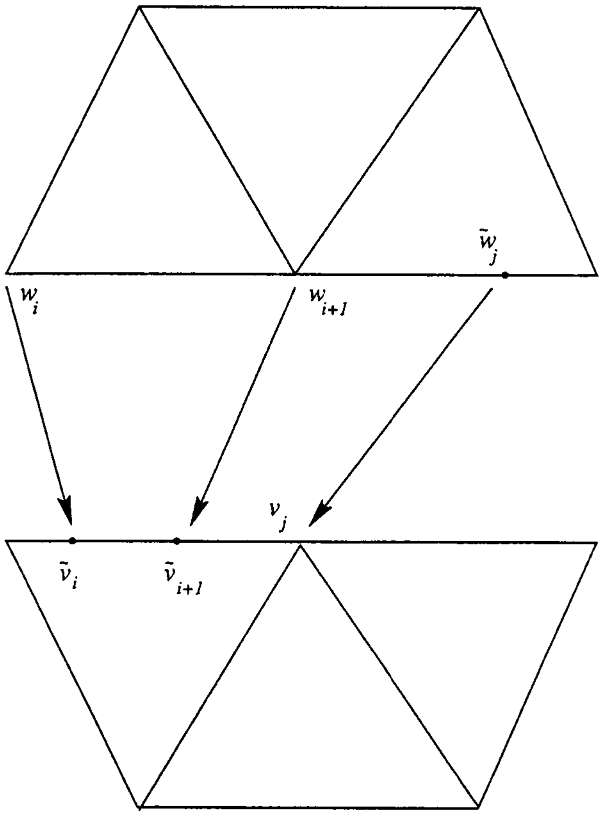

Figure 4.1: Addition of Vertices
Vertices $\tilde{v}_i$ and $\tilde{v}_{i+1}$ are added to T to correspond to $\varphi(w_i)$ and $\varphi(w_{i+1})$, respectively. The vertex $\tilde{w}_j$ is added to T^* to correspond to $\varphi(v_j)$.

of at most one v_j.

We remark that the reason we do not add an extra boundary vertex to T if $\varphi(w_i)$ is close (within $\frac{r}{3k}$) to some v_j is a technical one to be explained in Section 4.5 below.

Since we still want T to triangulate a closed disk, we must also add additional edges. For each face $\langle u, v_j, v_{j+1}\rangle$ of T, we add an edge from u to each $\tilde{v}_i$ lying on the edge $[v_j, v_{j+1}]$. Since $\langle u, v_j, v_{j+1}\rangle$ was embedded as a euclidean triangle, we embed our new edge $[u, \tilde{v}_i]$ as a line segment from u to $\tilde{v}_i$. We will denote our new augmented complex as $\mathcal{T}$. Similarly for each boundary vertex v_j of T, we add a vertex

$$\tilde{w}_j = \begin{cases} w_i, & \text{if } v_j = \tilde{v}_i \\ \varphi^{-1}(v_j), & \text{otherwise,} \end{cases}$$

to the boundary of T^* and add appropriate interior edges as above. Again we denote this augmented complex as $\mathcal{T}^*$. See Figure 4.2.

Lemma 4.1. *There is a one-to-one, order-preserving correspondence φ_T between the boundary vertices of $\mathcal{T}^*$ and the boundary vertices of $\mathcal{T}$ (and hence also between the boundary edges) given by*

$$\begin{aligned} \varphi_T(w_i) &= \tilde{v}_i \\ \varphi_T(\tilde{w}_j) &= v_j, \end{aligned} \tag{4.2}$$

for $i = 1, 2, \ldots, m$, and $j = 1, 2, \ldots, n$.

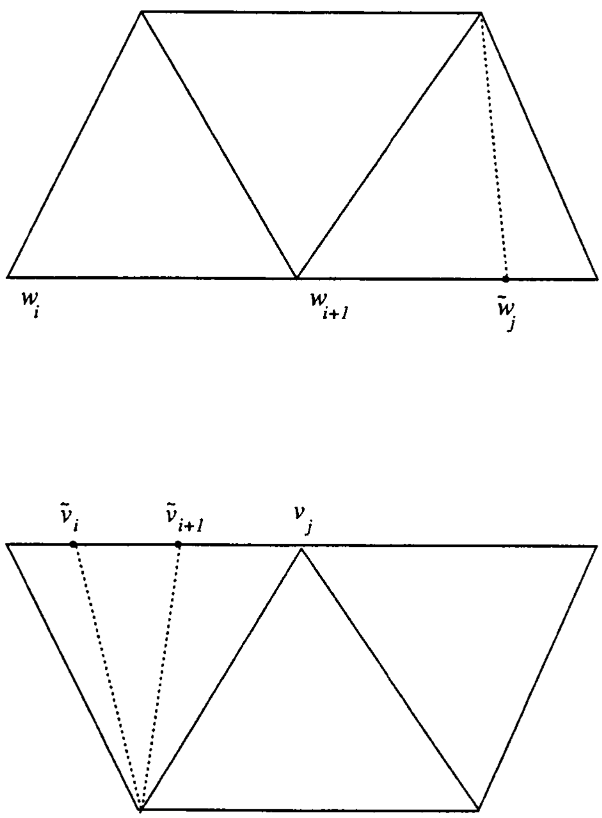

Figure 4.2: Augmentation of Complexes
Edges are now added so that our augmented complexes remain triangulations.

Proof. Since a boundary vertex of $\mathcal{T}^*$ could be labeled both as w_i for some i and as $\tilde{w}_j$ for some j, our first concern must be whether φ_T is even well-defined. But a careful observation of our definitions allays our fears as $w_i = \tilde{w}_j$ if and only if $\tilde{v}_i = v_j$.

Next recall that if $\tilde{v}_i = v_j$ then $|\varphi(w_i) - v_j|_{\partial T} < \frac{r}{3k}$. Thus since φ is k-bilipschitz,

$$\begin{aligned} \frac{r}{k} &\leq \frac{1}{k}|w_{i+1} - w_i|_{\partial T^*} \\ &\leq |\varphi(w_{i+1}) - \varphi(w_i)|_{\partial T} \\ &\leq |\varphi(w_{i+1}) - v_j|_{\partial T} + |\varphi(w_i) - v_j|_{\partial T} \\ &< |\varphi(w_{i+1}) - v_j|_{\partial T} + \frac{r}{3k}. \end{aligned}$$

A moment of algebra yields

$$\frac{r}{3k} < \frac{2r}{3k} < |\varphi(w_{i+1}) - v_j|_{\partial T},$$

which implies $\tilde{v}_{i+1} \neq v_j$. Similarly, $\tilde{v}_{i-1} \neq v_j$. Since φ is orientation-preserving, it is clear that $\tilde{v}_k \neq v_j$, if $k \neq i$. In other words, $\tilde{v}_i = \tilde{v}_j$ if and only if $i = j$. Consequently, $\tilde{w}_i = \tilde{w}_j$ if and only if $i = j$.

Now we see if $\varphi_T(v_i) = \varphi_T(v_j)$, then $\tilde{w}_i = \tilde{w}_j$, and hence $i = j$. Similarly, if $\varphi_T(\tilde{v}_i) = \varphi_T(\tilde{v}_j)$, then $w_i = w_j$, and again $i = j$. Finally, if $\varphi_T(v_j) = \varphi_T(\tilde{v}_i)$, then $\tilde{w}_j = w_i$, which implies $v_j = \tilde{v}_i$. Hence φ_T is one-to-one.

But in our augmentation of the boundaries, we ensured that $\mathcal{T}$ and $\mathcal{T}^*$

now have the same number of boundary vertices. Hence since φ_T is one-to-one, it must also be onto. Finally, it is clear φ_T must be orientation-preserving since φ is orientation-preserving.

□

Now we are able to complete our combinatorial welding. By Lemma 4.1, each boundary vertex of $\mathcal{T}$ is the image under φ_T of some boundary vertex of $\mathcal{T}$, and each boundary vertex of $\mathcal{T}^*$ is the image under φ_T^{-1} of some boundary vertex of $\mathcal{T}^*$. Thus we form a spherical complex $\mathcal{K}$ by identifying vertices (and edges) which correspond under φ_T. Again we emphasize that $\mathcal{K}$ is just a spherical abstract triangulation. No geometric structure has yet been imposed.

4.3 Discrete Quasisymmetries

The identification map introduced in Lemma 4.1 will play a critical role in our work.

Definition 4.1. The map φ_T constructed above can be extended linearly on the edges of $\mathcal{T}^*$. Since each edge $[w_i, \tilde{w}_j]$ is embedded as a euclidean line segment, each point on this edge is of the form $(1-t)w_i + t\tilde{w}_j$ for some $0 \le t \le 1$. Thus we extend φ_T to such an edge by setting

$$\varphi_T((1-t)w_i + t\tilde{w}_j) = (1-t)\varphi_T(w_i) + t\varphi_T(\tilde{w}_j).$$

Similarly we can extend φ_T to edges of the form $[w_i, w_{i+1}]$ in the same manner and define φ_T on all of ∂T^*. Such an extended map will be referred to as a **discrete quasisymmetric function** or **discrete quasisymmetry**.

Partial justification for this terminology is provided by the following proposition.

Proposition 4.2. *The discrete quasisymmetry φ_T constructed above is k-bilipschitz.*

Proof. First we note that any point on T^* lies on an edge of the form $[w_i, w_{i+1}]$ or $[w_i, \tilde{w}_j]$. Fix two points $x, y \in \partial T^*$ which lie on edges of the first type. The proof for the remaining cases is, of course, the same.

Now x and y can be written as convex combinations of pairs of boundary vertices; that is,

$$x = (1-t)w_i + tw_{i+1}$$
$$y = (1-s)w_j + sw_{j+1}$$

for some boundary vertices w_i, w_{i+1}, w_j, and w_{j+1} and some $t, s \in [0,1]$.

If $i = j$, that is, if x and y lie on the same edge, then we see

$$\begin{aligned}
|\varphi_T(x) - \varphi_T(y)|_{\partial T} &= |\varphi_T((1-t)w_i + tw_{i+1}) - \varphi_T((1-s)w_i + sw_{i+1})|_{\partial T} \\
&= |(1-t)\varphi(w_i) + t\varphi(w_{i+1}) - (1-s)\varphi(w_i) + s\varphi(w_{i+1})|_{\partial T} \\
&= |(s-t)\varphi(w_i) - (s-t)\varphi(w_{i+1})|_{\partial T} \\
&\leq k|s-t||w_i - w_{i+1}|_{\partial T^*} \\
&= k|(s-t)w_i - (s-t)w_{i+1}|_{\partial T^*} \\
&= k|((1-t)w_i + tw_{i+1}) - ((1-t)w_i + tw_{i+1})|_{\partial T^*} \\
&= k|x-y|_{\partial T^*}.
\end{aligned}$$

If $i \neq j$, then we may assume without loss of generality that w_{i+1} and w_j lie on the shorter subarc of T^* connecting x and y. In this case,

$$\begin{aligned}
|\varphi_T(x) - \varphi_T(y)|_{\partial T} &= |\varphi_T(x) - \varphi_T(w_{i+1})|_{\partial T} \\
&\quad + |\varphi_T(w_{i+1}) - \varphi_T(w_j)|_{\partial T} + |\varphi_T(w_j) - \varphi_T(y)|_{\partial T} \\
&\leq k|x - w_{i+1}|_{\partial T^*} + k|w_{i+1} - w_j|_{\partial T^*} + k|w_j - y|_{\partial T^*} \\
&= k|x-y|_{\partial T^*}.
\end{aligned}$$

Hence φ_T is k-Lipschitz. The proof that φ_T^{-1} is also k-Lipschitz is of course similar.

□

4.4 Conditions on the Degree

In later work, maintaining a bound on the degree of our complexes will be critical. With such a bound, we will be able to apply Corollary 3.12 to show our approximate welding maps are uniformly quasiconformal. Our assumption that φ be bilipschitz is precisely the condition we need for such a bound.

Lemma 4.3. *Suppose*

$$r = \min\{|w_i - w_{i+1}|_{\partial\mathcal{T}^*}, |v_j - v_{j+1}|_{\partial\mathcal{T}} : i = 1, 2, \ldots, m,\ j = 1, 2, \ldots, n\} \text{ and}$$
$$R = \max\{|w_i - w_{i+1}|_{\partial\mathcal{T}^*}, |v_j - v_{j+1}|_{\partial\mathcal{T}} : i = 1, 2, \ldots, m,\ j = 1, 2, \ldots, n\}.$$

If the degrees of $\mathcal{T}$ and $\mathcal{T}^*$ are at most M_I and the maximum degree of a fringe vertex of $\mathcal{T}$ or $\mathcal{T}^*$ is M_F, then the new degree of $\mathcal{T}$ and $\mathcal{T}^*$ after performing the construction above is at most

$$M = \max\left(M_I, M_F + M_F\left\lceil\frac{kR}{r}\right\rceil\right).$$

Moreover, the new degree of any fringe vertex is at most

$$M_F\left(1 + \left\lceil\frac{kR}{r}\right\rceil\right).$$

(Note that by $\lceil a\rceil$ we mean the smallest integer greater than a.)

Proof. First note the vertices which are added by our construction all have degree $3 \leq M_I \leq M$. Moreover, our construction changes the degree only of vertices on the fringe of the complex. The degree of such a vertex is at most M_F plus the number of new vertices added between its boundary neighbors. It can have at most M_F such boundary neighbors; thus it suffices to show that given any fringe vertex u with consecutive boundary neighbors v_j and v_{j+1}, at most $\lceil \frac{kR}{r} \rceil$ new vertices $\tilde{v}_i$ can be added to the edge $[v_j, v_{j+1}]$.

In order for a vertex $\tilde{v}_i$ to be added between v_j and v_{j+1}, $\varphi(w_i)$ must lie between v_j and v_{j+1}. That is, w_i must lie between $\varphi^{-1}(v_j)$ and $\varphi^{-1}(v_{j+1})$. By (4.1), we see

$$|\varphi^{-1}(v_j) - \varphi^{-1}(v_{j+1})|_{\partial T} \leq k|v_j - v_{j+1}|_{\partial T^*} \leq kR.$$

Since the distance between consecutive w_i's is at least r, we see that at most

$$\frac{kR}{r}$$

vertices w_j can lie between $\varphi^{-1}(v_j)$ and $\varphi^{-1}(v_{j+1})$.

The degree of $\mathcal{T}^*$ must of course be similarly bounded.

$\square$

4.5 Conditions on Angles

We have now established control over the number of vertices added to each edge, but not yet over the relative position of these vertices within each edge.

Recall that we did not add an extra vertex $\tilde{v}_i = \varphi(w_i)$ to T if it would have been placed too near an existing vertex v_j. Without this safeguard, it would be possible for one of the new vertices $\tilde{v}_i$ to be placed arbitrarily closely to a neighboring vertex v_j. In this case $\tilde{v}_i$ and v_j would have a mutual interior neighbor, say u, at which the angle $\angle v_j u \tilde{v}_i$ formed by the edges $[u, v_j]$ and $[u, \tilde{v}_i]$ would be arbitrarily small. Such a small angle could induce a large distortion in our later maps.

Proposition 4.4. *Suppose T and T^* are realized in such a way that the angles θ in each face of T and T^* are uniformly bounded away from 0 and π, say, $\sin\theta > m > 0$. Then the realizations of faces in the new triangulations $\mathcal{T}$ and $\mathcal{T}^*$ will have angles which are also uniformly bounded away from 0 and π. Moreover, this bound depends only on m, k, and the ratio $c = \frac{\mathfrak{R}}{\mathfrak{r}}$, where $\mathfrak{r}$ and $\mathfrak{R}$ are the minimum and maximum, respectively, lengths of edges of T and T^* which contain a boundary vertex.*

Proof. First note that only faces of the form $\langle u, v_j, v_{j+1}\rangle$ are altered by our addition of the $\tilde{v}_i$ vertices. The angles in all other faces of $\mathcal{T}$ remain bounded as they were. Thus it suffices to examine only faces of the form $\langle u, \tilde{v}_i, v_j\rangle$ and $\langle u, \tilde{v}_i, \tilde{v}_{i+1}\rangle$.

Let u be a fringe vertex with boundary neighbors v_j, v_{j+1}, and suppose $\tilde{v}_i \neq v_j, v_{j+1}$ is a new neighbor of v_j. Let α be the new angle formed at u in the triangle $\Delta u\, v_j\, \tilde{v}_i$, β the angle at v_j, and γ the angle at $\tilde{v}_i$. See Figure 4.3.

Now extend the edge $[u, v_j]$ if necessary and draw a line segment through $\tilde{v}_i$ and perpendicular to the (extended) edge $[u, v_j]$. Let h be the length of this line segment, that is, the distance of $\tilde{v}_i$ to the (extended) edge $[u, v_j]$. If

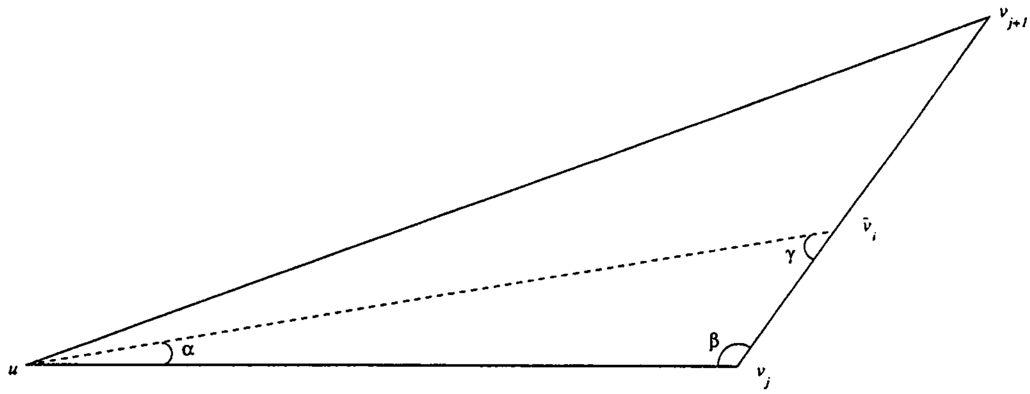

Figure 4.3: An Augmented Face
The face $\langle u, v_j, v_{j+1}\rangle$ with the addition of $\tilde{v}_i$. The angles α, β, and γ are indicated.

H is the length of the edge $[u, \tilde{v}_i]$, then

$$\sin\alpha = \frac{h}{H}.$$

Moreover

$$\begin{aligned}\sin\beta &= \sin(\pi - \beta)\\ &= \frac{h}{|v_j - \tilde{v}_i|}.\end{aligned}$$

See Figure 4.4.

Now recall that if

$$r = \min\{|w_i - w_{i+1}|_{\partial T^*}, |v_j - v_{j+1}|_{\partial T} : i = 1, 2, \ldots, m,\ j = 1, 2, \ldots, n\},$$

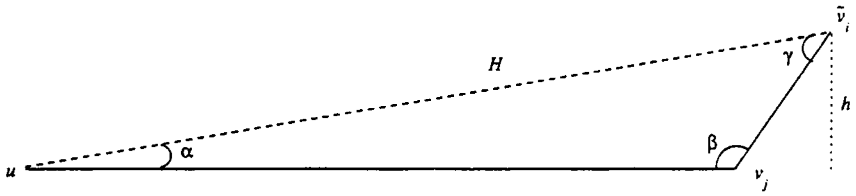

Figure 4.4: Adding a Perpendicular Segment
The face $\langle u, v_j, \tilde{v}_i \rangle$ with the segment of length h indicated.

then by our construction in Section 4.2,

$$\begin{aligned}
|v_j - \tilde{v}_i| &\geq \frac{r}{3k} \\
&\geq \frac{\mathfrak{r}}{3k} \\
&= \frac{\mathfrak{R}}{3kc} \\
&\geq \frac{\max\{|u - v_{j+1}|, |u - v_j|\}}{3kc} \\
&\geq \frac{H}{3kc}.
\end{aligned}$$

Hence

$$\begin{aligned}
\sin(\alpha) &= \frac{h}{H} \\
&= \frac{|v_j - \tilde{v}_i| \sin(\beta)}{H} \\
&\geq \frac{\frac{H}{3kc} \sin(\beta)}{H} \\
&= \frac{\sin(\beta)}{3kc} \\
&> \frac{m}{3kc}.
\end{aligned}$$

and α is bounded away from 0 and π by $\sin^{-1}(\frac{m}{3kc})$.

Of course the angle β remains unchanged by the addition of $\tilde{v}_i$ and is thus bounded as before. Since $\gamma = \pi - \alpha - \beta$, then γ must be bounded away from 0 and π as well.

Now since our construction also ensures

$$|\tilde{v}_i - \tilde{v}_{i+1}| \geq \frac{\mathfrak{r}}{k} = \frac{\mathfrak{R}}{kc} \geq \frac{1}{kc} \max\{|u - v_j|, |u - v_{j+1}\}|,$$

we can repeat the proof above to get a similar bound for angles in faces of the form $\langle \tilde{v}_i, u, \tilde{v}_{i+1} \rangle$.

$\square$

Chapter 5

Welding of Discs

We now use the combinatorial welding developed in Chapter 4 to construct a discrete version of conformal welding for discs. In particular, we will first prove

Theorem 5.1. *Given a bilipschitz quasisymmetry φ, there exist sequences of discrete analytic functions $\{f_n\}$ and $\{g_n\}$ converging uniformly on compact subsets of $\mathbb{D}$ and $\mathbb{D}^*$, respectively, to the conformal welding maps f and g induced by φ. Moreover, the discrete conformal welding curves Γ_n bounding the images of f_n and g_n are quasicircles converging uniformly in the Hausdorff metric to the quasicircle Γ induced by φ as $n \to \infty$.*

In Section 5.9, we will even remove the condition that φ be bilipschitz.

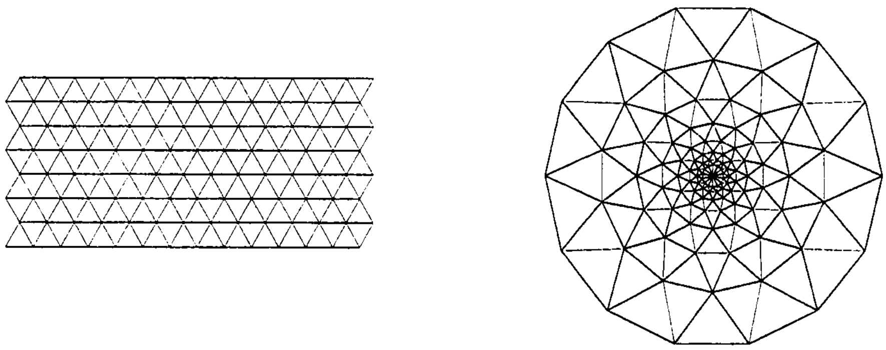

Figure 5.1: A Prototype Triangulation
The initial triangulation $R_{14,8}$ and the prototype triangulation $D_{14,8}$.

5.1 Prototype Triangulations

In order to simplify the remaining arguments, we will now fix a sequence of prototypical triangulations $\{T_{n,m}\}$ on which we can perform the operations described in Chapter 4. However, our arguments can easily be extended to other sequences of triangulations using the results of [50] or [23].

For each $n, m > 4$, let $R_{n,m}$ be a rectangular portion of the infinite hexagonal grid consisting of $n + 1$ vertices on the top and bottom and m vertices on each side. Now identify the left and right sides of this complex, yielding a triangulation of a cylinder, or equivalently, of an annulus. Finally add one additional vertex and edges from it to each of the n vertices on one of the boundaries of the annulus. That is, we "fill up the hole" in the annulus with a single vertex. We will refer to this vertex as v_0 and the entire complex as $T_{n,m}$. See Figure 5.1.

Notice $T_{n,m}$ is now (simplicially equivalent to) a triangulation of a closed disc and has the following properties:

1. $T_{n,m}$ is n-fold rotationally symmetric about v_0 .

2. The degree of v_0 is n.

3. The degrees of all neighbors of v_0 are 5.

4. The degrees of all boundary vertices of $T_{n,m}$ are 4.

5. The degrees of all other vertices of $T_{n,m}$ are 6.

Finally, choose one boundary vertex in each $T_{n,m}$ and label it as v_1 in each complex. The disguished vertices v_0 and v_1 will be used later for normalization.

5.2 Geometric Realization of Prototypes

Before we proceed with the use of our prototype triangulations, we first show the existence of the type of embeddings of $T_{n,m}$ we will need.

Lemma 5.2. *There exists an embedding of each $T_{n,m}$ in $\mathbb{C}$ such that*

1. *Edges of $T_{n,m}$ are realized as euclidean line segments and faces as euclidean triangles.*

2. *If $D_{n,m}$ is the closed region formed by the embedded image of $T_{n,m}$, then $\partial D_{n,m}$ is a regular n-gon inscribed in $\partial\mathbb{D}$.*

3. *There exists a natural b-bilipschitz homeomorphism $p_n : \partial D_{n,m} \to \partial\mathbb{D}$ where b does not depend on n or m.*

4. *The vertex v_0 corresponds to the origin.*

5. *The vertex v_1 corresponds to the point* 1.

Moreover, if $T^*_{n,m}$ is a copy of the complex $T_{n,m}$, but with reversed orientation, and w_∞ is the vertex in $T^*_{n,m}$ corresponding to v_0, then there exists an embedding of $T^*_{n,m} \setminus w_\infty$ in $D^*_{n,m} = S^2 \setminus (int\, D_{n,m})$ such that

1. *Edges of $T^*_{n,m}$ are realized as euclidean line segments and faces as euclidean triangles.*

2. *The collection of boundary edges of $T^*_{n,m}$ is also realized as a regular n-gon inscribed in $\partial\mathbb{D}$.*

3. *The vertex w_1, the copy in $T^*_{n,m}$ of v_1, corresponds to the point* 1.

Proof. Let $\mathcal{K}_{n,m}$ be the combinatorial double of $T_{n,m}$, that is, the triangulation formed by identifying the boundary vertices and edges of $T_{n,m}$ and $T^*_{n,m}$ which are copies of one another. We will when no possibility of confusion exists consider $T_{n,m}$ and $T^*_{n,m}$ as sub-complexes of $\mathcal{K}_{n,m}$.

Since $T_{n,m}$ was a triangulation of a closed disc, our complex $\mathcal{K}_{n,m}$ is simplicially equivalent to a triangulation of a sphere. Thus by the Koebe-Andreev-Thurston Theorem, there exists a unique circle packing $P_{n,m}$ of $\mathcal{K}_{n,m}$ in S^2 normalized so that C_{v_0}, C_{v_1}, and C_{w_∞} are centered at $0, 1$, and ∞, respectively. See Figure 5.2.

If we stereographically project $P_{n,m}$ to the plane, we obtain a new *euclidean* packing $\widehat{P}_{n,m}$. Recall that the spherical metric on $\mathbb{C}$ is given by

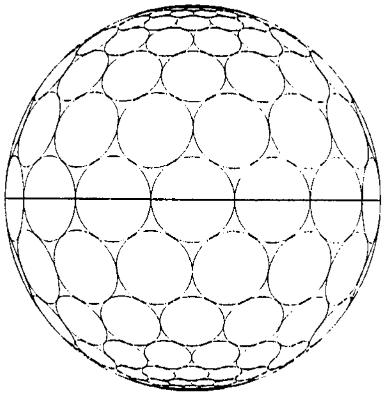

Figure 5.2: The packing $P_{14,8}$ on S^2.
Notice the packing is symmetric about the equator and circles which are the same combinatorial distance from v_0 have the same radii.

$|ds| = \frac{2}{1+|z|^2}|dz|$ and is clearly constant on euclidean circles $|z| = r$. Thus a spherical circle centered at the origin will stereographically project to a euclidean circle which is also centered at the origin. In particular, our circle C_{v_0} in $P_{n,m}$ will remain centered at 0 even after being projected to the plane.

However, the situation with C_{v_1} is not so fortunate. Its stereographic projection will still be a circle, of course, but its center will no longer remain at 1. Since the spherical density $\frac{2}{1+|z|^2}$ is smaller outside $\overline{\mathbb{D}}$ than inside, the new center must move radially outward to some point $1 + \epsilon_{n,m}$.

Next note that if $v \in T_{n,m}$ and $w \in T^*_{n,m}$ are copies of one another, then the circles C_v and C_w in $P_{n,m}$ must have the same radius. Otherwise, applying the Möbius rotation $M(z) = \frac{1}{z}$ to $P_{n,m}$ would result in different packing with the same normalization and, because $T_{n,m}$ and $T^*_{n,m}$ are combinatorially indistinguishable, the same underlying triangulation, thus violating the uniqueness part of Koebe-Andreev-Thurston Theorem. In particular, we see the seam $T_{n,m} \cap T^*_{n,m}$ must correspond exactly to this equator. In the same way, the rotational symmetry of $\mathcal{K}$ implies that circles centered on the equator must have the same spherical radii and thus stereographically project to euclidean circles in $\widehat{P}_{n,m}$ with the same radii. These circles are then centered at points

$$(1+\epsilon_{n,m})e^{i\frac{j-1}{n}}, \quad j = 1, \ldots, n. \tag{5.1}$$

Finally if we scale $\widehat{P}_{n,m}$ by $\frac{1}{1+\epsilon_{n,m}}$, then the portion $D_{n,m}$ of the carrier of this new packing corresponding to $T_{n,m}$ provides a geometric realization of $T_{n,m}$ in $\mathbb{C}$ in which faces are euclidean triangles. Note that v_0 does indeed correspond to the origin in this realization. Moreover, by (5.1), we see $\partial D_{n,m}$ is a regular n-gon with vertices on the unit circle. In particular, note that v_1 corresponds to the point 1. See Figure 5.3.

In order to associate $\partial D_{n,m}$ with $\partial \mathbb{D}$ we radially project $\partial D_{n,m}$ onto $\partial \mathbb{D}$ using a projection p_n as in Example 2.2. The use of p_n is a technical annoyance, but necessary since edges of euclidean triangles are not round. Recall that p_n was bilipschitz with constant b, where b was independent of n.

Similarly, let $D^*_{n,m}$ denote the carrier of our scaled packing $\widehat{P}_{n,m}$ corresponding to $T^*_{n,m}$. Since the circle for w_∞ remains centered at ∞ in $P_{n,m}$, $D^*_{n,m}$ is then a closed unbounded region with polygonal boundary. Indeed we see $D^*_{n,m}$ is the complement in S^2 of the interior of $D_{n,m}$.

Unfortunately, this also means that any face of $T^*_{n,m}$ containing w_∞ is not

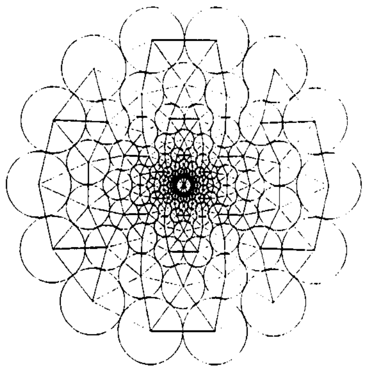

Figure 5.3: The packing $P_{14,8}$ projected to the plane.
Notice that the carrier provides an embedding of $T_{14,8}$ and $T^*_{14,8} \setminus w_\infty$.

embedded in $\mathbb{C}$ by this procedure. Indeed, there is a topological obstruction to embedding the simply connected $T^*_{n,m}$ in the punctured topological disc $\mathbb{D}^*$. The best we can manage is an embedding of $T^*_{n,m} \setminus w_\infty$.

Since the boundary edges of $T^*_{n,m}$ are identified in $\mathcal{K}_{n,m}$ with their respective copies in $T_{n,m}$, we see that the boundary edges of $T^*_{n,m}$ are embedded by the carrier of $\widehat{P}_{n,m}$ in the same way as the boundary edges of $T_{n,m}$. Hence the boundary edges of $T^*_{n,m}$ are also realized as the regular n-gon $\partial D_{n,m} = \partial D^*_{n,m}$. In particular, w_1 also corresponds to the point 1.

$\square$

It is an annoying complication that we cannot embed faces containing w_∞ in $\mathbb{C}$. To fix future notation we will denote by $G_{n,m}$ the unbounded region which "should" have provided an embedding of the faces containing w_∞. That is, $G_{n,m}$ is the complement in $D^*_{n,m}$ of the embedding of $T^*_{n,m} \setminus w_\infty$.

These embeddings of our prototype triangulations do possess other nice features, however. Both v_0 and w_∞ are surrounded by m disjoint chains of n edges which are embedded as euclidean polygons. For large n, these are very nearly concentric circles about 0. As such, they are approximately level curves for the hyperbolic density function on $\mathbb{D}$ and $\mathbb{D}^*$. Their images under our discrete maps will thus provide a good indication of the hyperbolic density on Ω and Ω^*.

5.3 Construction of Discrete Welding Maps

We now use the constructions of Chapter 4 to construct an approximation to the maps f and g and the conformal welding curve Γ induced by φ as described in the Conformal Welding Theorem.

Lemma 5.2 provides the embeddings we need; the only missing ingredient is an identification map from $\partial D_{n,m}$ to $\partial D^*_{n,m}$. Our φ acts only on $\partial\mathbb{D}$, not on $\partial D^*_{n,m}$. However, conjugating φ by p_n will produce a homeomorphism of $\partial D^*_{n,m}$ onto $\partial D_{n,m}$.

Since our radial projection maps p_n are bilipschitz with constant b, each $p_n^{-1}\circ\varphi\circ p_n$ is bilipschitz with constant kb^2. Thus we will use $p_n^{-1}\circ\varphi\circ p_n$ and the constructions of Chapter 4 to combinatorially weld each $T_{n,m}$ to $T^*_{n,m}$, forming augmented triangulations $\mathcal{T}_{n,m}$ and $\mathcal{T}^*_{n,m}$, and a spherical triangulation $\widetilde{\mathcal{K}}_{n,m}$. We also form a discrete quasisymmetry φ_n as in the proof of Lemma 4.1.

Then for each n, m, by the Koebe-Andreev-Thurston Theorem, we can find a circle packing $\widetilde{P}_{n,m}$ for $\widetilde{K}_{n,m}$ on S^2. Without loss of generality, we can normalize $\widetilde{P}_{n,m}$ so that the circles corresponding to v_0, v_1, and w_∞ are centered at $0, 1$, and ∞, respectively. This $\widetilde{P}_{n,m}$ at last gives a geometric structure to our once purely combinatorial welding. We will see that in settling on their appropriate size and location, the circles transmit the local changes in combinatorics induced by φ to the global geometry on the sphere in approximately the same way as the classical conformal welding maps.

By stereographic projection, the realization of $\widetilde{\mathcal{K}}_n$ via $\widetilde{P}_{n,m}$ on S^2 also gives us another embedding of $\mathcal{T}_{n,m}$ and $\mathcal{T}^*_{n,m} \setminus w_\infty$ in the plane. As in the proof of Lemma 5.2 the circles C_{v_0} and C_{w_∞} will remain centered at 0 and ∞, respectively, after the projection. However, as before, we must scale our projected packings by some small factor $\frac{1}{1+\tilde{\epsilon}_{n,m}}$ to place the center of the projection of C_{v_1} at 1. After this scaling, we let $\Omega_{n,m}$ and $\Omega^*_{n,m}$ be the euclidean carriers of the portions of this scaled packing corresponding to $\mathcal{T}_{n,m}$ and $\mathcal{T}^*_{n,m}$, respectively. As before, we cannot construct an embedding of $\mathcal{T}^*_{n,m}$ in $\mathbb{C}$, but only of $\mathcal{T}^*_{n,m} \setminus w_\infty$. We let $\widetilde{G}_{n,m}$ denote the open unbounded region formed by the complement in $\Omega^*_{n,m}$ of the embedding of $\mathcal{T}^*_{n,m} \setminus w_\infty$.

Now we define discrete welding maps

$$\begin{aligned} f_{n,m} &: D_{n,m} \to \Omega_{n,m} \\ g_{n,m} &: D^*_{n,m} \setminus G_{n,m} \to \Omega^*_{n,m} \setminus \widetilde{G}_n \end{aligned} \tag{5.2}$$

by mapping vertices to corresponding vertices and extending piecewise affinely as described in Section 3.5. Note that since $G_{n,m}$ and $\widetilde{G}_{n,m}$ are not formed by the union of *finite* euclidean triangles, we are forced to define $g_{n,m}$ only on a subset of D_n^*.

Proposition 5.3. *For each n and m and all $x \in \partial\mathbb{D}$, $g_{n,m}(x) = f_{n,m} \circ \varphi_n(x)$.*

Proof. If $x \in \partial\mathbb{D}$, then $p_n^{-1}(x)$ lies a line segment between some pair w_i, w_{i+1} of vertices of ∂D. That is, $x = (1-t)w_i + tw_{i+1}$ for some $0 \leq t \leq 1$. But our combinatorial welding was constructed precisely to ensure

$$\begin{aligned} g_{n,m}(w_i) &= f_{n,m} \circ \varphi_n(w_i) \\ g_{n,m}(w_{i+1}) &= f_{n,m} \circ \varphi_n(w_{i+1}). \end{aligned} \tag{5.3}$$

But $g_{n,m}$, $f_{n,m}$, and φ_n were all just linear extensions of maps defined on vertices. Thus

$$\begin{aligned} g_{n,m}(x) &= g_{n,m}((1-t)w_i + tw_{i+1}) \\ &= (1-t)g_{n,m}(w_i) + tg_{n,m}(w_{i+1}) \\ &= (1-t)f_{n,m} \circ \varphi_n(w_i) + tf_{n,m} \circ \varphi_n(w_{i+1}) \\ &= f_{n,m}((1-t)\varphi_n(w_i) + t\varphi_n(w_{i+1})) \\ &= f_{n,m} \circ \varphi_n((1-t)w_i + tw_{i+1}) \\ &= f_{n,m} \circ \varphi_n(x). \end{aligned} \tag{5.4}$$

□

5.4 Quasiconformality of the Discrete Maps

Now that we have defined our discrete welding maps, we show that they are well-behaved. In our constructions in Sections 4.4 and 5.1, we have been very careful to maintain a uniform bound (uniform in both n and m) on the degree of $\mathcal{T}_{n,m}$ and $\mathcal{T}^*_{n,m}$, except at the vertices v_0 and w_∞. Recall that the degree of both v_0 and w_∞ is n, and the degree of each neighbor of v_0 or w_∞ is 5. Moreover, the boundary edges of $T_{n,m}$ and $T^*_{n,m}$ were realized as line segments all having the same length. Consequently, by Lemma 4.3, the degree of all fringe vertices of $\mathcal{T}_{n,m}$ is at most $6\,(1 + \lceil k \rceil)$. Finally, each boundary vertex still has degree 3, and all remaining vertices have degree 6.

Thus by Lemma 3.7, the angles in triangles of $\Omega^*_{n,m}$ and triangles of $\Omega_{n,m}$ which do not contain the origin (the embedded image of v_0) are bounded away from 0 and π uniformly in n and m. Similarly, triangles in our original embeddings of $T^*_{n,m}$ and $T_{n,m}$ which do not contain the origin are also bounded uniformly in n and m. Moreover, according to Lemma 4.4, our augmentation during the combinatorial welding of $T_{n,m}$ and $T^*_{n,m}$, creates triangles whose angles are still uniformly bounded. Thus by Proposition 3.11, each $g_{n,m}$ is K_1-quasiconformal, and on triangles of $D_{n,m}$ which do not contain the origin, each $f_{n,m}$ is K_1-quasiconformal, where K_1 depends on k, but not on n or m. We denote by $F_{n,m}$ the complement in $D_{n,m}$ of this collection of triangles containing 0. That is, $F_{n,m}$ is the embedding of the open star of v_0. In keeping with our previous notation for $G_{n,m}$, we will refer to the region of $\Omega_{n,m}$ corresponding to $F_{n,m}$ as $\widetilde{F}_{n,m}$.

It is an unfortunate complication that as $n \to \infty$, the degree of v_0 becomes unbounded. Happily, however, we are able to bound the dilatation of $f_{n,m}$ on $F_{n,m}$ by choosing m large enough.

Lemma 5.4. *For fixed n, the dilatation of $f_{n,m}$ on $F_{n,m}$ decreases to 1 as $m \to \infty$.*

Proof. As $m \to \infty$, the complexes $T_{n,m}$ exhaust an infinite complex $T_{n,\infty}$, consisting of one vertex of degree n surrounded by infinitely many chains consisting of n vertices of degree 6. As described in Example 3.1, this complex is parabolic and thus has an essentially unique locally finite circle packing in $\mathbb{C}$. It is easy to see this packing must consist of a central circle surrounded by chains of n circles with all circles on each chain having the same radius. If, for example, we scale the packing so that the central circle corresponds to the unit circle, then the radius of every other circle in the entire packing is also determined.

Now consider the circle packings $P_{n,m}$ and $\widetilde{P}_{n,m}$ used in the proof of Lemma 5.2 and in Section 5.3 to construct $D_{n,m}$ and $D^*_{n,m}$, respectively. Let $Q_{n,m}$ and $\widetilde{Q}_{n,m}$ be euclidean packings formed by the portions of the stereographic projections of $P_{n,m}$ and $\widetilde{P}_{n,m}$, respectively, corresponding to the triangulation $T_{n,m}$.

For each m, re-scale $Q_{n,m}$ and $\widetilde{Q}_{n,m}$ so that the circle for v_0 corresponds to the unit circle. Then as $m \to \infty$, $Q_{n,m}$ and $Q_{n,m}$ converge to a packing Q for $T_{n,\infty}$. Thus the radii of circles on the same layer must be nearly equal for large m. In particular, we may choose m so that the angles in faces of carr $Q_{n,m}$ containing v_0 are nearly equal the corresponding angles in carr $\widetilde{Q}_n$. Thus the dilatation of $f_{n,m}$ must decrease to 1 as $m \to \infty$.

$\square$

Next we see that the domains $D_{n,m}$ of our discrete maps $f_{n,m}$ expand to fill the domain $\mathbb{D}$ of the classical conformal welding map f.

Proposition 5.5. *Any compact subset of $\mathbb{D}$ is eventually contained in $D_{n,m}$ for sufficiently large n.*

Proof. Recall that $\partial D_{n,m}$ was a regular n-gon inscribed in $\mathbb{D}$. Clearly then $\partial D_{n,m} \to \partial \mathbb{D}$ as $n \to \infty$, and any compact subset of $\mathbb{D}$ will eventually be contained in $D_{n,m}$.

$\square$

Next we move to the maps $g_{n,m}$. The domains of these discrete maps should fill out the domain $\mathbb{D}^*$ of the classical welding map g. We first prove the following preliminary lemma.

Lemma 5.6. *The spherical radii $s_{n,m}$ and $\widetilde{s}_{n,m}$ of the circle $C_{v_1} = C_{w_1}$ in the packings $P_{n,m}$ and $\widetilde{P}_{n,m}$, respectively, decrease to 0 as $n \to \infty$ if $m \geq \frac{n}{2}$.*

Proof. Note that C_{v_1} is surrounded in $\widetilde{P}_{n,\frac{n}{2}}$ by $\frac{n}{2} - 1$ generations of degree 6 circles.

These generations form $\frac{n}{2} - 1$ disjoint chains separating C_{v_1} from both C_{v_0} and C_{w_∞}. The i^{th} such chain will have length $6i$; thus by the Spherical

Length-Area Lemma,

$$s_{n,\frac{n}{2}} \leq \frac{2\pi}{\sqrt{\sum_{i=1}^{\frac{n}{2}} 6i}},$$

which converges to 0 as $n \to \infty$ since the harmonic series is divergent.

Of course, if $m \geq \frac{n}{2}$, then we can still form such chains. Thus the spherical radius of C_{v_1} in $\widetilde{P}_{n,m}$ will decrease to 0 as $n \to \infty$, if we take $m \geq \frac{n}{2}$.

Next by Lemma 4.3 the degree of all vertices on the "seam" $\mathcal{T}_{n,\frac{n}{2}} \cap \mathcal{T}^*_{n,\frac{n}{2}}$ is bounded by some M independently of n. It is not difficult to see that if we attempt to form disjoint chains about C_{v_1} in $\widetilde{P}_{n,m}$ by joining the i^{th} generation of circles about C_{v_1} in the portion corresponding to $T_{n,\frac{n}{2}}$ to the j^{th} generation in the portion corresponding to $T^*_{n,\frac{n}{2}}$, then we must be able to successfully complete such a chain across the "seam" at at least $\frac{n}{2M}$ vertices. That is, we are assured of forming at least $\frac{n}{2M}$ disjoint chains, the i^{th} one having length at most $6Mi$. Hence

$$\widetilde{s}_{n,m} \leq \frac{2\pi}{\sqrt{\sum_{i=1}^{\frac{n}{2M}} \frac{1}{6Mi}}},$$

which decreases to 0 as $n \to \infty$.

Of course in $P_{n,m}$, the degree of all vertices on the "seam" is exactly 6. Thus in $P_{n,m}$ as well, the radius of C_{v_1} must decrease to 0 as $n \to \infty$, if $m \geq \frac{n}{2}$.

$\square$

Since $\partial D_n^* = \partial D_n$ converges to $\partial\mathbb{D}$, we see the domains $D_{n,m}^* \setminus G_{n,m}$ will expand to fill out $\mathbb{D}^*$ if the spherical diameter of $G_{n,m}$ shrinks to 0.

Lemma 5.7. *For each n, the spherical radii $r_{n,m}$ and $\tilde{r}_{n,m}$ of the circle C_{w_∞} in $P_{n,m}$ and $\widetilde{P}_{n,m}$, respectively, decrease to 0 as $m \to \infty$. Consequently, the spherical diameter of $G_{n,m} \to 0$, $D_{n,m} \cup D_{n,m}^* \to \mathbb{C}$ and $\Omega_{n,m} \cup \Omega_{n,m}^* \to \mathbb{C}$ as $m \to \infty$.*

Proof. First fix n and observe that C_{w_∞} is separated from 0 and 1 in both $P_{n,m}$ and $\widetilde{P}_{n,m}$ by $m-1$ chains consisting of n circles each. Thus by the Spherical Length Area Lemma,

$$\begin{aligned}\tilde{r}_{n,m}, r_{n,m} &\leq \frac{2\pi}{\sqrt{\sum_{i=1}^{m-1} \frac{1}{n}}} \\ &\leq \frac{2\pi}{\sqrt{n}(m-1)}.\end{aligned}$$

Hence for each fixed n, we see $\tilde{r}_{n,m}, r_{n,m} \to 0$ as $m \to \infty$.

Now each neighboring vertex of w_∞ has degree 5. By the Spherical Ring Lemma, as $m \to \infty$ the radius of each neighboring circle must decrease to 0 as well. Thus the stereographic projections of the portion of $P_{n,m}$ and $\widetilde{P}_n$ corresponding to $\mathcal{T}_{n,m}^* \setminus w_\infty$ fill $\mathbb{C}$ as $m \to \infty$. However, in forming $D_{n,m}^*$ and $\Omega_{n,m}^*$, we scaled these stereographic projections by $\epsilon_{n,m}$ and $\widetilde{\epsilon}_{n,m}$, respectively. Thus we must show these scaling factors remain bounded as $m \to \infty$.

Recall $\epsilon_{n,m}$ and $\widetilde{\epsilon}_{n,m}$ were the distance between the spherical and euclidean centers of C_{v_1} in P_n and $\widetilde{P}_n$, respectively. But the proof of Lemma 5.6 provides a bound on the spherical radius of C_{v_1} which does not depend on m, so long as $m \geq \frac{n}{2}$. Thus the spherical radius of C_{v_1} in both $P_{n,m}$ and $\widetilde{P}_{n,m}$ remains bounded as $m \to \infty$. Since C_{v_1} is centered at the point 1 in $P_{n,m}$ and $\widetilde{P}_{n,m}$, its stereographic projection to $\mathbb{C}$ must be uniformly bounded away from ∞ for all m. Thus the spherical and euclidean radii of C_{v_1} in each packing are uniformly comparable. Hence $\epsilon_{n,m}$ and $\widetilde{\epsilon}_{n,m}$ remain uniformly bounded as $m \to \infty$. Consequently our scaling cannot prevent the spherical diameter of $G_{n,m}$ from decreasing to 0. Hence $D_{n,m} \cup D^*_{n,m} \to \mathbb{C}$ and $\Omega_{n,m} \cup \Omega^*_{n,m} \to \mathbb{C}$ as $m \to \infty$.

$\square$

Thus for each n, we choose $m > n$ large enough so that

1. The map $f_{n,m}$ is K_1-quasiconformal on $F_{n,m}$ (and hence on all of $D_{n,m}$).
2. The spherical radius of the complement of $D_{n,m} \cup D_{n,m}$ is less than $\frac{1}{n}$.
3. The spherical radius of the complement of $\Omega_{n,m} \cup \Omega^*_{n,m}$ is less than $\frac{1}{n}$.

With this choice of m, we define $D_n = D_{n,m}$, $D^*_n = D^*_{n,m}$, $F_n = F_{n,m}$, $\widetilde{G}_n = \widetilde{G}_{n,m}$, $f_n = f_{n,m}$, $g_n = g_{n,m}$, and $g_n = g_{n,m}$. Thus at last we have sequences $\{f_n\}$ and $\{g_n\}$ of K_1-quasiconformal discrete welding maps, which are eventually defined on any compact subset of $\mathbb{D}$ and $\mathbb{D}^*$, respectively.

5.5 Extension of the Discrete Maps

Note that Ω_n and Ω_n^* are complementary regions of a polygonal discrete welding curve

$$\Gamma_n = f_n(\partial D_n) = g_n(\partial D_n^*) = \partial\Omega_n = \partial\Omega_n^*.$$

If Γ_n is to approximate a quasicircle Γ, then one would hope it would be a quasicircle as well. In this case, we could use reflection in Γ_n to extend f_n and g_n across Γ_n.

Lemma 5.8. *For each n, the discrete quasisymmetry φ_n induces a k^2b^4-quasisymmetric homeomorphism $\widehat{\varphi}_n = p_n \circ \varphi_n \circ p_n^{-1}$ of $\partial\mathbb{D}$.*

Proof. By Proposition 4.2, each φ_n is k-bilipschitz. Because each p_n is b-bilipschitz, then each $\widehat{\varphi}_n$ must be kb^2-bilipschitz and consequently k^2b^4-quasisymmetric by Example 2.1.

□

Theorem 5.9. *For each $n = 1, 2, \ldots$, the curve Γ_n is a K_3-quasicircle, where K_3 depends only on k; in particular, K_3 is independent of n.*

Proof. By Lemma 5.8, each $\widehat{\varphi}_n$ is k^2b^4- quasisymmetric, and hence $\widehat{\varphi}_n^{-1}$ is also k^2b^4-quasisymmetric. Thus by the Douady-Earle Extension Theorem, $\widehat{\varphi}_n^{-1}$ has a $K_2 = K_2(k)$-quasiconformal extension Φ_n to $\mathbb{D}$. Observe that $p_n^{-1} \circ \Phi \circ p_n$ has the effect of quasi-conformally re-arranging the embeddings of vertices in ∂D_n so that they match up with the embeddings of vertices in

∂D_n^*. That is, for all vertices $v_i \in \partial D_n$,

$$p_n^{-1} \circ \Phi \circ p_n(v_i) = p_n^{-1} \circ \Phi^{-1}(v_i) = w_j,$$

for some boundary vertex w_j of D_n^*.

Now define

$$B_n(x) = \begin{cases} f_n \circ p_n^{-1} \circ \Phi_n^{-1}(x) & \text{if } x \in \overline{\mathbb{D}}; \\ g_n(x) \circ p_n^{-1}, & \text{if } x \in \mathbb{D}^*. \end{cases} \tag{5.5}$$

If $x \in \partial\mathbb{D}$, then by Proposition 5.3

$$\begin{aligned} B_n(x) &= f_n \circ p_n^{-1} \circ \Phi_n^{-1}(x) \\ &= f_n \circ p_n^{-1} \circ \widehat{\varphi}_n(x) \\ &= f_n \circ p_n^{-1} \circ p_n \circ \varphi_n \circ p_n^{-1}(x) \\ &= f_n \circ \varphi_n \circ p_n^{-1}(x) \\ &= g_n \circ p_n^{-1}(x) \end{aligned} \tag{5.6}$$

Thus B_n is continuous. Off $\partial\mathbb{D}$, B_n is $K_3 = K_1K_2$-quasiconformal. But $\partial\mathbb{D}$ has measure 0, so by Remark 2.1, B_n is K_3-quasiconformal on all of $\mathbb{C}$.

But finally, we note $B_n(\partial\mathbb{D}) = g_n(\partial\mathbb{D}) = \Gamma_n$. Hence Γ_n is a K_3-quasicircle.

□

Since $\partial D_n = \partial D_n^*$ is a b-quasicircle for each n, then by Lemma 2.16 we can extend each f_n be a $K = K_2 K_3^2 b^2$-quasiconformal map of the entire plane by first reflecting $\mathbb{C} \setminus D_n$ in ∂D_n, then applying f_n, and finally reflecting in Γ_n. Note that each f_n now fixes the points $0, 1$, and ∞.

Similarly, we extend each g_n by reflecting $D_n^* \setminus G_n$ in ∂D_n, applying g_n, and then reflecting in Γ_n. Of course, g_n was originally defined only on $D_n^* \setminus G_n$, not on all of D_n^*. Thus our extended g_n is defined only on an annular region about 0, not on all of $\mathbb{C}$. Fortunately, however, by Lemma 5.7, the domain of g_n does expand to fill $\mathbb{C} \setminus \{0\}$ as $n \to \infty$.

5.6 Convergence of the Discrete Maps

Now since each f_n fixes $0, 1$, and ∞, by Theorem 2.9, the family $\{f_n\}$ is normal and has a subsequence converging uniformly on compact subsets of $\mathbb{C}$ to a K-quasiconformal homeomorphism f. We will re-number as necessary and assume the sequence $\{f_n\}$ itself converges. Note that if we show f and g are indeed the unique conformal welding maps corresponding to φ, then any convergent subsequence of $\{f_n\}$ will have the same limit. Since any subsequence of our original sequence is again normal and thus has a further convergent subsequence, clearly the full original sequence will then have been shown to converge.

Similarly, each map g_n fixes 1 and omits 0 and ∞; thus Theorem 2.9 implies the existence of a subsequence converging uniformly on compact subsets of $\mathbb{C} \setminus \{0\}$ to a map g. Again we will re-number and assume the sequence

$\{g_n\}$ itself converges.

Unfortunately, in this case Theorem 2.9 does not ensure that g is non-constant. However, if g were constant, then it would be identically equal to 1 since $\{g_n\}$ fixes 1. But for each n, the curve $g_n(\{|z| = \frac{1}{2}\})$ must completely surround 0. Thus some point $g_n(z_n)$ of $g_n(\{|z| = \frac{1}{2}\})$ must be at a distance of more than one from the point 1. But $\{|z| = \frac{1}{2}\}$ is compact, so some subsequence of $\{z_n\}$ must converge to some point $z \in \{|z| = \frac{1}{2}\}$. Since $\{g_n\}$ converges uniformly on $\{|z| = \frac{1}{2}\}$, the sequence $\{g_n(z_n)\}$ must converge to $g(z)$. But $|g_n(z_n)-1| > 1$ for all n; hence $|g(z)-1| \geq 1$. Thus no subsequence of $\{g_n\}$ can converge to a constant map, and g must be a K-quasiconformal homeomorphism of $\mathbb{C} \setminus \{0\}$.

Note that by Remark 2.1, 0 and ∞ are removable singularities for g. Thus we may take g to be a K-quasiconformal self-map of S^2. Similarly, we may assume f to be defined on all of S^2.

Remark 5.1. It is here we see one of the reasons it was necessary to extend each f_n and g_n. Originally, they fixed the point 1 on the *boundary* of their domains. But then

$$\begin{aligned} 1 \notin & \bigcup_j \operatorname{int}\left(\bigcap_{n>j} \operatorname{range}(f_n)\right) \\ &= \operatorname{range}(f). \end{aligned} \tag{5.7}$$

Thus we could not conclude range(f) contains more than one point.

The sequence

$$F_n(z) = \begin{cases} \frac{z}{\left(1+\frac{\arg z}{2\pi}\right)^n} & \text{if } -\pi \leq \arg z \leq 0; \\ \frac{z}{\left(1-\frac{\arg z}{2\pi}\right)^n} & \text{if } 0 < \arg z < \pi, \end{cases}$$

where $\arg z \in [-\pi, \pi)$, is an example of a family defined on $\mathbb{D}$, fixing zero in the interior of its domain and 1 on the boundary of its domain, yet $\lim_{n\to\infty} F_n$ is not a homeomorphism .

5.7 Conformality of the Limit Maps

The results of this section should come as no surprise to those familiar with the use of discrete analytic functions to approximate classical analytic functions [15, 17, 23, 25, 47, 50, 52].

Lemma 5.10. *As $n \to \infty$, the mesh of the embedding of $\mathcal{T}_n$ in D_n and of $\mathcal{T}_n^* \setminus w_\infty$ in D_n^* decreases to zero. In particular, any compact subset of $\mathbb{D}$ or of $\mathbb{D}^*$ can be separated from $\partial\mathbb{D}$ by arbitrarily many generations of degree six circles by taking n large.*

Proof. The proof follows from the Rodin-Sullivan Length-Area Lemma in exactly the same way Lemma 5.7 followed from the Spherical Length-Area Lemma. □

Our next lemma now follows easily from the results cited in Chapter 3.

Lemma 5.11. *The maps f and g are conformal on $\mathbb{D}$ and $\mathbb{D}^*$, respectively.*

Proof. Choose compact set $E \subset \mathbb{D}\backslash\{0\}$, and fix $\epsilon > 0$. By Lemma 5.10, as $n \to \infty$, the number of generations of degree six circles in P_n separating E from $\partial\mathbb{D}$ can be made arbitrarily large. Similarly, the number of generations of degree six circles separating E from 0 can be made arbitrarily large. Thus by the Hex Packing Lemma, the maximum dilatation of f_n on E decreases to one as $n \to \infty$.

Thus we may choose N so large that for $n \geq N$, f_n is $(1+\epsilon)$-quasiconformal on E. Hence the limit f of $\{f_n\}_{n\geq N}$ must be $(1+\epsilon)$-quasiconformal on E. But ϵ and E were arbitrary; consequently, f is conformal on $\mathbb{D}\backslash\{0\}$. Since $\{0\}$ has measure zero, clearly f must be conformal on all of $\mathbb{D}$ by Remark 2.1.

A similar proof holds for g. □

5.8 Welding Property of the Limit Maps

At last we connect all the dots to prove Theorem 5.1.

Proof of Theorem 5.1. By Lemma 5.11, $f_n \to f$, $g_n \to g$, where f and g are conformal on $\mathbb{D}$ and $\mathbb{D}^*$, respectively. But f and g are K-quasiconformal on all of $\mathbb{C}$, so $f(\partial\mathbb{D}) = g(\partial\mathbb{D})$ is indeed a quasicircle.

Now the discrete quasisymmetries φ_n had different domains for each n; however, the maps $\varphi_n \circ p_n^{-1}$ are all defined on $\partial\mathbb{D}$. Moreover, it is clear

$\{\varphi_n \circ p_n^{-1}\}$ converges uniformly to φ as $n \to \infty$. Similarly, the domain of $f_n^{-1} \circ g_n$ varies with each n. However, $f_n^{-1} \circ g_n \circ p_n^{-1}$ is defined on $\partial\mathbb{D}$ for all n, and clearly $f_n^{-1} \circ g_n \circ p_n^{-1} \to f^{-1} \circ g$ uniformly as $n \to \infty$.

Thus by Proposition 5.3,

$$\begin{aligned} f^{-1} \circ g &= \lim_{n\to\infty} f_n^{-1} \circ g_n \circ p_n^{-1} \\ &= \lim_{n\to\infty} \varphi_n \circ p_n^{-1} \\ &= \varphi \end{aligned} \tag{5.8}$$

on $\partial\mathbb{D}$. Since the maps promised by the Conformal Welding Theorem are unique, they must be exactly our maps f and g. Note then that as described in Section 5.6, the entire original sequences we constructed converge, not just subsequences.

The fact that $\Gamma_n \to \Gamma$ in Hausdorff metric follows directly from the uniform convergence of f_n and g_n on $\partial\mathbb{D}$. $\square$

5.9 Quasisymmetric Identification Maps

Recall that Theorem 5.1 is stated only for bilipschitz quasisymmetries. Fortunately, the following result of Kelingos [29, 34] shows that the bilipschitz quasisymmetries are dense in the set of all quasisymmetries.

Lemma 5.12. *A k-quasisymmetry $\varphi : \partial\mathbb{D} \to \partial\mathbb{D}$ can be uniformly approximated by a k-quasisymmetry $\tilde{\varphi}$ which has an analytic extension to a neigh-*

borhood of $\partial\mathbb{D}$. In fact, $\tilde{\varphi}$ is bilipschitz with constant k; that is

$$\frac{1}{k}|x-y|_{\mathbb{D}} \leq |\tilde{\varphi}(x)-\tilde{\varphi}(y)|_{\mathbb{D}} \leq k|x-y|_{\mathbb{D}}. \tag{5.9}$$

Moreover, the conformal welding maps induced by $\tilde{\varphi}$ approximate uniformly on compact subsets the welding maps induced by φ.

Corollary 5.13 now follows immediately via a standard diagonalization argument.

Corollary 5.13. *Given a quasisymmetric map φ on $\partial\mathbb{D}$, the construction employed above yields sequences $\{f_n\}$ and $\{g_n\}$ of discrete welding maps converging locally uniformly on $\mathbb{D}$ and $\mathbb{D}^*$, respectively, to the conformal welding maps induced by φ. The extension properties of the limit maps and the Hausdorf convergence of Γ_n to Γ hold as well.*

Chapter 6

Welding of Half-Planes

Next we will develop a system for approximating the welding of half-planes. Throughout this chapter we will take φ to be a real k-bilipschitz quasisymmetry fixing 0 and 1. We will use large "square" pieces of the regular hexagonal grid H_n of Example 3.1 to exhaust $\mathbb{U}$ and $\mathbb{L}$, the upper and lower half-planes, respectively. If these pieces are combinatorially welded together, the resulting circle packing will induce maps converging to the conformal welding maps.

Theorem 6.1. *Given a bilipschitz quasisymmetry φ, there exist sequences of discrete analytic functions $\{f_n\}$ and $\{g_n\}$ converging uniformly on compact subsets of $\mathbb{L}$ and $\mathbb{U}$, respectively, to the conformal welding maps f and g induced by φ. Moreover, the discrete conformal welding curve Γ_n formed by the common boundary of the images of f_n and g_n is a quasicircle converging uniformly in the Hausdorff metric to the quasicircle Γ induced by φ.*

6.1 Prototype Triangulations

For each n, let a and b be the smallest multiples of $\frac{1}{n}$ such that

$$a \leq \varphi(-n) \tag{6.1}$$
$$b \geq \varphi(n).$$

Let T_{L_n} and T_{U_n} denote the sub-complexes of $\operatorname{carr} H_n$ contained in the squares $[a, b] \times [0, b-a]$ and $[-n, n] \times [-2n, 0]$, respectively. We will label the vertices of T_{L_n} lying at 0 and 1 as v_0 and v_1.

6.2 Construction of Discrete Welding Maps

The combinatorial welding developed in Chapter 4 can easily be adapted to weld T_{L_n} to T_{U_n}. Condition (6.1) ensures that the image under φ of every vertex of $T_{U_n} \cap \mathbb{R}$ lies on an edge of $T_{L_n} \cap \mathbb{R}$. As before, form an augmented complex $\mathcal{T}_{L_n}$ by adding vertices to T_{L_n} as described in Section 4.2. Conversely, the image under φ^{-1} of each vertex of $T_{L_n} \cap (a, b)$ lies on an edge of $T_{U_n} \cap \mathbb{R}$. Again we add vertices to T_{U_n} to form an augmented complex $\mathcal{T}_{U_n}$.

Note that in most cases, we will not be so fortunate as to have $a = \varphi(-n)$ and $b = \varphi(n)$. That is, we would often expect $\varphi([-n, n]) \subset (a, b)$, and hence $\varphi^{-1}(a), \varphi^{-1}(b) \notin [-n, n]$. If however, we delete any such offending vertices at a or b, we can ensure the vertices of $\mathcal{T}_{L_n} \cap \mathbb{R}$ are in one-to-one correspondence with the vertices of $\mathcal{T}_{U_n} \cap \mathbb{R}$. That is, we can form a discrete quasisymmetry $\varphi_n : \mathcal{T}_{U_n} \cap \mathbb{R} \to \mathcal{T}_{L_n} \cap \mathbb{R}$ by mapping vertices to vertices and extending linearly on the edges. Identifying vertices corresponding under φ_n then yields a welded complex $\mathcal{K}_n$ which triangulates a closed disc. We note that Lemma 4.3 and Proposition 4.4 also hold.

Now Corollary 3.2 gives the existence of a circle packing for $\mathcal{K}_n$ in $\mathbb{C}$ which we normalize so that C_{v_0} and C_{v_1} are centered at 0 and 1, respectively. We will denote the carrier of the portions of this packing corresponding to L_n and U_n by Ω_n and Ω_n^*, respectively.

Since φ is an orientation-preserving real homeomorphism, it must be increasing. Thus $a, b \to \infty$ as $n \to \infty$. In particular, this means $L_n \cup U_n$ expands to fill the entire plane as $n \to \infty$. Hence on each compact subset of the upper of lower half-plane, the discrete analytic functions

$$\begin{aligned} f_n &: L_n \to \Omega_n \\ g_n &: U_n \to \Omega_n^* \end{aligned} \tag{6.2}$$

induced by the circle packings constructed above and in Section 6.1 are defined for sufficiently large n. By Lemma 4.3 our assumption that φ is bilipschitz implies the degree of $\mathcal{K}_n$ is bounded uniformly in n. Hence by Corollary 3.12, each of the maps f_n and g_n are K_1-quasiconformal, where K_1 is independent of n.

Furthermore, the proof used for Proposition 5.3 can be repeated here to show

$$g_n = f_n \circ \varphi_n$$

on $[-n, n]$.

6.3 Extension of the Discrete Maps

The critical step in our construction is the extension of the maps f_n and g_n across $\mathbb{R}$. If $\{f_n\}$ and $\{g_n\}$ can then be shown to be normal, a subsequence will converge uniformly on compact subsets of $\mathbb{R}$. This uniform convergence will allow us to prove that our limit maps are indeed the welding maps we seek.

Lemma 6.2. *Each of the maps f_n and g_n can be extended across $\mathbb{R}$ to a K-quasiconformal map defined on a portion of $\mathbb{L}$ and $\mathbb{U}$, respectively. Moreover, given any compact subset E of $\mathbb{C}$, then for sufficiently large n, both f_n and g_n will be defined on E.*

Proof. Note that Lemma 4.2 implies that each discrete quasisymmetry φ_n is k-quasisymmetric on $[-n, n]$. We now appeal to Lemma 2.10 to extend φ_n to a k'-quasisymmetry on all of $\mathbb{R}$.

Hence by the Beurling-Ahlfors Extension Theorem, each extended φ has a $K_2 = K_2(k)$-quasiconformal extension Φ_n to the upper half-plane $\mathbb{U}$. We now extend f_n by setting

$$f_n = g_n \circ \Phi_n^{-1}$$

on $\Phi_n(U_n)$. Note that this is indeed a $K = K_1 K_2$-quasiconformal extension of f_n as

$$\begin{aligned} f_n &= g_n \circ \varphi_n^{-1} \\ &= g_n \circ \Phi_n^{-1} \end{aligned} \tag{6.3}$$

on $[a, b]$.

Now it is clear from our construction that L_n expands to fill $\mathbb{L}$ as $n \to \infty$; hence given any compact subset E of $\mathbb{C}$, L_n will cover $E \cap \overline{\mathbb{L}}$ for large n. To ensure that f_n is eventually defined on $E \cap \overline{\mathbb{U}}$ we must show $\Phi_n(U_n)$ covers $E \cap \overline{\mathbb{U}}$ for large n.

First note that by Proposition 2.13, $\Phi_n \to \Phi$ locally uniformly as $n \to \infty$, where Φ is the Beurling-Ahlfors extension of φ. Now for each $i = 1, 2, \ldots$, $\Phi(U_i)$ must contain a relatively open neighborhood $B(0, R_i) \cap \overline{\mathbb{U}}$ of 0. We can assume R_i is the largest possible radius of such a neighborhood. Then since Φ is a proper map, we must have $R_i \to \infty$ as $i \to \infty$.

Next recall that for each fixed i, $\Phi_n \to \Phi$ uniformly on U_i as $n \to \infty$, since each U_i is compact. Thus for each i, we can find N_i so that

$$\mathrm{dist}(\Phi(\partial U_n \setminus (-n,n)),0) > \frac{R_i}{2}$$

for all $n \geq N_i$. In particular,

$$B\left(0,\frac{R_i}{2}\right) \subset \Phi_n(U_n)$$

for $n \geq N_i$.

But $E \cap \overline{\mathbb{U}}$ must be contained in $B\left(0, \frac{R_i}{2}\right)$ for some sufficiently large i. Hence for $n \geq N_i$ $E \subset \Phi_n(U_n)$, and f_n is defined on E.

Similarly, we can extend g_n by defining

$$g_n = f_n \circ \imath \circ \Phi_n \circ \imath$$

on $\imath \circ \Phi_n^{-1} \circ \imath(L_n)$, where $\imath$ is the reflection in $\mathbb{R}$. Since Φ_n^{-1} must converge to Φ^{-1} locally uniformly and $\imath(L_n)$ expand to fill $\mathbb{U}$ as $n \to \infty$, the argument used above also shows that on any compact set of $\mathbb{C}$, g_n will be defined for sufficiently large n.

□

6.4 Convergence of the Discrete Maps

Since each f_n fixes both 1 and 0 and omits ∞, by Theorem 2.9 $\{f_n\}$ is normal and has a subsequence converging locally uniformly to a K-quasiconformal homeomorphism f defined on all of $\mathbb{C}$. By re-numbering, we will assume the entire sequence $\{f_n\}$ converges to f. Since the domain of f is the entire plane, then by Liouville's Theorem, the range of f must be the entire plane. In fact, we see the singularity at ∞ can be removed by setting $f(\infty) = \infty$. Indeed, $f(\mathbb{R} \cup \{\infty\})$ is a Jordan curve on S^2 passing through $0, 1$, and ∞.

In the same way, a subsequence of $\{g_n\}$ converges to a K-quasiconformal homeomorphism g of $\mathbb{C}$ onto itself. Again we re-number as necessary and will assume the entire sequence $\{g_n\}$ converges.

6.5 Conformality of the Limit Maps

By construction, the number of generations of vertices separating any given compact set in $\mathbb{L}$ from $\mathbb{R}$ goes to infinity as $n \to \infty$. Thus just as in the proof of Lemma 5.11, the Hex Packing Lemma implies the maximum dilatation of f_n on every compact subset of $\mathbb{L}$ decreases to one as $n \to \infty$. Hence f must be conformal on $\mathbb{L}$. In the same way, g is, of course, also conformal on $\mathbb{U}$.

6.6 Welding Property of the Limit Maps

Finally, we have constructed all the necessary machinery to prove our theorem.

Proof of Theorem 6.1. With the preliminary lemmas behind us, the proof of this theorem now proceeds in exactly the same manner as the proof of Theorem 5.1. First recall $f_n \to f$, $g_n \to g$, where f and g are conformal on

$\mathbb{L}$ and $\mathbb{U}$, respectively. Since f and g are K-quasiconformal on all of $\mathbb{C}$, then $f(\mathbb{R} \cup \{\infty\}) = g(\mathbb{R} \cup \{\infty\})$ is indeed a quasicircle.

Moreover, since

$$f_n = g_n \circ \varphi_n$$

for each n, and f_n, g_n, and φ_n converges locally uniformly on $\mathbb{R}$ to f, g, and φ, respectively, we have

$$f = g \circ \varphi.$$

Thus by the uniqueness part of the Conformal Welding Theorem, $f|\mathbb{L}$ and $g|\mathbb{U}$ must be the welding maps corresponding to φ. Note that as described in Section 5.6, the entire original sequences we constructed converge, not just subsequences.

Furthermore, note that by our construction $f|\mathbb{U}$ and $g|\mathbb{L}$ are extensions across Γ of the welding maps f and g, respectively. Again the convergence of $\Gamma_n \to \Gamma$ in Hausdorff metric follows directly from the uniform convergence of f_n and g_n on $\mathbb{R}$.

□

6.7 Quasisymmetric Identification Maps

If φ is not necessarily bilipschitz, but still quasisymmetric, then for each $m = 1, 2, \ldots$, we can uniformly approximate φ on compact subintervals by a

k_m-bilipschitz map φ_m. If each φ_m is extended to $\mathbb{R}$ by Lemma 2.11 then the welding maps induced by φ_m converge to the welding maps induced by φ as $m \to \infty$. Thus by a standard diagonalization argument, the techniques used above will produce discrete analytic approximations to the welding maps induced by φ. Thus as in Chapter 5, we have the following corollary.

Corollary 6.3. *Given a quasisymmetric map φ on $\mathbb{R}$, the construction employed above yields sequences of discrete welding maps $\{f_n\}$ and $\{g_n\}$ converging locally uniformly on $\mathbb{L}$ and $\mathbb{U}$, respectively, to the conformal welding maps induced by φ. The extension properties of the limit maps and the Hausdorff convergence of Γ_n to Γ hold as well.*

6.8 Locally Quasisymmetric Maps

As mentioned in Remark 2.2, quasisymmetry is a global property, and the conclusion of the the Conformal Welding Theorem is correspondingly global. That is, when φ is a quasisymmetry, Γ is the image of a circle under a quasiconformal map of the entire plane, or, equivalently, there is a quasiconformal reflection fixing Γ and interchanging the components Ω and Ω^* of $S^2 \setminus \Gamma$. If φ is only locally quasisymmetric, then an essentially unique conformal welding still exists, but the curve Γ no longer admits a global quasiconformal reflection. Instead, Γ admits only local reflections.

Theorem 6.4. *If φ is a locally quasisymmetric real homeomorphism, then there exist conformal maps f and g of $\mathbb{L}$ and $\mathbb{U}$, respectively, such that their* *boundary values satisfy*

$$g = f \circ \varphi.$$

Each point of $\Gamma = f(\mathbb{R}) = g(\mathbb{R})$ *has a neighborhood* $\mathcal{V}$ *and a orientation reversing quasiconformal map* $\imath_x$ *fixing* $\Gamma \cap \mathcal{V}$ *and interchanging* $\mathcal{V} \cap \Omega$ *and* $\mathcal{V} \cap \Omega^*$. *Moreover, the maps* f *and* g *are unique up to composition with a Möbius transformation.*

This follows from Kôtaro Oikawa's observation that local quasisymmetries have quasiconformal extensions [38].

Lemma 6.5. *If* φ *is a* k*-quasisymmetric homeomorphism of* $[-1, 1]$ *fixing* -1 *and* 1, *then there exists a* $K = K(k)$*-quasiconformal extension of* φ *to the triangle* $\{z \| \mathrm{Re}\ z| + \mathrm{Im}\ z \geq -1, \mathrm{Im}\ z \leq 0\}$.

6.9 Discrete Local Approximation

One might notice that our discrete welding maps have all been constructed by *locally* altering the combinatorics of our prototype complexes. It has been the geometry imposed by our circle packings that produced global maps from these local changes. Thus one might wonder if our approximation scheme might work using a *locally bilipschitz* map φ. Indeed this is the case.

Theorem 6.6. *If* φ *is locally bilipschitz on* $\mathbb{R}$, *and the maps* f_n *and* g_n *are formed as in Theorem 6.1, then* $f_n \to f$ *and* $g_n \to g$ *uniformly on compact* *subsets of* $\mathbb{L}$ *and* $\mathbb{U}$*, respectively, where* f *and* g *are the the conformal welding maps induced by* φ*.*

Proof. First we note that for each $x \in \mathbb{R}$, there is a $t > 0$ so that φ is k_x-bilipschitz on $[x-t, x+t]$. Thus if n is large enough so that $[x-t, x+t] \subset \partial U_n$ and $\varphi([x-t, x+t]) \subset \partial L_n$, the proof of Lemma 4.3 can be used locally to show that there is a uniform bound on the degrees of the vertices of $\mathcal{T}_{U_n}$ and lying on $[x-t, x+t]$ or sharing an edge with a vertex lying on $[x-t, x+t]$. Of course, the same holds for vertices of $\mathcal{T}_{L_n}$ lying on $\varphi([x-t, x+t])$ or sharing an edge with such a vertex. Consequently, if $\mathcal{T}_{L_n}$ and $\mathcal{T}_{U_n}$ are welded together producing discrete analytic maps f_n and g_n as in Section 6.2, then by Corollary 3.12, there is a uniform bound K_{1_x} on the dilatation of f_n and g_n on interior faces and on faces which contain boundary vertices lying on $\varphi([x-t, x+t])$ and $[x-t, x+t]$, respectively.

As before, our next hurdle is to show that each g_n can be extended across $[x-t, x+t]$. Recall that in combinatorially welding T_{U_n} and T_{L_n} we also form discrete quasisymmetries φ_n. Note that the proof of Proposition 4.2 can be applied to each φ_n to see that φ_n is k_x-bilipschitz on $[x-t, x+t]$. In particular, each φ_n is k_x-quasisymmetric on $[x-t, x+t]$.

Now define linear maps

$$\begin{aligned} A_{x,n}(z) &= \frac{z-x}{t} \\ B_{x,n}(z) &= \frac{z-\varphi_n^{-1}(x)}{\varphi_n^{-1}(x-t)-\varphi_n^{-1}(x+t)}, \end{aligned} \tag{6.4}$$

and note that $A_{x,n}$ and $B_{x,n}$ map the domain and range, respectively, of $\varphi_n|[x-t,x+t]$ onto $[-1,1]$. Since pre- and post-composition of a quasisymmetry with affine maps does not change the quasisymmetry constant, we see the map

$$\widehat{\varphi}_{x,n}(y) = B_{x,n} \circ \varphi_n \circ A_{x,n}^{-1}(y) \tag{6.5}$$

is k_x-quasisymmetric on $[-1,1]$ and fixes -1 and 1. Thus $\widehat{\varphi}_{x,n}$ has a $K_{2_x} = K_{2_x}(k_x)$-quasiconformal extension to the triangle

$$\Delta = \{z||\text{Re } z| + \text{Im } z \geq -1, \text{Im } z \leq 0\}$$

with base $[-1,1]$ and apex $(0,-1)$.

Now consider the triangle

$$\Delta_x = \{z||\text{Re } z - x| + \text{Im } z \geq -t, \text{Im } z \leq 0\}$$

with base $[x-t, x+t]$ and apex $(x,-t)$. Note that Δ_x does not depend on n. We will extend each g_n $K_{1,x}K_{2,x}$-quasiconformally to Δ_x by

$$g_n(z) = f_n \circ B_{x,n}^{-1} \circ \Phi_{x,n} \circ A_{x,n}(z)$$

on Δ_x. Note that by (6.5) and the proof of Proposition 5.3, for $w \in [x-t, x+t]$

$$\begin{aligned} f_n \circ B_{x,n}^{-1} \circ \Phi_{x,n} \circ A_{x,n}(w) &= f_n \circ B_{x,n}^{-1} \circ \widehat{\varphi}_{x,n} \circ A_{x,n}(w) \qquad (6.6) \\ &= f_n \circ B_{x,n}^{-1} \circ B_{x,n} \circ \varphi_n \circ A_{x,n}^{-1} \circ A_{x,n}(z) \\ &= f_n \circ \varphi_n(w) \\ &= g_n \circ (w). \end{aligned}$$

Thus we have truly defined an extension of g_n to Δ_x.

In the same fashion, we can apply the above construction to φ_n^{-1} on $\varphi([x-t, x+t]) \subset L_n$ to $K_{3,x}K_{4,x}$-quasiconformally extend each f_n to some triangle Δ_x^* with base $\varphi([x-t, x+t])$ and apex in $\mathbb{U}$.

Now each map f_n and g_n is quasiconformal in fixed neighborhoods of 0 and 1; thus by Theorem 2.9, $\{f_n\}$ and $\{g_n\}$ have subsequences converging locally uniformly to some quasiconformal homeomorphisms f and g, on $\mathbb{L}$ and $\mathbb{U}$, respectively. As in Section 6.5, the Hex Packing Lemma implies f and g are conformal on $\mathbb{L}$ and $\mathbb{U}$, respectively.

Moreover, because we can extend each f_n and g_n locally, for each $x \in \mathbb{R}$, the sequences $\{g_n\}$ and $\{f_n\}$ are K_x-quasiconformal and $K_{\varphi(x)}$-quasiconformal on $\mathbb{U} \cup \Delta_0 \cup \Delta_1 \cup \Delta_x$ and $\mathbb{L} \cup \Delta_0^* \cup \Delta_1^* \cup \Delta_{\varphi(x)}^*$, respectively. Thus a subsequence of $\{g_n\}$ and $\{f_n\}$ converges uniformly on any compact subset of $\mathbb{U} \cup \Delta_0 \cup \Delta_1 \cup \Delta_x$ and $\mathbb{L} \cup \Delta_0^* \cup \Delta_1^* \cup \Delta_{\varphi(x)}^*$, respectively. Since $g_n = f_n \circ \varphi_n$ on $\Delta_x \cap \mathbb{R}$, we must have $g(x) = f \circ \varphi(x)$.

Again by Liouville's Theorem, we must have $f(\infty) = g(\infty)$. As quasiconformal homeomorphisms must map Jordan domains to Jordan domains, we see $\Gamma = f(\mathbb{R}) = g(\mathbb{R})$ must be a Jordan curve. Hence by the uniqueness part of Theorem 6.4, as before, the entire sequences $\{f_n\}$ and $\{g_n\}$ must converge, not just subsequences. $\square$

Chapter 7

Approximation of Quasisymmetries

Throughout this chapter let Γ be a K-quasicircle passing through 1 and separating 0 from ∞. We will refer to the bounded and unbounded components of the complement of Γ in $\mathbb{C}$ as Ω and Ω^*, respectively. We will assume Γ to be positively oriented with respect to Ω.

We now consider the converse problem to Theorem 5.1; that is, we will construct a sequence $\{\varphi_n\}$ converging uniformly to the quasisymmetry φ induced by Γ.

Theorem 7.1. *Given a K-quasicircle Γ as above, there exists a sequence $\{\varphi_n\}$ constructed using the boundary values of discrete analytic functions and converging uniformly to the quasisymmetry φ induced Γ and normalized as in Theorem 2.18.*

The Rodin-Sullivan Theorem [47] itself will supply discrete analytic approximations to the conformal welding maps f and g. The goal of our proof will be to show uniform convergence of these maps not only on compact subsets of $\mathbb{D}$ or $\mathbb{D}^*$, but on $\partial\mathbb{D}$ as well. Then the boundary values of the discrete analytic maps can be used to approximate φ.

7.1 Construction of Range Packings

As in Example 3.1, let H_n be the regular euclidean hexagonal packing consisting of infinitely many generations of degree six circles, each circle having radius $\frac{1}{2n}$, about some circle C_{v_0}. We will assume C_{v_0} is centered at the origin and one of its neighbors is centered on the positive real axis. Note that the carrier of H_n gives a tiling of the plane by equilateral triangles of side length $\frac{1}{n}$.

Now consider the sub-complex formed by deleting from the carrier of H_n all triangles which hit Γ or Ω^*. Unfortunately, this triangulation might not yet be suitable for our purposes. In particular, doubling it across its boundary might not yield a sphere which is *triangulated.* Any boundary vertex without an interior neighbor will have degree 2 in the combinatorial double, and hence cannot be part of a triangulation. Thus to remedy this situation, we further delete any face which does not contain an interior vertex. Note that if u is an interior vertex, then no faces containing u are deleted, so u remains an interior vertex. Thus no new boundary vertices are formed by this trimming.

In general, this complex may have many components, but we will consider

Figure 7.1: A Cow-Shaped Quasicircle.
A cow-shaped quasicircle Γ and a portion of a packing H_n before and after trimming.

only the component T_n containing v_0. See Figure 7.1. Note that every boundary vertex of T_n now has degree at least 3; thus doubling T_n across its boundary will yield a triangulation of a sphere.

Let Ω_n be the portion of carr H_n corresponding to T_n. As before, we will not be overly concerned with the distinction between T_n and the embedding for it provided by Ω_n. In particular, we will refer to points in $\partial\Omega_n$ corresponding to boundary vertices of T_n as "boundary vertices of Ω_n."

Note that now every boundary vertex of Ω_n is at most one triangle away from Γ. That is, every boundary vertex v must have been a vertex of a triangle in carr H_n which was removed to form T_n. Thus Γ must hit an equilateral triangle Δ_v of side length $\frac{1}{n}$ of which v is a vertex. Hence there is a line segment γ_v connecting v to Γ having length at most $\frac{1}{n}$ and lying inside Δ_v. In particular, we may choose γ_v short enough so that $\gamma_v \cap \Gamma$ is a single point Γ_v.

A similar construction will be used to build a sequence of degree 6 complexes contained in Ω^*. Unfortunately, H_n accumulates at infinity; thus, in order to ensure that our complexes have only finitely many vertices, we cannot use H_n directly. Instead, we stereographically project each H_n to S^2, apply a Möbius rotation of S^2 fixing 1 and interchanging 0 and ∞, and stereographically project the resulting packing back to $\mathbb{C}$. Each of these new euclidean packings $\widetilde{H}_n$ will now accumulate only at zero; hence, only finitely many circles will lie in Ω^*. We now modify each $\widetilde{H}_n$ by first removing any faces which hit Ω or Γ and then removing extraneous vertices as before. Of course, these packings no longer have constant euclidean radii, but the maximum radius of boundary circles in $\widetilde{H}_n$ does decrease to 0 as $n \to \infty$. Thus to simplify later computations, we can re-number our complexes so that the maximum radius of boundary circles in $\widetilde{H}_n$ is $\frac{1}{2n}$. Now by the same argument as above, each vertex w on the boundary of $\operatorname{carr} \widetilde{H}_n$ is connected to Γ by a line segment γ_w lying outside $\operatorname{carr} \widetilde{H}_n$ and having length at most $\frac{1}{n}$.

The stereographic projection of the trimmed portion of $\widetilde{H}_n$ to S^2 gives an embedding of a constant degree 6 complex T_n^* in a region Ω_n^* containing ∞. Unfortunately, this packing does not induce an embedding in $\mathbb{C}$ of T_n^* since one vertex (which we will refer to as w_∞ in each complex) lies at ∞. The best $\widetilde{H}_n$ can provide is an embedding of $T_n^* \setminus w_\infty$.

In analogy with our construction in Chapter 5, we will denote the open unbounded region formed by the complement in Ω_n^* of the embedding of $T_n^* \setminus w_\infty$ by $\widetilde{G}_n$; that is, $\widetilde{G}_n$ is the region which "should" have provided a realization of faces containing ∞. Similarly, we will let $\widetilde{F}_n$ be the interior of the collection of faces in Ω_n containing v_0, that is, containing 0.

Remark 7.1. Note that as $n \to \infty$, $\Omega_n \to \Omega$ and $\Omega_n^* \to \Omega^*$. Moreover, it is clear $\widetilde{F}_n \to \{0\}$ as $n \to \infty$. But $\widetilde{G}_n$ is just the stereographic projection to $\mathbb{C}$ of rotated faces from the carrier of some H_m which contained 0. The spherical diameter of this collection of faces clearly decreases to 0 before the rotation and thus must decrease to 0 after the rotation as well.

7.2 Geometric Lemmas

Next we need two geometric lemmas. These observations will provide the key to showing uniform convergence of the boundary values of our discrete analytic functions.

Lemma 7.2. *Using the notation established above, for large n there exist homeomorphisms $l_n : \partial\Omega_n \to \Gamma$ and $u_n : \partial\Omega_n^* \to \Gamma$ such that for all $z \in \partial\Omega_n$ and $w \in \partial\Omega_n^*$,*

$$\begin{aligned} |l_n(z) - z| &\leq \frac{57\widetilde{K}}{n} \\ |u_n(w) - w| &\leq \frac{57\widetilde{K}}{n}, \end{aligned} \tag{7.1}$$

where $\widetilde{K}$ depends only on K. In particular, we have

$$|l_n^{-1} \circ u_n(w) - w| \leq \frac{114\widetilde{K}}{n}. \tag{7.2}$$

Proof. First recall that each boundary vertex v of Ω_n is connected to $\Gamma_v \in \Gamma$ by a line segment γ_v of length at most $\frac{1}{n}$. We may assume $\gamma_v \cap \Gamma = \{\Gamma_v\}$.

Next choose a boundary vertex v_1 of $\partial\Omega_n$. Let A be the polygonal Jordan curve forming the boundary of Ω_n and parameterize A over $[0,1]$ so that it is positively oriented with respect to Ω_n and $A(0) = v_1$. Similarly, parameterize Γ over $[0,1]$ so that it is positively oriented with respect to Ω and $\Gamma(0) = \Gamma_{v_1}$.

Now we construct a finite sequence $v_1, v_2, \ldots, v_p, v_{p+1} = v_1$ of boundary vertices of Ω_n such that

1. If $v_i = A(t_i)$, $\quad i = 1, 2, \ldots, p$, then $0 = t_1 < t_2 < \cdots < t_p < 1$.
2. If $\Gamma_{v_i} = \Gamma(s_i)$, $\quad i = 1, 2, \ldots, p$, then $0 = s_1 < s_2 < \cdots < s_p < 1$.
3. The segment $A((t_i, t_{i+1}))$, $\quad i = 1, 2, \ldots, p$, contains at most 36 boundary vertices of Ω_n.

Starting from v_1, proceed around A in the positive direction until reaching a vertex v_2 such that $\gamma_{v_1} \cap \gamma_{v_2} = \emptyset$. Note that if a boundary vertex w lies in $\mathfrak{G}_T(v_1, 3)$, that is, w is 3 generations away from v_1, then faces containing w do not intersect faces containing v_1. In particular, we have $\gamma_v \cap \gamma_w = \emptyset$. (Note that for large n, $\mathfrak{G}_{T_n}(v_1, 3) \neq \emptyset$.) Note $\mathfrak{G}_{T_n}(v_1, 1)$ and $\mathfrak{G}_{T_n}(v_1, 2)$ can contain at most 6 and 12 vertices, respectively, since T_n was formed by deleting vertices from H_n. Thus since the Jordan curve A cannot hit a vertex twice, A can hit at most 18 vertices before reaching $\mathfrak{G}_{T_n}(v_1, 3)$. Hence at most 18 vertices can lie on A between v_1 and v_2.

Note that if v_2 corresponds to $A(t_2)$ and Γ_{v_2} corresponds to $\Gamma(s_2)$, then $0 = t_1 < t_2 < 1$ and $0 = s_1 < s_2 < 1$.

Now suppose boundary vertices $v_1, v_2, \ldots, v_m$ of Ω_n have been choosen to satisfy conditions 1, 2, and 3 above. Travel along A positively from v_m until encountering either v_1 or a vertex $v_{m+1} = A(t_{m+1})$ such that $\gamma_{v_{m+1}} \cap \gamma_{v_m} = \emptyset$ and $\gamma_{v_{m+1}} \cap \gamma_{v_1} = \emptyset$. Note that as described above, there are at most 18 vertices w such that $\gamma_w \cap \gamma_{v_m} \neq \emptyset$ and there are at most 18 vertices u such that $\gamma_u \cap \gamma_{v_1} \neq \emptyset$. Thus A can hit at most 36 vertices before hitting one which satisfies our second search criterion. Hence, if A first encounters v_1, then $A((t_m, 1))$ can contain at most 36 vertices and our construction is concluded. Likewise, if A first encounters a vertex v_{m+1} as described above and $v_{m+1} = A(t_{m+1})$, then $0 = t_1 < t_2 < \cdots < t_m < t_{m+1} < 1$ and we can be assured that $A((t_m, t_{m+1}))$ contains at most 36 boundary vertices. Moreover, $\Gamma_{v_{m+1}}$ cannot equal $\Gamma(s_1)$ or $\Gamma(s_m)$ since $\gamma_{v_{m+1}} \cap \gamma_{v_m} = \emptyset$ and $\gamma_{v_{m+1}} \cap \gamma_{v_1} = \emptyset$.

Suppose now $\Gamma_{v_{m+1}} = \Gamma(s_{m+1})$, but $0 = s_1 < s_{m+1} < s_m < 1$. Let

$$J = A([t_1, t_{m+1}]) \cup \gamma_{v_{m+1}} \cup \Gamma([s_1, s_{m+1}]) \cup \gamma_{v_1}.$$

See Figure 7.2.

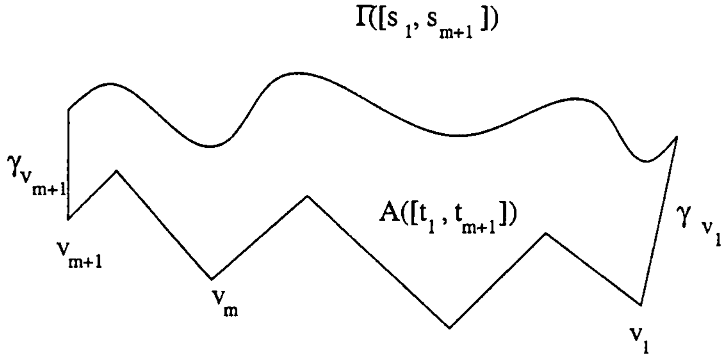

Figure 7.2: The Jordan curve J.

Note that by our construction

$$\begin{aligned} A \cap \gamma_{v_1} &= v_1 = A(t_1) \\ A \cap \gamma_{v_{m+1}} &= v_{m+1} = A(t_{m+1}) \\ \Gamma \cap \gamma_{v_1} &= \Gamma_{v_1} = \Gamma(s_1) \\ \Gamma \cap \gamma_{v_{m+1}} &= \Gamma_{v_{m+1}} = \Gamma(s_{m+1}) \\ A \cap \Gamma &= \emptyset \\ \gamma_{v_1} \cap \gamma_{v_{m+1}} &= \emptyset. \end{aligned} \tag{7.3}$$

Thus it is easy to see J is a Jordan curve, and hence by the Jordan Curve Theorem, divides the plane into two complementary components, one of which is bounded and one of which is unbounded. Note that J was constructed so as not to enclose any point of Ω_n; that is, Ω_n must lie in the unbounded complementary component of J.

Since γ_{v_m} misses $\Gamma([s_1, s_{m+1}])$, γ_{v_1}, and $\gamma_{v_{m+1}}$, we see

$$\gamma_{v_m} \cap J = \gamma_{v_m} \cap A([t_1, t_{m+1}]) = \{v_m\}.$$

Thus $\gamma_{v_m} \setminus \{v_m\}$ must lie entirely in one of the complementary components of J. Since near v_m, the curve J forms a portion of $\partial\Omega_n$, if $\gamma_{v_m} \setminus \{v_m\}$ lies in the unbounded complementary component of J, then $\gamma_{v_m} \setminus \{v_m\}$ must hit Ω_n. But $\gamma_{v_m} \cap \Omega_n = \{v_m\}$; hence, $\gamma_{v_m} \setminus \{v_m\}$ must lie entirely in the bounded complementary component of J.

Now since Γ is a K-quasicircle, it is the image of $\partial\mathbb{D}$ under some (orientation preserving) quasiconformal map F of $\mathbb{C}$ onto itself. Since Γ is positively oriented with respect to Ω, F^{-1} must map Ω onto $\mathbb{D}$. By composing F^{-1} with a suitable rotation, we may assume without loss of generality that $F^{-1}(\Gamma_{v_1}) = F^{-1}(\Gamma(s_1)) = 1$. Since $J \subset \bar{\Omega}$, then $F^{-1}(J) \subset \bar{\mathbb{D}}$. In particular, note that the bounded complementary component of J is mapped onto the bounded complementary component of $F^{-1}(J)$. See Figure 7.3.

Let $e^{i\theta_j} = F^{-1}(\Gamma_{v_j})$, $0 \le \theta_j < 2\pi$, $\quad j = 1, m, m+1$. Since $s_1 < s_{m+1} < s_m$, we must have $0 = \theta_{s_1} < \theta_{s_{m+1}} < \theta_{s_m}$. But then $e^{i\theta_{s_m}} = F^{-1}(\Gamma_{v_m})$ lies in the unbounded complementary component of $F^{-1}(J)$. Hence $\Gamma_{v_m} \in \gamma_{v_m} \setminus \{v_m\}$ must lie in the unbounded complementary component of J. But $\gamma_{v_m} \setminus \{v_m\}$ lies in the bounded complementary component of J, and hence we have a contradiction. Thus we must have $0 < s_1 < s_m < s_{m+1} < 1$. Hence by induction, we can construct a sequence $v_1, v_2, \ldots, v_p$ satisfying conditions 1, 2, and 3.

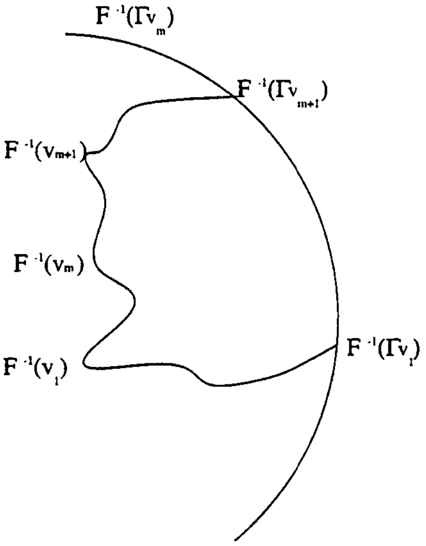

Figure 7.3: The image of J lying in $\mathbb{D}$.

Next, note that any point of $\partial\Omega$ can be written as $A((1-r)t_i + rt_{i+1})$ for some $i = 1, 2, \ldots, p$. Hence we define our map l_n on $\partial\Omega_n$ by

$$l_n(A((1-r)t_i + rt_{i+1})) = \Gamma((1-r)s_i + rs_{i+1});$$

that is, we send each v_i to Γ_{v_i} and extend linearly in between. Since the sequence $\Gamma(s_i)$ proceeds positively around Γ, l_n must be a homeomorphism.

Now since there are at most 36 boundary vertices on $A((t_i, t_{i+1}))$, we have

$$|v_i - v_{i+1}| \leq \frac{36}{n}, \quad i = 1, 2, \ldots, p.$$

Furthermore, if $z \in A((t_i, t_{i+1}))$, then

$$|z - v_i| \le \frac{1}{2}\frac{36}{n} = \frac{18}{n}.$$

Hence by Propositon 2.15,

$$\begin{aligned}
|l_n(z) - z| &\le |l_n(z) - l_n(v_i)| + |l_n(v_i) - v_i| + |v_i - z| \\
&\le \operatorname{diam}(\Gamma([s_i, s_{i+1}])) + \frac{1}{n} + \frac{18}{n} \\
&\le \widetilde{K}|\Gamma(s_i) - \Gamma(s_{i+1})| + \frac{19}{n} \\
&\le \widetilde{K}(|\Gamma(s_i) - v_i| + |v_i - v_{i+1}| + |v_{i+1} - \Gamma(s_{i+1})|) + \frac{19}{n} \\
&\le \widetilde{K}\left(\frac{1}{n} + \frac{36}{n} + \frac{1}{n}\right) + \frac{19}{n}\widetilde{K} \\
&\le \frac{57\widetilde{K}}{n},
\end{aligned}$$

where $\widetilde{K}$ depends only on K.

The maps u_n can be constructed in precisely the same manner. Condition (7.2) now follows easily.

□

Since we designed Ω_n and Ω_n^* to almost fill out the complementary components of the K-quasicircle Γ, we would certainly expect $\partial\Omega_n$ and $\partial\Omega_n^*$ to be quasicircles themselves. The next lemma shows this is in fact the case.

Lemma 7.3. *For each n, $\partial\Omega_n$ and $\partial\Omega_n^*$ are K_1-quasicircles, where K_1 depends only on K. In particular, there exist K_1^2-quasiconformal reflections $\jmath_n$ and $\jmath_n^*$ in $\partial\Omega_n$ and $\partial\Omega_n^*$, respectively.*

Proof. We will give the proof for $\partial\Omega_n$; the proof for $\partial\Omega_n^*$ is of course the same.

As in the proof of Lemma 7.2, we let A denote the Jordan curve forming $\partial\Omega_n$. Fix n and $w, z \in A$. As in the statement of Proposition 2.15, we let $A_{w,z}$ denote the sub-arc of A connecting w and z and having the smaller diameter.

Note that by Lemma 7.2, for all $a, b \in A_{w,z}$,

$$\begin{aligned} |a-b| \le{} & |a - l_n(a)| + |l_n(a) - l_n(b)| + |l_n(b) - b| \\ & \frac{57\widetilde{K}}{n} + \operatorname{diam}(l_n(A_{w,z})) + \frac{57\widetilde{K}}{n} \\ & \frac{114\widetilde{K}}{n} + \operatorname{diam}(l_n(A_{w,z})). \end{aligned} \tag{7.4}$$

Thus

$$\operatorname{diam}(A_{w,z}) \le \frac{114\widetilde{K}}{n} + \operatorname{diam}(l_n(A_{w,z})). \tag{7.5}$$

Next we let $\Gamma_{l_n(w),l_n(z)}$ denote the sub-arc of Γ connecting $l_n(w)$ and $l_n(z)$ and having the smaller diameter. Unfortunately, it is not necessarily the case that $\Gamma_{l_n(w),l_n(z)} = l_n(A_{w,z})$. See Figure 7.4

If $\Gamma_{l_n(w),l_n(z)} \neq l_n(A_{w,z})$, then $\Gamma_{l_n(w),l_n(z)}$ and $l_n(A_{w,z})$ must be complemen-

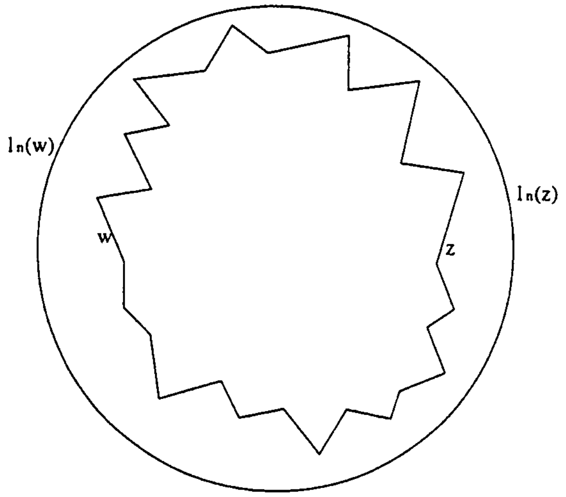

Figure 7.4: Curves for which $\Gamma_{l_n(w),l_n(z)} \neq l_n(A_{w,z})$.
If z and w are nearly "antipodal," then $\Gamma_{l_n(w),l_n(z)}$ need not equal $l_n(A_{w,z})$. In this example, Γ corresponds to the unit circle and $\Gamma_{l_n(w),l_n(z)}$ lies in the upper semicircle. However, l_n can be chosen to map $A_{w,z}$ onto the lower semicircle.

tary closed subarcs of Γ. Thus we let $A^c_{w,z} = A \setminus (A_{w,z} \setminus \{z, w\})$ so that $A_{w,z}$ and $A^c_{w,z}$ are complementary closed subarcs of A. Since $l_n(A_{w,z}) \neq \Gamma_{l_n(w), l_n(z)}$, then $l_n(A^c_{w,z}) = \Gamma_{l_n(w), l_n(z)}$. Again, by Lemma 7.2, for all $a, b \in A^c_{w,z}$,

$$\begin{aligned}
|a - b| &\leq |a - l_n(a)| + |l_n(a) - l_n(b)| + |l_n(b) - b| \\
&\leq \frac{114\widetilde{K}}{n} + \operatorname{diam}(l_n(A^c_{w,z})) \\
&\leq \frac{114\widetilde{K}}{n} + \operatorname{diam}(\Gamma_{l_n(w), l_n(z)}).
\end{aligned}$$

Thus $\operatorname{diam}(A^c_{w,z}) \leq \frac{144\widetilde{K}}{n} + \operatorname{diam}(\Gamma_{l_n(w), l_n(z)})$, and by equation (7.5),

$$\begin{aligned}
\operatorname{diam}(A_{w,z}) &\leq \frac{114\widetilde{K}}{n} + \operatorname{diam}(l_n(A_{w,z})) \\
&\leq \frac{114\widetilde{K}}{n} + \operatorname{diam}(A^c_{w,z}) \\
&\leq \frac{228\widetilde{K}}{n} + \operatorname{diam}(\Gamma_{l_n(w), l_n(z)}).
\end{aligned}$$

If $\Gamma_{l_n(w), l_n(z)} = l_n(A_{w,z})$, then by Equation (7.4), we must also have

$\operatorname{diam}(A_{w,z}) \leq \frac{228\widetilde{K}}{n} + \operatorname{diam}(\Gamma_{l_n(w),l_n(z)})$. Thus in any case,

$$\begin{aligned}
\operatorname{diam}(A_{w,z}) &\leq \frac{228\widetilde{K}}{n} + \operatorname{diam}(\Gamma_{l_n(w),l_n(z)}) \qquad (7.6)\\
&\leq \frac{228\widetilde{K}}{n} + \widetilde{K}|l_n(z) - l_n(w)|\\
&\leq \frac{228\widetilde{K}}{n} + \widetilde{K}(|l_n(z) - z| + |z - w| + |w - l_n(w)|)\\
&\leq \frac{342\widetilde{K}^2}{n} + \widetilde{K}|z - w|.
\end{aligned}$$

If $|z - w| \geq \frac{1}{n}$, then (7.6) becomes

$$\begin{aligned}
\operatorname{diam}(A_{w,z}) &\leq \frac{342\widetilde{K}^2}{n} + \widetilde{K}|z - w|\\
&\leq 342\widetilde{K}^2|z - w| + \widetilde{K}|z - w|\\
&\leq \left(342\widetilde{K}^2 + \widetilde{K}\right)|z - w|.
\end{aligned}$$

Recall that $\partial\Omega_n$ was formed from the union of sides of equilateral triangles of side length $\frac{1}{n}$. Thus, if $|z - w| < \frac{1}{n}$, then z and w must lie either on a euclidean line segment of length $\frac{1}{n}$ or on two different line segments of length $\frac{1}{n}$ which meet at angle $\frac{\pi}{3}$ or $\frac{2\pi}{3}$. In either case, clearly $\operatorname{diam}(A_{w,z}) \leq 2|z-w| \leq \left(342\widetilde{K}^2 + \widetilde{K}\right)|z - w|$. Thus $A = \partial\Omega_n$ is a K_1-quasicircle, where K_1 depends only on $\widetilde{K}$ (and thus only on K). The second assertion of the Lemma then follows from Lemma 2.16.

$\square$

7.3 Construction of Domain Packings

Now we wish to construct a circle packing lying in $\mathbb{D}$ for each of the complexes we embedded in Ω. The existence of such a packing is of course guaranteed by Corollary 3.2. However, since we are also interested in forming a correspondence between $\partial\Omega_n$ and $\partial\mathbb{D}$, we will use the combinatorial "doubling trick" already employed in Chapter 5 rather than appeal to Corollary 3.2 directly.

If T_n is doubled across its boundary, the Koebe-Andreev- Thurston Theorem gives a circle packing P_n on S^2 for the doubled complex. We may normalize so that the circle for v_0 is centered at the origin, the circle for the doubled copy of v_0 is centered at infinity, and the point corresponding to $l_n^{-1}(1)$ is located at 1. That is, if

$$l_n^{-1}(1) = (1-t)a + tb$$

for some neighboring bounday vertices a and b with $0 \leq t < 1$, and if $\widehat{a}$ and $\widehat{b}$ are the euclidean centers of C_v and C_w, respectively, in our new packing P_n, then we may normalize so that

$$(1-t)\widehat{a} + t\widehat{b} = 1.$$

By symmetry, the boundary circles of T_n are all centered on $\partial\mathbb{D} \subset S^2$. See Figure 7.5.

We stereographically project to the plane the portion of this packing

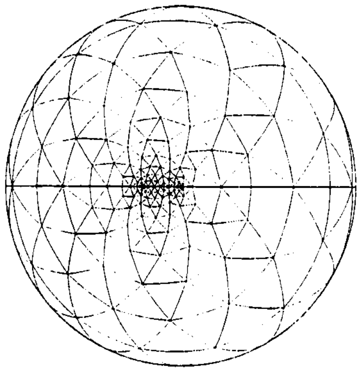

Figure 7.5: A Doubled Complex.
The doubled complex on S^2 for the Ω_n corresponding to Figure 7.1.

corresponding to Ω_n and let D_n denote its euclidean carrier.

Of course, ∂D_n is a polygon circumscribing $\mathbb{D}$, not $\partial \mathbb{D}$ as desired. See Figure 7.6. However, since the spherical carrier was precisely equal to $\mathbb{D}$, the switching of geometries induces a map

$$p_n : \partial \mathbb{D} \to \partial D_n$$

by mapping the spherical centers of boundary circles to the euclidean centers of the stereographic projection of these circles and then extending linearly on the edges.

In a similar way, we can double the complex T_n^* used to define Ω_n^* in Section 7.1 and pack the resulting complex on S^2. We normalize this packing using w_∞ in the same way we used v_0 above. Again we stereographically project the portion corresponding to T_n^* to $\mathbb{C}$ and denote its euclidean carrier

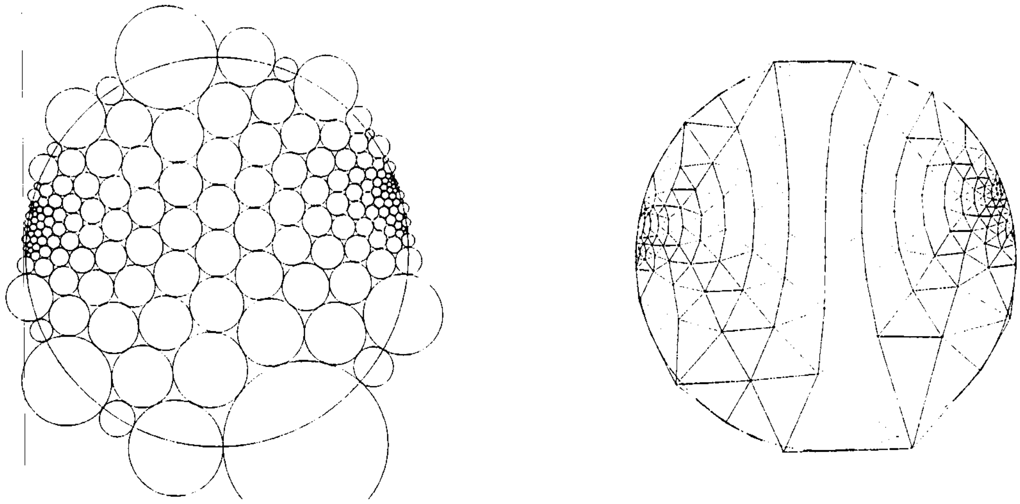

Figure 7.6: A Euclidean Complex
The packing (left) of Figure 7.5 stereographically projected to a neighborhood of $\mathbb{D}$. Note the centers of boundary circles lie outside $\mathbb{D}$. The triangles of the carrier (right) extending outside $\mathbb{D}$ are clearly visible.

by D_n^*. Once more, we obtain a piecewise linear map

$$p_n^* : \partial\mathbb{D} \to \partial D_n^*.$$

As in Chapter 5, we denote by F_n the interior of the collection of faces in $\mathbb{D}_n$ containing 0 and denote by G_n the open unbounded region formed by the complement in D_n^* of our geometric realization of $T_n^* \setminus w_\infty$.

Lemma 7.4 (Domain Lemma). *As $n \to \infty$, the radii of circles corresponding to vertices on ∂D_n and ∂D_n^* decrease uniformly to 0. Consequently both p_n and p_n^* converge uniformly to the identity map on $\partial\mathbb{D}$ as $n \to \infty$. Moreover, the spherical diameter of both F_n and G_n decrease to 0 as $n \to \infty$. As a result, $D_n \to \mathbb{D}$ and $D_n^* \to \mathbb{D}^*$ as $n \to \infty$.*

Proof. Since Γ is compact and misses 0, there is a lower bound d on the distance of points on Γ from 0. By our construction, the distance of points on $\partial\Omega_n$ from 0 is greater than $d - \frac{2}{n}$. Thus each boundary circle of Ω_n is separated in the packing H_n from v_0 by at least

$$\left\lfloor \frac{d - \frac{2}{n}}{\frac{2}{n}} \right\rfloor = \left\lfloor \frac{nd-2}{2} \right\rfloor$$

generations of circles. That is, there are at least $\lfloor \frac{nd-2}{2} \rfloor$ chains of circles in H_n about each boundary circle separating it from 0. But recall that in H_n the i^{th} such chain has length $6i$.

Now when H_n is intersected with the inside of Γ, these chains become half-chains in Ω_n. Thus in the spherical packing for the combinatorial double of Ω_n constructed above, each circle on the original boundary of Ω_n is surrounded by $\lfloor \frac{nd-2}{2} \rfloor$ chains of circles separating it from both 0 and ∞. Note that the i^{th} chain in the doubled complex now has length at most $12i$. Thus by the Spherical Length-Area Lemma, the spherical radius of any circle corresponding to a vertex on ∂D_n is less than

$$\frac{2\pi}{\sqrt{\sum_{i=1}^{n} \frac{1}{12i}}} \to 0.$$

Since the euclidean projection of these circles are bounded away from ∞, their euclidean radii must be uniformly comparable to their spherical radii. Thus the euclidean radii of circles on $\partial\Omega_n$ must decrease uniformly to 0. It is easy to see in this case that both p_n and p_n^* converge uniformly to the identity map on $\partial\mathbb{D}$ as $n \to \infty$.

Finally, note that as $n \to \infty$, the number of generations of degree 6 vertices surrounding w_∞ and each of its neighbors in T_n^* increases without bound. Hence by the Spherical Length-Area Lemma, the spherical radius of C_{w_∞} in the packing for T_n^* used to define D_n^* decreases to 0. Thus the spherical diameter of G_n must decrease to 0. Of course, the same argument also shows that the spherical diameter of F_n decreases to 0. It now follows that $D_n \to \mathbb{D}$ and $D_n^* \to \mathbb{D}^*$ as $n \to \infty$. $\square$

7.4 Construction of the Approximating Maps

At last we can define our approximating maps. The embeddings constructed above induce discrete analytic functions

$$\begin{aligned} f_n &: D_n \to \Omega_n \\ g_n &: D_n^* \setminus G_n \to \Omega_n^* \setminus \widetilde{G}_n. \end{aligned} \tag{7.7}$$

This allows us to at last define our approximations

$$\varphi_n = (p_n)^{-1} \circ f_n^{-1} \circ l_n^{-1} \circ u_n \circ g_n \circ p_n^*$$

to the quasisymmetry φ induced by Γ.

Lest we lose sight of the simple geometry in this maze of compositions, let us recap what φ_n actually does. First φ_n maps the boundary of $\mathbb{D}$ to the boundary of the carrier D_n of a euclidean packing for $\mathcal{T}_n^*$. This is merely a technical correction to allow us to define φ_n on $\partial\mathbb{D}$ itself rather than on a polygon about $\partial\mathbb{D}$. Then we move to the boundary of the carrier of another circle packing for the complex T_n^*, but this one re-packed to lie in the inside Ω^*. Next we "jump across" Γ to the carrier of a packing lying in Ω. A re-packing of this complex takes us back to a polygon about $\partial\mathbb{D}$, and a final technical correction moves us to $\partial\mathbb{D}$. The unfortunate technical considerations aside, this is precisely a discrete version of $f^{-1} \circ g$.

Note that by Corollary 3.12, the families $\{f_n\}$ and $\{g_n\}$ are uniformly

K_1-quasiconformal, where K_1 depends only on the bound C_6 from the Ring Lemma.

7.5 Extension of the Approximating Maps

As before, the key to convergence is extension and the key to extension is reflection. Recall that D_n and D_n^* were formed by *doubling* T_n and T_n^*, respectively. Thus the packings used to realize T_n and T_n^* actually provide two embeddings – one in each hemisphere of S^2. In particular, we have two complementary realizations in $\mathbb{C}$ of $T_n \setminus v_0$ and two complementary realizations in $\mathbb{C}$ of $T_n^* \setminus w_\infty$. Consequently, we have copies $\widehat{D}_n$, $\widehat{D}_n^*$, $\widehat{F}_n$, and $\widehat{G}_n$ of D_n, D_n^*, F_n, and G_n, respectively.

Lemma 7.5. *There exists a discrete reflection $\imath_n$ in ∂D_n interchanging $D_n \setminus F_n$ with $\widehat{D}_n \setminus \widehat{F}_n$. Similarly, there exists a discrete reflection $\imath_n^*$ in ∂D_n^* interchanging $D_n^* \setminus G_n$ with $\widehat{D}_n^* \setminus \widehat{G}_n$. Moreover, $\imath_n$ and $\imath_n^*$ are both K_1-quasiconformal, where K_1 is independent of n.*

Proof. We define our discrete analytic reflection $\imath_n$ by mapping realizations of vertices of $T_n \setminus v_0$ in $D_n \setminus F_n$ to the corresponding realizations in $\widehat{D}_n \setminus \widehat{F}_n$ and then extending affinely. The construction of $\imath_n^*$ is, of course, similar.

Note $\imath_n$ and $\imath_n^*$ are now K_1-quasiconformal by Corollary 3.12, where K_1 depends only on the degree of T_n and T_n^*. But the degree of these complexes does not change with n; hence K_1 is independent of n as well. ☐

Now by Lemma 7.3 we can extend each f_n and g_n by setting

$$\begin{aligned} f_n &= \jmath_n \circ f_n \circ \imath_n \quad \text{on } \widehat{D}_n \setminus \widehat{F}_n \\ g_n &= \jmath_n^* \circ g_n \circ \imath_n^* \quad \text{on } \widehat{D}_n^* \setminus \widehat{G}_n. \end{aligned} \tag{7.8}$$

Finally, the Domain Lemma implies that on each compact subset of $\mathbb{C}$, g_n and f_n are defined for sufficiently large n.

7.6 Convergence of the Approximating Maps

We now have all the pieces to prove our theorem.

Proof of Theorem 7.1. First note each f_n and g_n omit both 0 and ∞ while fixing 1; thus by Theorem 2.9, subsequences of $\{f_n\}$ and $\{g_n\}$ converge uniformly on compact subsets of $\mathbb{C}$ to K_1-quasiconformal homeomorphisms f and g, respectively. We will renumber and assume without loss of generality that $\{f_n\}$ and $\{g_n\}$ themselves converge.

Now, by taking n sufficiently large, any compact subset of $\mathbb{D}$ can be separated from $\partial\mathbb{D}$ by arbitrarily many generations of degree 6 vertices in D_n. Thus by the Hex Packing Lemma, the dilatation of f_n on any compact subset of $\mathbb{D}$ can be made arbitrarily close to 1 by taking n large. Hence the limit map f must be conformal on $\mathbb{D}$, and similarly g must be conformal on $\mathbb{D}^*$.

Next note that by the Domain Lemma, $\{p_n\}$ and $\{p_n^*\}$ converge uniformly to the identity on $\partial\mathbb{D}$. Thus $\{g_n \circ p_n^*\}$ converges uniformly to g on $\partial\mathbb{D}$.

Moreover, since by (7.2)

$$|l_n^{-1} \circ u_n(z) - z| \leq \frac{114\widetilde{\mathcal{K}}}{n}$$

for all $z \in \partial\Omega_n$, we see $\{l_n^{-1} \circ u_n \circ g_n \circ p_n^*\}$ also converges uniformly to g on $\partial\mathbb{D}$.

A similar argument implies $\{f_n \circ p_n = (p_n^{-1} \circ f_n^{-1})^{-1}\}$ converges uniformly to f on $\partial\mathbb{D}$. It is easy to show that if $\eta_n \to \eta$ and $\xi_n \to \xi$ uniformly and ξ^{-1} is uniformly continuous, then $\xi_n^{-1} \circ \eta_n$ converges uniformly to $\xi^{-1} \circ \eta$, where this composition is defined. Hence we have

$$\varphi_n = {p_n}^{-1} \circ f_n^{-1} \circ l_n^{-1} \circ u_n \circ g_n \circ p_n^* \to f^{-1} \circ g \tag{7.9}$$

uniformly on $\partial\mathbb{D}$. Finally we see $g^{-1} \circ f$ is quasisymmetric on $\partial\mathbb{D}$ by Theorem 2.18. Since $g^{-1} \circ f$ is normalized as in 2.18, it must be the desired quasisymmetry corresponding to Γ. $\square$

Chapter 8

Computational Aspects

8.1 Experimentation

One of the great advantages of circle packing techniques is the ease with which one can experiment. Thanks to Ken Stephenson's wonderful software package `CirclePack`, it is easy to create and display circle packings. Indeed, most of the figures contained herein were produced using `CirclePack`.

During the early phases of this research, the opportunity for experimentation was invaluable. After writing programs to create several prototype triangulations and weld them together in various ways, the author used `CirclePack` to create packings for the combinatorially welded complexes and observe the behavior of the discrete welding curve. It quickly became apparent that these discrete welding curves did behave as expected.

In fact, these early experiments were extremely useful in developing intuition about the manner in which a quasisymmetry φ influences the shape of its conformal welding curve Γ. In particular, experimenting with weldings induced by monomials as in Example 2.3, led to the observation that intervals on which φ acts as a contraction should map under g to portions of Γ which turn "toward" Ω. While this statement is far from rigorous, it is nonetheless very useful in understanding the behavior of Γ. For example, if φ is a quasisymmetry of $\partial\mathbb{D}$ with $\varphi' < 1$ on an interval I, then $|\varphi(I)|_{\mathbb{D}} < |I|_{\mathbb{D}}$, and thus the harmonic measure $\omega(\varphi(I);\mathbb{D},0)$ of $\varphi(I)$ with respect to $\mathbb{D}$ and 0 will be smaller than the harmonic measure $\omega(I,\mathbb{D}^*,\infty)$ of I with respect to $\mathbb{D}^*$ and ∞. Consequently, we must have $\omega(f\circ\varphi(I);\Omega,0) < \omega(g(I);\Omega^*,\infty)$ since f and g are conformal maps fixing 0 and ∞, respectively. Hence Γ must bend "towards" Ω and "away from" Ω^*.

This phenomenon was first observed experimentally and only later rigorously understood. In our combinatorial welding, a small derivative for φ means that many edges of $T^*_{n,m}$ will be attached to relatively few edges of $T_{n,m}$. In particular, many vertices will be added to only a few edges of $T_{n,m}$; hence, some fringe vertices will have several new boundary neighbors between their two old boundary neighbors. When realized via circle packing, these new neighbors will serve to push the old boundary vertices apart, forcing the fringe circles to increase their radii, and thus bending the discrete welding curve toward $\Omega_{n,m}$. See Figure 8.1.

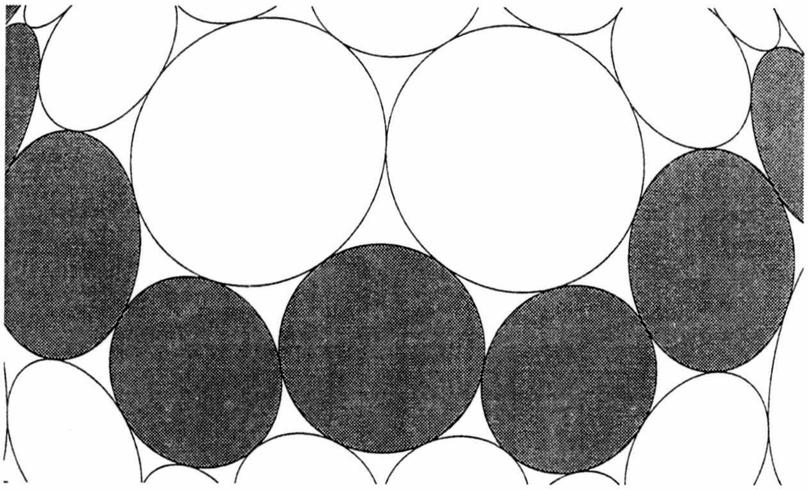

Figure 8.1: Welding a Contraction
A discrete welding corresponding to an interval on which φ is a contraction. Circles corresponding to the welding curve are shaded. Note that the degree of the two large fringe circles has increased, causing the curve to bend toward Ω.

8.2 Successful Failures

Unfortunately, the opportunity to test conjectures experimentally can often leave one with lots of pictures but no proof. Many different prototype triangulations were welded in various ways, and while the early experiments were very convincing, each construction eventually proved problematic.

For example, one of the early methods devised to combinatorially weld two disc triangulations involved adding edges reaching from the boundary of one triangulation to the other. The packings thus produced seemed to approximate the conformal welding curve very closely. For example, the quasisymmetry $\varphi(e^{i\theta}) = e^{i(\theta+\sin\theta)}$ satisfies $\varphi'(e^{i\theta}) > 1$ for $-\frac{\pi}{2} < \theta < \frac{\pi}{2}$, and $0 \leq \varphi'(e^{i\theta}) < 1$ for $\frac{\pi}{2} < \theta < \frac{3\pi}{2}$. Welding prototype triangulations $T_{36,7}$ and $T^*_{36,7}$ by adding edges produced the packing of Figure 8.2. Notice that as expected the discrete welding curve bends toward Ω^* when φ is an expansion and towards Ω when φ is a contraction.

Another class of quasisymmetries for which this method of discrete welding was tried was the piecewise linear real quasisymmetries, for example

$$\varphi(x) = \begin{cases} 7x, & \text{if } x \leq 0 \\ x, & \text{if } x > 0. \end{cases}$$

Yitzhak Katznelson, Subhashis Nag, and Dennis Sullivan [28] have shown if a quasisymmetry is non-differentiable but still Lipschitz at a point (such as 0 and ∞ for the φ above), then the induced conformal welding curve will

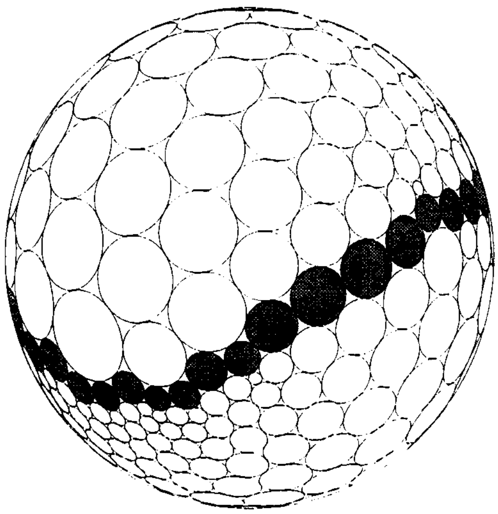

Figure 8.2: An Early Discrete Welding
An early packing produced using $\varphi(e^{i\theta}) = e^{i(\theta+\sin\theta)}$. The circles corresponding to the discrete welding curve are shaded.

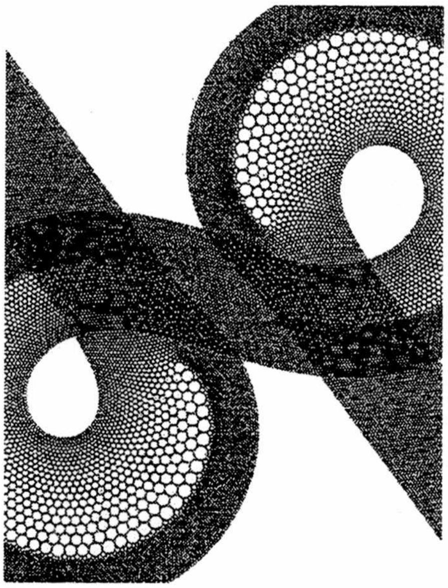

Figure 8.3: A Spiraling Welding
An early packing for a complex welded by a piecewise linear quasisymmetry.

be an infinite spiral about the image of that point. Our discrete welding curve for φ should thus have two spirals. Due to computational limitations, the resulting welded triangulations was not packed as described in Chapter 6, but instead packed subject to the constraint that all boundary circles have the same radii. The resulting circle packing is not univalent, but does demonstrate quite dramatically the tendency to spiral. See Figure 8.3.

Unfortunately, however, welding triangulations by adding edges creates additional faces in the welded complex that do not have combinatorial copies in the original triangulations. Thus they can not lie in the image of the discrete welding maps; instead they form a "dead region" separating the images of the discrete maps. This provides an obstacle to quasiconformally extending the discrete maps, and consequently dooms the proof.

Such failed attempts to construct a discrete welding were not a total loss, however. Without the insight gained from these experiments, a workable procedure for welding triangulations would have been much more difficult to develop.

8.3 Monomial Quasisymmetries

Real quasisymmetries of the form $\varphi(x) = x|x|^{\alpha-1}$ were studied as far back as Beurling and Ahlfors's original paper on extending quasisymmetries [13]. Thus, once a convergent method of discrete welding was discovered, one of the first real quasisymmetries for which our discrete welding procedure was used was $\varphi(x) = x^3$. As explained in Example 2.3, the conformal welding curve for this map consists of two rays meeting at the origin at an angle $\frac{\pi}{2}$.

Figure 8.4 shows the results of combinatorially welding using this φ. The discrete welding curve is clearly visible. This particular packing contains 28397 circles and required approximately 14 minutes for a 400 mHz Pentium II to produce.

The next interesting monomial is $\varphi(x) = x^5$, which results in a conformal welding curve with angle $\frac{\pi}{3}$. Welding the same prototype triangulations as before, we form Figure 8.5.

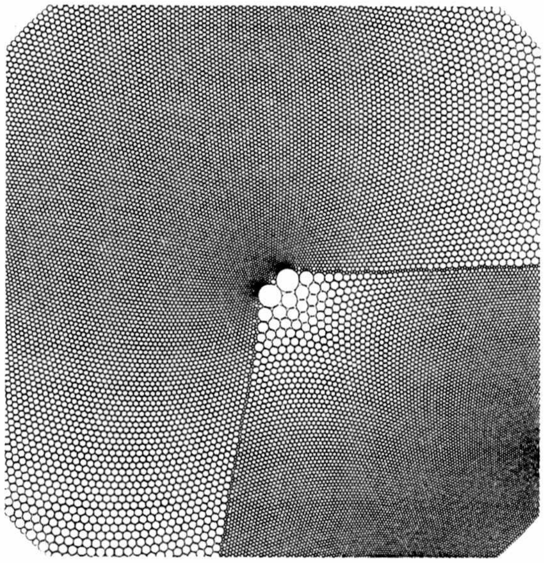

Figure 8.4: A Discrete Welding for $\varphi(x) = x^3$.
A discrete conformal welding curve with a nearly-right angle.

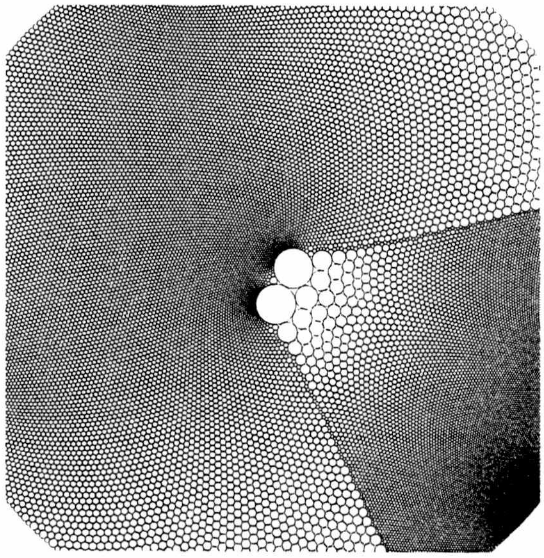

Figure 8.5: A Discrete Welding for $\varphi(x) = x^5$.
A discrete conformal welding curve with angle nearly $\frac{\pi}{3}$.

8.4 Quasisymmetries Induced by Blaschke Products

Once our method of discrete welding was perfected, it became possible to study classical welding questions by observing the discrete approximations. One very interesting class of quasisymmetries was suggested by David Tischner [53]. The square root of a two-fold Blaschke product B extends to a quasisymmetric map φ of $\partial\mathbb{D}$. If we normalize B so that one root is at 0 and the other lies at iy on the imaginary axis, then the induced quasisymmetry is given by

$$\varphi(e^{i\theta}) = \sqrt{e^{i\theta}\left(\frac{e^{i\theta} - iy}{1 - iye^{i\theta}}\right)}.$$

Note that if $y = 0$, then φ is just the identity map. For $y = 1$, φ is no longer a homeomorphism of $\partial\mathbb{D}$; in fact, we see that as $y \to 1$, then $\varphi'(1) \to \infty$. An obvious question then is, "What happens to the conformal welding curve as $y \to 0$ and $y \to 1$?"

As one might expect, the conformal welding curve does seem to approach the unit circle (the welding curve induced by the identity map) as $y \to 0$. See Figure 8.6. The same prototype triangulation was used in each case.

On the other hand, as $y \to 1$, the welding curve must bend into Ω more and more. The curve degenerates by squeezing the point corresponding to 1 down to 0. See Figure 8.7.

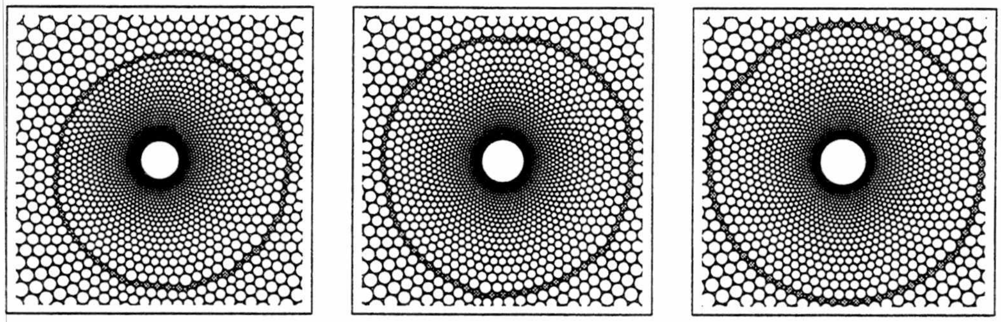

Figure 8.6: Discrete Blaschke Welding for Small y.
The discrete welding for (from left) $y = 0.3$, 0.1, and 0.05. The circles corresponding to the discrete welding curve are shaded in each case.

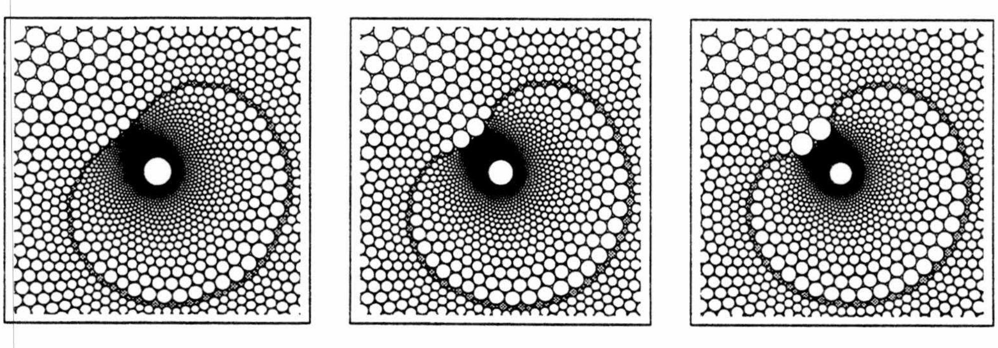

Figure 8.7: Discrete Blaschke Welding for Large y.
The discrete welding for (from left) $y = 0.85$, 0.95, and 0.99. The circles corresponding to the discrete welding curve are shaded in each case.

8.5 Practical Limitations

Unfortunately, there are at present several technical limitations which prevent our discrete welding from being a practical method for numerically approximating conformal welding maps and curves. For example, quasisymmetries may in general have derivative equal to 0 almost everywhere. Such a map would be very difficult to encode in a subroutine which our current software could use.

Even more troubling is the total lack of error estimates for our discrete approximations. With the exception of He's estimate [22] on the convergence of the dilatation of discrete analytic maps, nothing is known about the rate of convergence for discrete analytic maps. In most cases, it appears that very coarse approximations are reasonably accurate, but we have found examples in which the convergence is painfully slow. For example, welding discs using a quasisymmetry with two non-differentiable, but bilipschitz, singularities will yield a curve with two infinite spirals [28]. Unfortunately, while our discrete approximations do give the general shape of the curve at a relatively coarse stage, the spirals emerge very slowly. In fact, the most accurate picture we have generated to date is Figure 8.8. The curve was formed by welding $T_{2000,50}$ to $T^*_{2000,50}$, using a total of 201502 circles. It required almost 14 hours for a 400 mHz Pentium II to compute its discrete welding curve and was, needless to say, somewhat disappointing.

Note that this quasisymmetry is bilipschitz; hence the conformal welding curve is a Bishop-Jones curve, and our welding can be done directly. But

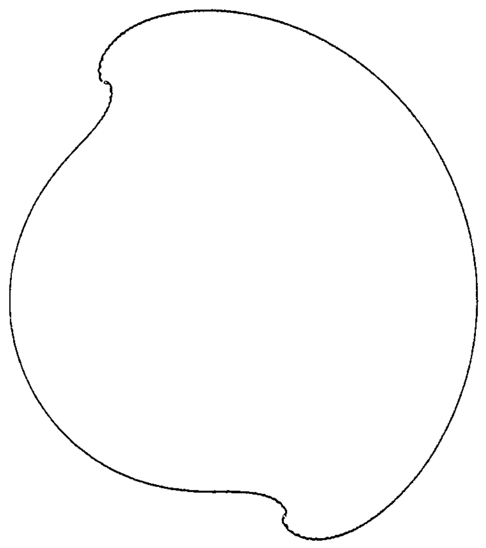

Figure 8.8: A Double Spiral.
An approximation of a conformal welding curve having two infinite spirals.

recall that for quasisymmetries which are not bilipschitz, a diagonalization process must be employed. This further complicates the goal of finding error estimates; indeed it is doubtful if such estimates could be found.

Finally, an additional weakness in our approximation scheme for discs is the need to "choose m sufficiently large" to ensure $f_{n,m}$ is uniformly quasiconformal on $F_{n,m}$ and the spherical radius of $G_{n,m}$ is less than $\frac{1}{n}$. The Spherical Length-Area Lemma provides some guide to choosing m to satisfy the latter condition, but there are as yet no estimates for the former.

Fortunately, our method seems to perform much better in practice than the "worst case" estimates would indicate. Indeed, the main features of the conformal welding curves are usually apparent even at very coarse stages in the approximation.

Bibliography

Bibliography

[1] William Abikoff and Taiping Ye, *Computing the Douady-Earle extension*, Lipa's Legacy, Contemp. Math., vol. 211, Amer. Math. Soc., 1995, pp. 1–8.

[2] Lars Ahlfors, *On quasiconformal mappings*, Journal d'Analyse Mathematique **3** (1953/54), 1–58.

[3] ———, *Riemann surfaces*, Princeton University Press, Princeton, New Jersey, 1960.

[4] ———, *Quasiconformal reflections*, Acta Math. **109** (1963), 291–301.

[5] ———, *Lectures on quasiconformal mappings*, D. van Nostrand, Princeton, New Jersey, 1966.

[6] E. M. Andreev, *Convex polyhedra in Lobacevskii space*, Math. USSR Sbornik **10** (1970), 413–440 (English).

[7] ———, *Convex polyhedra of finite volume in Lobacevskii space*, Math. USSR Sbornik **12** (1970), 255–259 (English).

[8] G. areth Jones and David Singerman, *Complex functions: An algebraic and geometric viewpoint*, Cambridge University Press, Cambridge, 1987.

[9] Kari Astala and Michel Zinsmeister, *Teichmüller spaces and BMOA*, Math. Ann. **289** (1991), no. 4, 613–625.

[10] A. Beardon.

[11] Alan F. Beardon and Kenneth Stephenson, *The uniformization theorem for circle packings*, Indiana Univ. Math. J. **39** (1990), 1383–1425.

[12] Lipman Bers, *Simultaneous uniformization*, Bull. Amer. Math. Soc. **66** (1960), 94–97.

[13] A. Beurling and L. Ahlfors, *The boundary correspondence under quasiconformal mappings*, Acta Mathematica **96** (1956), 125–141.

[14] Chris Bishop and Peter Jones, *Harmonic measure, l^2 estimates and the Schwarzian derivative*, Journal D'Analyse (1994), no. 62, 77–113.

[15] Philip L. Bowers and Kenneth Stephenson, *Uniformizing dessins and Belyĭ maps via circle packing*, submitted.

[16] A. Douady and C. Earle, *Conformally natural extension of homeomorphisms of the circle*, Acta Math. **157** (1986), 145–149.

[17] Tomasz Dubejko, *Approximation of analytic functions with prescribed boundary conditions by circle packing maps*, Discrete and Computational Geometry **17** (1997), 67–77.

[18] Tomasz Dubejko and Kenneth Stephenson, *Circle packing: Experiments in discrete analytic function theory*, Experimental Mathematics **4** (1995), no. 4, 307–348.

[19] Frederick P. Gardiner, *Teichmüller theory and quadratic differentials*, Wiley, 1987.

[20] Frederick W. Gehring, *Characteristic properties of quasidisks*, Les Presses De L'Universiteé De Montréal, Montréal, 1982.

[21] H. Grötzsch, *Über die Verzerrung bei Schlichten Nichtkonformen Abbildungen und über eine damit zusammenhängende Erweiterung des Picardschen Satzes*, Ber. Verh. Sächs. Akad. wiss. Leipzig **80** (1928), 503–507.

[22] Zheng-Xu He, *An estimate for hexagonal circle packings*, J. Differential Geometry **33** (1991), 395–412.

[23] Zheng-Xu He and Burt Rodin, *Convergence of circle packings of finite valence to Riemann mappings*, Comm. in Analysis and Geometry **1** (1993), 31–41.

[24] Zheng-Xu He and Oded Schramm, *Hyperbolic and parabolic packings*, Discrete & Computational Geom. **14** (1995), 123–149.

[25] ______, *On the convergence of circle packings to the Riemann map*, Invent. Math. **125** (1996), 285–305.

[26] Alfred Huber, *Représentation conforme. courbe déterminée par une relation entreses applications conformes intérieure et extérieure*, C. R. Acad. Sci. Paris Sér. I Math. **303** (1986), no. 13.

[27] ______, *Eine Lösungsformel für Reguläre Konforme Verheftungen*, Archives of Mathematics **67** (1996), 195 – 198.

[28] Y. Katznelson, Subhashis Nag, and Dennis P. Sullivan, *On comformal welding homeomorphisms associated to Jordan curves*, Annales AcademiæScientiarium Fennicæ**15** (1990), 293 – 306.

[29] J.A. Kelingos, *Boundary correspondence under quasiconformal mappings*, Michigan Math. J. **13** (1966), 235 – 249.

[30] Koebe, *Kontaktprobleme der Konformen Abbildung*, Ber. Sächs. Akad. Wiss. Leipzig, Math.-Phys. Kl. **88** (1936), 141–164.

[31] Jan G. Krzyż, *Quasicircles and harmonic measure*, Annales Academiæ-Scientiarum FennicæSeries AI Mathematica **12** (1987), 19 – 24.

[32] A. Lecko and D. Partyka, *An alternative proof of a result due to Douady and Earle*, Annales Universitatis Mariae Curie - Sklodowska - Lublin - Polonia **17** (1988), 59 – 68.

[33] O. Lehto, *Univalent functions and Teichmüller spaces*, Springer-Verlag, 1987.

[34] O. Lehto and K.I. Virtanen, *Quasiconformal mappings in the plane*, second ed., Springer - Verlag, Berlin - Heidelberg - New York, 1973.

[35] Subhashis Nag, *The complex analytic theory of Teichmüller spaces*, Wiley, 1988.

[36] ______, *Matrices: Canonical mappings in string theory*, Rev. Roumaine Math. Pures. Appl. **39** (1991), no. 8, 789–827.

[37] Kinjiro Nishikaw and Fumio Maitani, *Moduli of ring domains obtained by a conformal welding*, Kodai Mathematics Journal **20** (1997), 161 - 171.

[38] Kôtaro Oikawa, *Welding of polygons and the type of Riemann surfaces*, Kodai Math. Sem. Rep. **13** (1961), 37 - 52.

[39] D. Partyka, *A sewing theorem for complementary Jordan domains*, Annales Universitatis Mariae Curie - Sklodowska - Lublin - Polonia **16** (1987), 99 - 103.

[40] Osmo Pekonen, *The interface of Teichmüller theory and string theory*, Rev. Roumaine Math. Pures Appl. **38** (1994), no. 8, 829–854.

[41] ______, *Universal Teichmüller space in geometry and physics*, Journal of Geometry and Physics **15** (1995), 227–251.

[42] Albert Pfluger, *Quasiconforme abbildungen und logarithmische kapazität*, Ann. Inst. Fourier (Grenoble) (1951), no. 2, 69–80.

[43] ______, *Über die Konstruktion Riemanischen Flächen durch Verheftung*, J. Indian Math. Soc. **24** (1961), 401 - 412.

[44] Ch. Pommerneke, *Boundary behavior of conformal maps*, Springer - Verlag, Berlin - Heidelberg - New York, 1992.

[45] John G. Ratliffe, *Foundations of hyperbolic manifolds*, Springer - Verlag, Berlin - Heidelberg - New York, 1994.

[46] Andrew Repp, *Discrete Riemann maps and the parabolicity of tilings*, Ph.D. thesis, Virginia Polytechnic Institute and State University, May 1998.

[47] Burt Rodin and Dennis Sullivan, *The convergence of circle packings to the Riemann mapping*, J. Differential Geometry **26** (1987), 349–360.

[48] Kenneth Stephenson, Notes for Seminar in Analysis, Fall 1997 and Spring 1998, University of Tennessee.

[49] ______, Notes for Seminar in Analysis, Fall 1993 and Spring 1994, University of Tennessee.

[50] ______, *Circle packings in the approximation of conformal mappings*, Bulletin, Amer. Math. Soc. (Research Announcements) **23, no. 2** (1990), 407–415.

[51] William Thurston, *The geometry and topology of 3-manifolds*, Princeton University Notes, preprint.

[52] ______, *The finite Riemann mapping theorem*, 1985, Invited talk, An International Symposium at Purdue University on the occasion of the proof of the Bieberbach conjecture, March 1985.

[53] David Tishner, Personal Conversation, June 1998.

[54] Juhani V. Vainio, *Conditions for the possibility of conformal sewing*, Annales AcademiæScientiarum FennicæSeries AI Mathematica **53** (1985), 1 – 43.

[55] ———, *On the type of sewing functions with a singularity*, Annales AcademiæScientiarum FennicæSeries AI Mathematica **14** (1989), 161 – 167.

[56] ———, *Properties of real sewing functions*, Annales AcademiæScientiarum FennicæSeries AI Mathematica **20** (1995), 87 – 95.

[57] Jussi Väisälä, *Quasisymmetry and unions*, Manuscripta Mathematica **68** (1990), 101 – 111.

[58] Eric W. Weisstein, Web page. http://www.astro.virginia.edu/~eww6n /math, April 1998.

Index

Index

$|I|_J$, 12

$|x-y|_J$, 12

$\lceil\ \rceil$, 51, 67

$\lfloor\ \rfloor$, 113

$A_{w,z}$, 106

abstract triangulation, 27

Ahlfors, Lars, 6, 9, 14, 18, 31, 125

b, 18

barycentric coordinates, 38

Bers, Lipman, 6, 21

Beurling, Arne, 6, 14, 31, 125

Beurling-Ahlfors Extension Theorem, 14

bilipschitz, 13, 42, 49, 57, 79

  local, 90

Bishop, Chris, 21

Bishop-Jones curve, 21, 129

carr, 28, 98

carrier, 28, 98

Canright, Geoffrey, iii

chain, 31

circle packing, 28

  hexagonal, 30, 96

  univalent, 28

combinatorial structure, 41, 42

combinatorial welding, 42

complex

  augmented, 45, 64

  CP, 27, 29–30

  hyperbolic, 30

  parabolic, 30, 68

  simplicial, 26

complex derivatives, 9

  polar, 16

complex dilatation, 10

conformal structure, 5, 41

  extension of, 20

conformal welding
  definition, 20
  example, 22
conformal welding curve, 22
  definition, 20
conformal welding maps, 20
Conformal WeldingTheorem, 21
cow, 97
CP-complex, 27, 29–30

$D_{n,m}$, 59, 62
D^*_n, 62
dilatation, 9
  complex, 10
discrete analytic function, 38
discrete conformal welding curve,
    57, 81
discrete quasisymmetry, 49
Domain Lemma, 113
Douady, Adrien, 14
Douady-Earle Extension Theorem,
    15
doubling, 60, 96, 110

$\epsilon_{n,m}$, 61, 71
$\widetilde{\epsilon}_{n,m}$, 65, 71
Earle, Clifford, 14
embedding, 26
essentially unique, 21, 29
extremal length, 6, 31

$F_{n,m}$, 67
F_n, 113
$\widetilde{F}_{n,m}$, 67
$\widetilde{F}_n$, 98
$\{f_n\}$, 57, 81
f, 21, 75
$f_{n,m}$, 66
flower, 28, 30, 36
fringe, 28, 51–53, 67

$G_{n,m}$, 63
G_n, 113
Γ, 57, 81
Γ_n, 57, 81
Γ_v, 97, 100
$\Gamma_{x,y}$, 18
$\mathfrak{G}_{\mathcal{K}}$, 29
$\mathfrak{G}_{T_n}$, 100
$\widetilde{G}_{n,m}$, 65

$\widetilde{G}_n$, 98

γ_v, 97, 100

$\{g_n\}$, 57, 81

g, 21, 75

$g_{n,m}$, 66

generation, 29, 30, 37, 70, 100, 113, 114

Grötzsch, Herbert, 6, 9

H_n, 30, 39, 81

$\widetilde{H}_n$, 98

He, Zheng-Xu, 40

Hex Packing Lemma, 37, 39

hexagonal packing, 30

hyperbolic, 30

$\imath_n^*$, 116–117

$\imath_n$, 116–117

$\jmath_n$, 106, 117

$\jmath_n^*$, 106, 117

Jones, Peter, 21

Jordan Curve Theorem, 102

$\mathcal{K}$, 42

$\mathcal{K}_{n,m}$, 60

$\widetilde{\mathcal{K}}_{n,m}$, 64

Katznelson, Yitzhak, 122

Kelingos, John, 13, 14, 79

Koebe-Andreev-Thurston Theorem, 29, 60, 62

Krzyż, Jan, 21

$\mathbb{L}$, 22, 81

$l_n(z)$, 99

Lehto, Ollie, 21

Length-Area Lemma, 31, 77

  Spherical, 32

Liouville's Theorem, 10, 87, 93

Livingston, Sherman, iii

M_F, 51

M_I, 51

μ, 9

Maitani, Fumio, 21

modulus

  definition, 6

  estimation of, 7, 32

  of quadrilaterals, 7, 8

  of ring domains, 7, 8

Nag, Subhashis, 122

Nishikawa, Kinjiro, 21
normal family, 11

Ω, 21
Ω^*, 21
$\Omega^*_{n,m}$, 65
Ω^*_n, 98
$\Omega_{n,m}$, 65
Ω_n, 97
Oikawa, Kôtaro, 21, 90

$P_{n,m}$, 60, 69
$\widetilde{P}_{n,m}$, 65, 69
$\widehat{P}_{n,m}$, 60, 62
p_n, 62, 111
    definition, 16
p^*_n, 113
parabolic, 30, 68
Partyka, Dariusz, 21
Pfluger, Albert, 9, 21
φ_T, 47, 48
Plaut, Conrad, iii

$Q_{n,m}$, 68
$\widetilde{Q}_{n,m}$, 68
quadrilateral, 7
quasicircle, 15–19, 103
    definition, 15
        geometric, 18
quasiconformal
    definition
        analytic, 9
        geometric, 8
    extension, 19
    reflection, 19, 75, 106
quasidisc, 15
quasisymmetry, 12–15
    definition, 12
    local, 12, 89

Richter, Stefan, iii
Riemann Surface, 5
Riemann surface, 24
ring domain, 7
Ring Lemma, 36, 39
    Spherical, 36
Rodin, Burt, 31, 36
Rodin-Sullivan Theorem, 39

S^2, 6, 60
Schramm, Oded, 40

simplex, 26
simplicial complex, 26
Spherical Length-Area Lemma, 32, 71, 114
Spherical Ring Lemma, 36, 71
Stephenson, Ken, iii, 40
Sullivan, Dennis, 31, 36, 122

T, 41
$T \setminus w$, 27
T^*, 41
$T^*_{n,m}$, 60, 63
T^*_n, 98
$T_{n,m}$, 60
$T^*_{n,m}$, 62
T_n, 97
$\{T_{n,m}\}$, 58
Teichmüller theory, 6
Thurston, William, 27
Tischner, David, 127
triangle
  topological, 25
triangulation
  abstract, 27, 41
  of surface, 25

$\mathbb{U}$, 22, 81
u, 45
$u_n(z)$, 99
univalent, 28
Universal Teichmüller Space, 24

v_0, 60
v_1, 42, 59, 60
v_j, 43, 52
Väisälä, Jussi, 21
Vainio, Juhani, 21

w_1, 42, 60
w_∞, 60
w_i, 43, 47
Williams, Carol, iii

Vita

George Brock Williams, Jr. was born July 26, 1971, in Newton, Mississippi, the son of George and Dorothy Williams. He graduated from Heidelberg Academy in May of 1989 as the class valedictorian. In August 1989, he entered Mississippi State University, where he was active in the University Honors Program and a member of the Baptist Student Union Executive Council. During the summer of 1992, he served as a BSU summer missionary in Minnesota. Upon graduating *summa cum laude* from Mississippi State in May 1993, he entered the University of Tennessee as a Graduate Teaching Assistant. In December 1994, he married his wife Carol. His doctoral degree was conferred in May of 1999.